

IOWA STATE UNIVERSITY

Digital Repository

Retrospective Theses and Dissertations

Iowa State University Capstones, Theses and
Dissertations

1991

Synthesis and analysis of elastic high-speed cam-operated mechanisms

Hsin-Ting Jonathan Liu
Iowa State University

Follow this and additional works at: <https://lib.dr.iastate.edu/rtd>



Part of the [Mechanical Engineering Commons](#)

Recommended Citation

Liu, Hsin-Ting Jonathan, "Synthesis and analysis of elastic high-speed cam-operated mechanisms" (1991). *Retrospective Theses and Dissertations*. 9549.
<https://lib.dr.iastate.edu/rtd/9549>

This Dissertation is brought to you for free and open access by the Iowa State University Capstones, Theses and Dissertations at Iowa State University Digital Repository. It has been accepted for inclusion in Retrospective Theses and Dissertations by an authorized administrator of Iowa State University Digital Repository. For more information, please contact digirep@iastate.edu.

INFORMATION TO USERS

This manuscript has been reproduced from the microfilm master. UMI films the text directly from the original or copy submitted. Thus, some thesis and dissertation copies are in typewriter face, while others may be from any type of computer printer.

The quality of this reproduction is dependent upon the quality of the copy submitted. Broken or indistinct print, colored or poor quality illustrations and photographs, print bleedthrough, substandard margins, and improper alignment can adversely affect reproduction.

In the unlikely event that the author did not send UMI a complete manuscript and there are missing pages, these will be noted. Also, if unauthorized copyright material had to be removed, a note will indicate the deletion.

Oversize materials (e.g., maps, drawings, charts) are reproduced by sectioning the original, beginning at the upper left-hand corner and continuing from left to right in equal sections with small overlaps. Each original is also photographed in one exposure and is included in reduced form at the back of the book.

Photographs included in the original manuscript have been reproduced xerographically in this copy. Higher quality 6" x 9" black and white photographic prints are available for any photographs or illustrations appearing in this copy for an additional charge. Contact UMI directly to order.



University Microfilms International
A Bell & Howell Information Company
300 North Zeeb Road, Ann Arbor, MI 48106-1346 USA
313/761-4700 800/521-0600



Order Number 9126217

**Synthesis and analysis of elastic high-speed cam-operated
mechanisms**

Liu, Hsin-Ting Jonathan, Ph.D.

Iowa State University, 1991

U·M·I
300 N. Zeeb Rd.
Ann Arbor, MI 48106



NOTE TO USERS

**THE ORIGINAL DOCUMENT RECEIVED BY U.M.I. CONTAINED PAGES
WITH POOR PRINT. PAGES WERE FILMED AS RECEIVED.**

THIS REPRODUCTION IS THE BEST AVAILABLE COPY.



Synthesis and analysis of elastic high-speed cam-operated mechanisms

by

Hsin-Ting Jonathan Liu

A Dissertation Submitted to the
Graduate Faculty in Partial Fulfillment of the
Requirements for the Degree of
DOCTOR OF PHILOSOPHY

Major: Mechanical Engineering

Approved:

Signature was redacted for privacy.

In Charge of Major Work

Signature was redacted for privacy.

For the Major Department

Signature was redacted for privacy.

For the Graduate College

Iowa State University
Ames, Iowa
1991

Copyright © Hsin-Ting Jonathan Liu, 1991. All rights reserved.

TABLE OF CONTENTS

INTRODUCTION	1
PART I. SYNTHESIS AND STEADY STATE ANALYSIS OF HIGH-SPEED ELASTIC CAM-FOLLOWER LINKAGES WITH CONCENTRATED MASSES, PART 1: THEORY	
	4
ABSTRACT	5
INTRODUCTION	6
DERIVATION OF SYSTEM EQUATIONS	12
SYNTHESIS	17
Initial synthesis	17
Improved synthesis	22
ANALYSIS	26
EXAMPLE	30
CONCLUSIONS	42
REFERENCES	43
PART II. SYNTHESIS AND STEADY STATE ANALYSIS OF HIGH-SPEED ELASTIC CAM-FOLLOWER LINKAGES WITH	

CONCENTRATED MASSES, PART 2: STEADY STATE ANALYSIS	46
ABSTRACT	47
INTRODUCTION	48
EXAMPLE	52
CONCLUSIONS	74
REFERENCES	75
PART III. SYNTHESIS AND STEADY STATE ANALYSIS OF HIGH-SPEED ELASTIC CAM-FOLLOWER LINKAGES WITH A CURVED BEAM COUPLER BY FINITE ELEMENT METHOD	77
ABSTRACT	78
INTRODUCTION	79
DERIVATION OF SYSTEM EQUATIONS	80
SYNTHESIS	86
Initial synthesis	86
Improved synthesis	89
ANALYSIS	92
EXAMPLE	93
CONCLUSIONS	116
REFERENCES	117
GENERAL CONCLUSIONS	120

APPENDIX A: INTRODUCTION TO THE NUMERICAL SCHEME USED TO CARRY OUT HSU'S METHOD INVOLVING THE TRANSITION MATRICES IN PART I	123
APPENDIX B: A SYSTEM OF EQUATIONS DERIVED FROM THE GOVERNING EQUATIONS BY CENTRAL FI- NITE DIFFERENCE SCHEME IN PART III	126
APPENDIX C: METHOD TO FIND THE CHARACTERISTIC MUL- TIPLIERS FOR THE ANALYSIS EQUATIONS IN PART III	128
APPENDIX D: FORTRAN PROGRAMS FOR PARTS I AND II .	130
APPENDIX E: FORTRAN PROGRAMS FOR PART III	147
REFERENCES	181
ACKNOWLEDGEMENTS	183

INTRODUCTION

Dynamically induced elastic deflections of a light weight cam-follower mechanism operating at a high speed may cause the response to deviate from the desired one, and it may be unacceptable if the design is based on kinematics alone. Further, the governing dynamic equations generally are periodic due to the changing geometry of the follower linkage and the constant rotation of the driving link. For a linear periodic system, it is well known that multiple instability regions may exist, and magnitudes of the characteristic multipliers (eigenvalues of the discrete transition matrix for a whole period) determine the stability.

In the synthesis of elastic cam-follower mechanisms, some work has been done on follower linkages which have translating motions and are governed by equations with constant coefficients (Johnson, 1959; Chen, 1973; Wiederrick and Roth, 1975; Gupta and Wiederrick 1983; Tsay and Huey, 1989). Only limited results, however, are available for follower linkages having oscillating motions and governed by periodic equations (Flugrad, 1986), or having other types of motions governed by periodic equations (Midha and Turcic, 1980; Cronin and LaBouff, 1981). For the elastic, high-speed, cam-operated mechanisms considered in this dissertation, the governing equations are inhomogeneous, periodic, linear, ordinary, differential equations. The steady state solutions and their relationship with the characteristic multipliers

become important in the synthesis.

The objectives of this research include the development of a systematic procedure to synthesize the cam profile to produce a desired output motion at a given design speed and damping ratio, the study of the relationship between characteristic multipliers and steady state solutions, and the search for a technique to select better design speeds.

Parts I and II of the dissertation, entitled *Synthesis and steady state analysis of high-speed elastic cam-follower linkages with concentrated masses*, consider a cam driving a lumped mass through a massless, elastic, slider-crank follower linkage with concentrated masses located at two pin joints. The output shaft and the links are subjected to torsional and axial deflections, respectively. An iterative procedure taking the elasticity, damping and changing geometry of the linkage into account is developed for synthesizing the cam profile to produce a desired output motion at a given design speed. Three first order differential equations with constant coefficients and periodic forcing terms are solved in sequence for synthesis. A system of three second order differential equations with periodic coefficients and forcing terms is then solved for analysis. Besides stability, a single dominant pair of complex characteristic multipliers is found to have important effects on the response of the cam systems. The influence of damping on vibration and the effects of the difference in damping ratios used for synthesis and analysis are investigated. All the results are based upon the steady states calculated numerically by Hsu's method (Hsu and Cheng, 1973, 1974; Hsu, 1974).

Part III of the dissertation, entitled *Synthesis and steady state analysis of high-speed elastic cam-follower linkages with curved beam couplers by finite element method*,

considers a cam driving a lumped mass through an elastic, slider-crank, follower linkage with a curved beam coupler. A systematic procedure using the finite element method to synthesize the cam profile and to analyze the response is developed. The finite element method developed by Midha et al. (1978) to model high-speed elastic linkages is used here. The curved beam coupler is approximated by an assembly of four straight beams of equal length. For small elastic displacements, the Coriolis, normal and tangential components of the coordinate accelerations are neglected (Midha et al., 1978). This leads to the uncoupling of rigid body and elastic components. Systems of inhomogeneous, periodic, linear, ordinary, differential equations are thus obtained for synthesis and analysis after imposing appropriate boundary conditions. The equations are solved by the central finite difference method (Sandor and Zhuang, 1985). An iterative procedure is developed for synthesis since the rigid body dependent system mass and stiffness matrices are unknown for synthesis.

PART I.

**SYNTHESIS AND STEADY STATE ANALYSIS OF HIGH-SPEED
ELASTIC CAM-FOLLOWER LINKAGES WITH CONCENTRATED
MASSES, PART 1: THEORY**

ABSTRACT

A cam driving a lumped inertia through a massless, elastic, slider-crank follower linkage with two concentrated masses located at the pin joints is considered. An iterative procedure taking the elasticity, damping, and changing geometry of the linkage into account is developed for synthesizing the cam profile to produce a desired output motion at a given design speed. The steady state solutions for the inhomogeneous, periodic, linear, ordinary differential equations are solved numerically by Hsu's method.

INTRODUCTION

Much research has recently been done on the analysis of elastic linkages. This is due to higher desired operating speeds with resulting dynamic effects that are no longer negligible. Because more accurate modeling techniques are now employed, periodic terms associated with the changing geometry of the mechanisms appear in the governing equations. Unlike an equation with constant coefficients which has only one natural frequency, equations with periodic coefficients may have many unstable frequency regions. The investigation of this parameter induced instability, called parametric instability (Bolotin, 1964; Hsu, 1963, 1965; Flugrad and Liu, 1988), and the related vibrations are important in designing elastic linkages governed by periodic systems of equations (Capellen, 1967; Capellen and Krumm, 1971; Carnegie and Pasricha, 1974; Zodaks and Midha, 1987a).

In the synthesis of elastic cam-follower mechanisms, some work has been done on follower linkages that have translating motions and are governed by equations with constant coefficients (Johnson, 1959; Chen, 1973; Wiederrick and Roth, 1975; Gupta and Wiederrick 1983; Tsay and Huey, 1989). Only limited results, however, are available for follower linkages that have oscillating motions governed by periodic equations (Flugrad, 1986).

The present study is an extension of the earlier work by Flugrad (1986) in which a systematic procedure was used to formulate equations for synthesis and analysis of an undamped, elastic, cam-driven mechanism with a single lumped output inertia and a massless, elastic, slider-crank follower linkage. The resulting equations were linearized with respect to small elastic deflections, but the nonlinearities associated with the gross rigid body motion of the mechanism were retained. The equation

of motion for the output link was found to be an inhomogeneous Hill equation with periodicity dependent on the changing geometry of the mechanism. Numerical results substantiated the existence of multiple instability regions in the neighborhood of the design speed.

In the present study, the lumped output inertia is joined by two other masses, M_c and M_d , located at the two pin joints. These are shown in Fig. 1. Damping is also included. The procedure used by Flugrad (1986) is used here to formulate governing equations for small elastic deflections. Three first order differential equations with constant coefficients and periodic forcing terms are solved in sequence for synthesis. An iterative procedure is used for synthesis because some parameters dependent on the undeformed linkage positions are unknown in the synthesis. A system of three second order differential equations with periodic coefficients and forcing terms is then solved for analysis. The steady state solution for this inhomogeneous periodic system is found numerically by Hsu's method (Hsu, 1974; Hsu and Cheng, 1974). Following is a brief discussion of Hsu's method as it applies to inhomogeneous periodic linear systems.

Equation (1) is the matrix expression for the system of inhomogeneous, periodic, linear, ordinary, differential equations:

$$\dot{\mathbf{X}} = \mathbf{A}(t)\mathbf{X} + \mathbf{B}(t) \quad (1)$$

where $\mathbf{A}(t) = \mathbf{A}(t + T)$, \mathbf{A} is an $n \times n$ coefficient matrix, $\mathbf{B}(t) = \mathbf{B}(t + T)$, \mathbf{B} is an $n \times 1$ forcing vector, T is the period for both \mathbf{A} and \mathbf{B} , and the initial value for \mathbf{X} is $\mathbf{X}(t_0)$. The existence and uniqueness of a solution for equation (1) is assured if $\mathbf{A}(t)$ and $\mathbf{B}(t)$ depend continuously on time for $t > t_0$. The general solution for

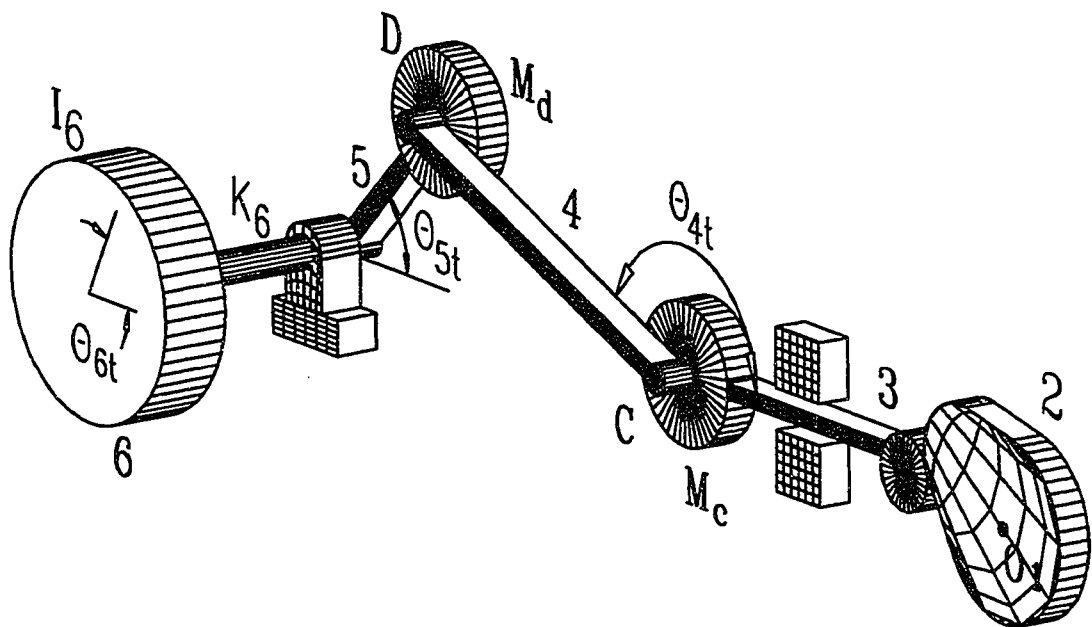


Figure 1: A cam-operated system

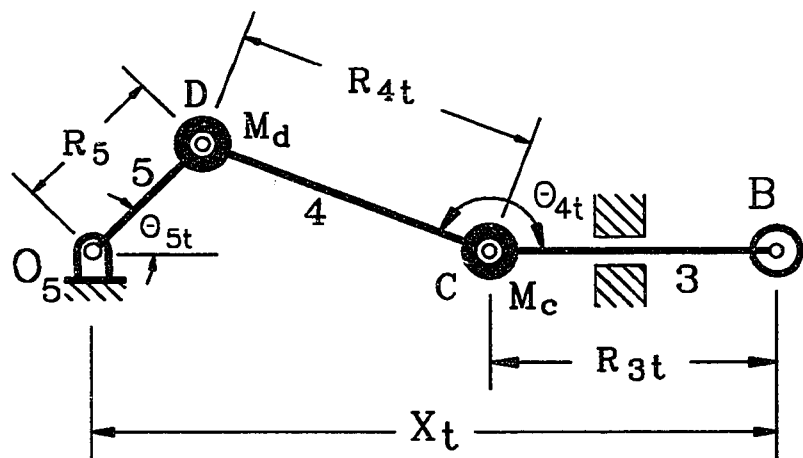


Figure 2: The elastic follower linkage with concentrated masses

equation (1) is

$$\mathbf{X}(t) = \Phi(t, t_0)\mathbf{X}(t_0) + \int_{t_0}^t \Phi(t, \tau)\mathbf{B}(\tau)d\tau \quad (2)$$

where $\Phi(t, t_0)$ is the transition matrix which can be expressed as

$$\Phi(t, t_0) = e^{\int_{t_0}^t \mathbf{A}(\tau)d\tau} \quad (3)$$

For the cam-follower system considered here, the gross rigid body motion of the follower linkage leads to the periodically varying coefficient matrix \mathbf{A} and the forcing vector \mathbf{B} . Besides Φ , the initial condition which will generate a periodic steady state is needed to determine the steady state solution. This periodic initial condition can be found by imposing the requirement that the responses at the beginning and the end of the period are equal, i.e., we let $\mathbf{X}(t_0 + T) = \mathbf{X}(t_0)$ in equation (2):

$$\mathbf{X}(t_0) = [\mathbf{I} - \Phi(t_0 + T, t_0)]^{-1} \int_{t_0}^{t_0+T} \Phi(t_0 + T, \tau)\mathbf{B}(\tau)d\tau \quad (4)$$

Of course, $[\mathbf{I} - \Phi(t_0 + T, t_0)]$ must be nonsingular. The existence of the periodic steady state solution is assured if the system is asymptotically stable.

Except for special cases, the analytical expression for Φ doesn't exist, but its approximation can be found numerically (Pipes, 1953; Hsu and Cheng, 1973; Hsu, 1974). For constant \mathbf{A} , the $\Phi(t_0 + \Delta t, t_0)$ can theoretically be evaluated by the following infinite series of the matrix exponential:

$$\Phi(t_0 + \Delta t, t_0) = \mathbf{I} + \mathbf{A} \Delta t + \mathbf{A}^2 (\Delta t)^2 / 2! + \mathbf{A}^3 (\Delta t)^3 / 3! + \dots \quad (5)$$

For the cam systems studied here, for very small Δt , the higher order terms are negligible, and equation (5) can be approximated by the first few terms. If the whole period T is divided into n intervals (they need not be equally spaced) so that for each

interval the time duration Δt is small and \mathbf{A} is nearly constant, then equation (5) is applicable in each interval. In addition, the transition matrix for the whole period is the successive product of Φ for each such interval:

$$\bar{\Phi}(t_0 + T, t_0) = \Phi(t_0 + T, t_{n-1}) \Phi(t_{n-1}, t_{n-2}) \cdots \Phi(t_2, t_1) \Phi(t_1, t_0) \quad (6)$$

The approximate transition matrix found by this method has been shown to approach the true transition matrix as the number of intervals approaches infinity (Hsu, 1974). The integration in equation (4) can be approximated numerically by summing the response to each impulse $\mathbf{B}(\tau)d\tau$ (see Appendix A), or by other integration schemes. Solutions were considered satisfactory if the difference in solutions obtained by using a greater number of intervals was less than the specified tolerance of 10^{-5} for δx in equation (20). In this study, the appropriate number of intervals used in the period, 2π , turned out to be 216,000 for synthesis and 1,800 for analysis.

Midha et al. (1979), Midha and Turcic (1980), and Turcic and Midha (1984) adopted a similar idea of replacing the periodically varying system with a number of consecutive constant systems and applied a general modal analysis. By considering the compatibility of displacements and velocities at the ends of the intervals, which is a property of the transition matrix, a large system of linear algebraic equations was obtained. Instead of modal analysis, Gao et al. (1988) used multi-step algorithms (Newmark, Houbolt, Park, and α method) to generate the algebraic equations for each interval.

The Fourier series method has also been used (Bolotin, 1964; Nath and Ghosh, 1980; Cleghorn et al., 1984) to obtain the steady state responses. Both sides of the equations are approximated by a truncated Fourier series. A large system of linear algebraic equations is thus generated by equating Fourier coefficients on both sides.

A perturbation method, which employs a relatively small parameter, can also be used for obtaining approximate solutions. Bogoliubov and Mitropolski (1961) developed the general asymptotic expansion method to obtain general solutions for both nonlinear and linear equations by using the concept of variation of parameters and by forcing secular terms to vanish. The general solutions and stability conditions for Mathieu's equation were derived in their monograph.

Compared to Hsu's method, the other methods have certain difficulties that are not easy to resolve. When solving a large system of algebraic equations, although the system of equations may be banded, small numbers which require a higher precision floating system may be generated. The accuracy of the perturbation method depends on the smallness of the small parameter and this sufficiently small quantity may not be easy to find. Also, the truncation of the Fourier series may adversely affect the accuracy of the solution. For the systems studied here, Hsu's method overcomes the problems listed above and is more suitable. The only requirement is that the time interval be small enough to make numerical evaluation of Φ and the integration of equation (4) accurate. The high dimension matrix computation can easily be handled by digital computers.

DERIVATION OF SYSTEM EQUATIONS

As shown in Fig. 1, the cam-driven system consists of a lumped output mass with inertia, I_6 , and an elastic slider crank linkage with two concentrated masses, M_c and M_d , located at two pin joints. This system is designed to transfer the constant rotation of the cam to output link 6. The slider, which acts as a translating roller follower, is assumed to remain in contact with the cam. The slider, connecting link, and the crank are all considered massless. Links 3 and 4 possess axial spring rates K_3 and K_4 respectively, while link 5 and the cam are assumed to be rigid.

Output link 6 is connected to the crank by a massless, elastic shaft with torsional spring rate K_6 . Any external torque that might be applied to link 6 is ignored here. In addition, it is assumed that no backlash exists in the joints of the mechanism and that all fixed bearings are rigid. Linear dimensions shown in Fig. 2 for the follower linkage, as well as angular positions of links 4, 5, and 6 are defined as the sum of two components. The first is a term associated with the undeformed configuration of the mechanism and the second represents a relatively small deflection due to the elasticity of the device. These, along with other important parameters, are summarized in Table 1.

For the output member, the equation of motion is derived by summing moments about the axis of rotation:

$$I_6 \ddot{\theta}_{6t} + C_6(\dot{\theta}_{6t} - \dot{\theta}_{5t}) + K_6(\theta_{6t} - \theta_{5t}) = 0$$

Resolving θ_{5t} into its rigid and elastic components, θ_5 and $\delta\theta_5$, and employing a dimensionless speed ratio, Ω , we have

$$\Omega^2 \theta''_{6t} + 2\zeta\Omega(\theta'_{6t} - \theta'_5 - \delta\theta'_5) + (\theta_{6t} - \theta_5 - \delta\theta_5) = 0 \quad (7)$$

Table 1: List of mechanism dimensions and associated parameters

R_n, X	= linear dimensions of undeformed configuration for n=3,4,5,7,8,f
$\delta R_n, \delta X$	= linear deflections due to elastic deformations for n=3,4
R_{nt}, X_t	= overall linear dimensions including effect of deformations, $R_{nt} = R_n + \delta R_n$ for n=3,4 and $X_t = X + \delta X$
r_n, x	= dimensionless parameters of undeformed configuration, $r_n = R_n/R_5$ for n=3,4,7,8,f and $x = X/R_5$
$\delta r_n, \delta x$	= dimensionless deflections arising from elastic deformations, $\delta r_n = \delta R_n/R_5$ for n=3,4 and $\delta x = \delta X/R_5$
θ_n	= angular position coordinates for the undeformed mechanism with n=4-8
$\delta\theta_n$	= angular deflections due to elastic deformations, for n=4-6
θ_{nt}	= overall angular positions including effect of deformations, $\theta_{nt} = \theta_n + \delta\theta_n$, for n=4-6
I_6	= mass moment of inertia for output link 6
K_3, K_4	= axial spring rates for links 3 and 4
K_6	= torsional spring rate for link 6
ϕ	= angular position of cam
ω	= constant rotational speed of cam
ω_n	= frequency parameter defined by $\omega_n^2 = K_6/I_6$
C_n	= damping coefficient for nth link, n=3,4,6
ζ	= dimensionless damping ratio, $\zeta = C_6/(2I_6\omega_n)$
Ω	= dimensionless speed ratio $\Omega = \omega/\omega_n$
m_c, m_d	= dimensionless masses for masses M_c and M_d , $m_n = M_n R_5^2/I_6$, for n=c,d
D_3, D_4	= dimensionless damping coefficients for links 3 and 4, $D_n = C_n R_5^2/C_6$, for n=3,4
S_3, S_4	= dimensionless spring rates for links 3 and 4, $S_n = K_n R_5^2/K_6$, for n=3,4

where primes denote differentiation with respect to the cam rotation angle, ϕ .

For the slider crank linkage, both kinematic constraints and motion equations exist. The kinematic constraints include both rigid body and elastic constraints given by equations (8) and (9) (Flugrad, 1986), respectively.

$$\begin{aligned} \cos \theta_5 - r_4 \cos \theta_4 + r_3 - x &= 0 \\ \sin \theta_5 - r_4 \sin \theta_4 &= 0 \end{aligned} \quad (8)$$

$$\begin{aligned} -\delta \theta_5 \sin \theta_5 + r_4 \delta \theta_4 \sin \theta_4 - \delta r_4 \cos \theta_4 + \delta r_3 - \delta x &= 0 \\ \delta \theta_5 \cos \theta_5 - r_4 \delta \theta_4 \cos \theta_4 - \delta r_4 \sin \theta_4 &= 0 \end{aligned} \quad (9)$$

Equations (9) have been linearized with regard to the elastic deformations, and, hence, they are valid only for small displacements.

In addition to kinematic constraints, equations of motion are required to completely describe the behavior of the follower linkage. Free body diagrams for the linkage elements are shown in Fig. 3. For the crank, link 5, moments are summed about point O_5 .

$$C_6(\dot{\theta}_{6t} - \dot{\theta}_{5t}) + K_6(\theta_{6t} - \theta_{5t}) - R_5 F_{45} \sin(\theta_{4t} - \theta_{5t}) = M_d R_5^2 \ddot{\theta}_{5t} \quad (10)$$

The connecting link, link 4, is a two force member.

$$F_{54} = F_{34} = C_4 \delta \dot{R}_4 + K_4 \delta R_4 \quad (11)$$

For link 3, summation of horizontal forces produces

$$\begin{aligned} F_s - F_{r3} &= C_3 \delta \dot{R}_3 + K_3 \delta R_3 \\ F_{43} \cos \theta_{4t} + (C_3 \delta \dot{R}_3 + K_3 \delta R_3) &= M_c (\ddot{X}_t - \ddot{R}_{3t}) \end{aligned} \quad (12)$$

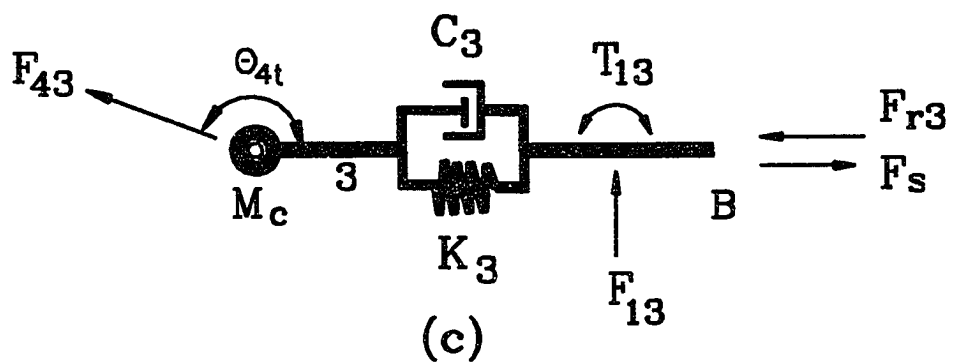
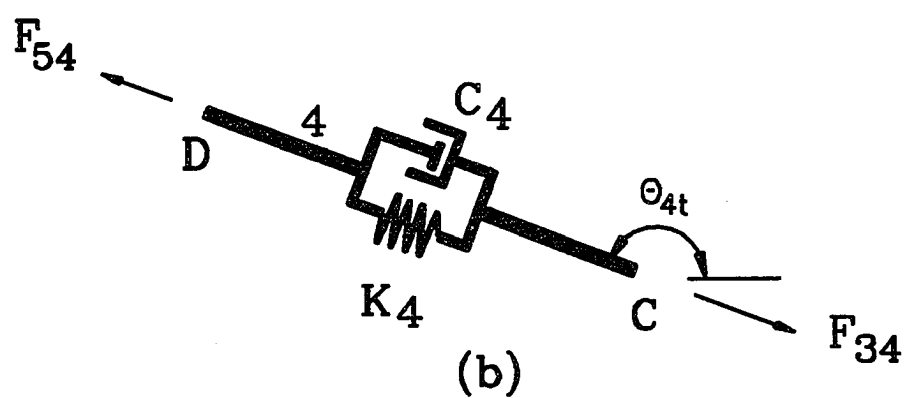
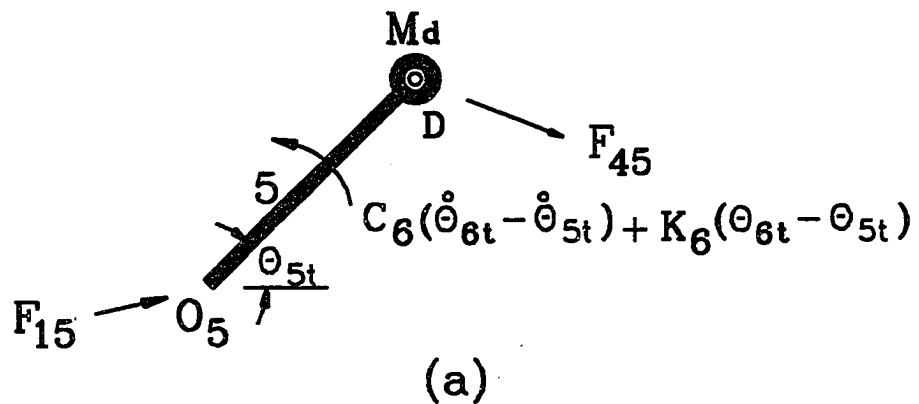


Figure 3: The links of the elastic follower linkage

where F_s represents the force due to a follower return spring which is not shown. F_{13} and T_{13} in Fig. 3(c) are bearing reactions. Expansion of $\sin(\theta_{4t} - \theta_{5t})$ and linearization of terms involving the small angles $\delta\theta_4$ and $\delta\theta_5$ produces

$$\sin(\theta_{4t} - \theta_{5t}) = \sin(\theta_4 - \theta_5) + (\delta\theta_4 - \delta\theta_5) \cos(\theta_4 - \theta_5) \quad (13)$$

Combining equations (10) and (11), substituting equation (13), ignoring products involving small deflections and their derivatives, and, finally, employing dimensionless quantities, one obtains,

$$\begin{aligned} 2\zeta\Omega(\theta'_{6t} - \theta'_5 - \delta\theta'_5) + (\theta_{6t} - \theta_5 - \delta\theta_5) - (2\zeta\Omega D_4 \delta r'_4 + S_4 \delta r_4) \sin(\theta_4 - \theta_5) \\ = m_d \Omega^2 (\theta''_5 + \delta\theta''_5) \end{aligned} \quad (14)$$

Similar treatment for equations (11), (12), and (13) yields

$$(2\zeta\Omega D_4 \delta r'_4 + S_4 \delta r_4) \cos \theta_4 + 2\zeta\Omega D_3 \delta r'_3 + S_3 \delta r_3 = m_c \Omega^2 (x'' + \delta x'' - \delta r''_3) \quad (15)$$

In summary, seven equations governing the overall motion of the output link and the follower linkage are needed: two pairs of algebraic kinematic constraints for the follower rigid body motion (equations (8)) and follower elastic deflection (equations (9)); three dynamical ordinary differential equations for the output member (equation (7)), and for the follower linkage (equations (14) and (15)). Nine variables ($x, \theta_4, \theta_5, \theta_{6t}, \delta r_3, \delta r_4, \delta x, \delta\theta_4$, and $\delta\theta_5$) appear in these seven equations. The synthesis of the cam profile and the analysis of the synthesized mechanism are based on the solutions to these seven equations.

SYNTHESIS

Initial synthesis

The objective for synthesis is to accurately determine the profile of the cam needed to produce the desired motion of the output member at a given operating speed. The approach is to solve the seven governing equations developed in the last section augmented by additional valid constraints.

For synthesis, the motion of the output member, given by θ_{6t} , is known, since it is specified as a function of the cam rotation angle, ϕ . One more imposed constraint will make the number of equations equivalent to the number of unknown variables. For initial synthesis, this constraint can be chosen as $\delta\theta_5 = 0$. Since $\delta\theta_5$ is small, the initially synthesized cam profile deviates from its true shape by only a small amount, which makes convergence for subsequent iterations fast. Equation (7) can thus be solved for θ_5 by first rearranging it as

$$\theta'_5 + [1/(2\zeta\Omega)] \theta_5 = (\Omega/2\zeta) \theta''_{6t} + \theta'_{6t} + [1/(2\zeta\Omega)] \theta_{6t} \quad (16)$$

Since θ_{6t} , θ'_{6t} , and θ''_{6t} are all periodic with period 2π , θ_5 is expected to be periodic with the same period. Hsu's method can be applied to solve for the steady state directly. For this first order equation with constant coefficient, the A in equations (3) and (5) becomes $-1/(2\zeta\Omega)$, and the transition matrix becomes a scalar, $\Phi(t, t_0) = e^{-(t-t_0)/(2\zeta\Omega)}$. Once θ_5 is determined, the rigid body constraints given by equations (8), can be solved in closed form for θ_4 and x ,

$$\begin{aligned} \theta_4 &= \sin^{-1}(\sin \theta_5 / r_4) \\ x &= \cos \theta_5 - r_4 \cos \theta_4 + r_3 \end{aligned} \quad (17)$$

The steady state δr_4 can then be determined by rewriting equation (14) and using it in conjunction with equation (7),

$$\delta r'_4 + [S_4/(2\zeta\Omega D_4)] \delta r_4 = -(\theta''_{6t} + m_d\theta''_5)\Omega/[2\zeta D_4 \sin(\theta_4 - \theta_5)] \quad (18)$$

and the θ''_5 term can be obtained by differentiating equation (16).

The δx used in synthesizing the cam profile is found next. Equations (9) can be solved for δr_3 by eliminating $\delta\theta_5$,

$$\delta r_3 = \delta x + \delta r_4 / \cos \theta_4 \quad (19)$$

Substituting δr_3 , $\delta r'_3$, and $\delta r''_3$, obtained by differentiating equation (19) into equation (15), one obtains

$$\begin{aligned} \delta x' + [S_3/(2\zeta\Omega D_3)]\delta x &= [1/(2\zeta\Omega D_3)] \left\{ m_c\Omega^2 x'' - (m_c\Omega^2/\cos\theta_4) \delta r''_4 \right. \\ &+ (-2\zeta\Omega D_4 \cos\theta_4 - 2m_c\Omega^2\theta'_4 \sin\theta_4/\cos\theta_4^2 - 2\zeta\Omega D_3/\cos\theta_4) \delta r'_4 \\ &+ [-S_4 \cos\theta_4 - m_c\Omega^2 (2\theta'^2_4 \sin^2\theta_4/\cos^3\theta_4 + \theta'^2_4/\cos\theta_4 \\ &\left. + \theta''_4 \sin\theta_4/\cos^2\theta_4) - 2\zeta\Omega D_3\theta'_4 \sin\theta_4/\cos^2\theta_4 - S_3/\cos\theta_4] \delta r_4 \right\} \end{aligned} \quad (20)$$

where $\delta r''_4$ is found by differentiating equation (18), and θ'_4 , θ''_4 , and x'' are found by differentiating equations (8),

$$\theta'_4 = \theta'_5 \cos\theta_5 / (r_4 \cos\theta_4) \quad (21)$$

$$\theta''_4 = [\theta''_5 \cos\theta_5 - \theta'^2_5 \sin\theta_5 + r_4\theta'^2_4 \sin\theta_4] / (r_4 \cos\theta_4) \quad (22)$$

$$x'' = -\theta''_5 \sin\theta_5 - \theta'^2_5 \cos\theta_5 + r_4\theta''_4 \sin\theta_4 + r_4\theta'^2_4 \cos\theta_4 \quad (23)$$

The steady state δx in equation (20) can be found by Hsu's method. The $\delta x''$ needed for the following iterative synthesis and the analysis in the following section can then

be determined by differentiating equation (20) which results in the $\delta r_4'''$ term. This $\delta r_4'''$ term can be found by differentiating equation (18) twice which results in the term θ_5'''' . This θ_5'''' can be determined by differentiating equation (16) which results in the highest derivative, θ_{6t}'''' , of θ_{6t} . This indicates that the continuity of the fifth derivative of θ_{6t} with respect to ϕ is required to synthesize a cam profile.

In differentiating equation (20) to find $\delta x''$, many terms need to be evaluated and some of them possess large values and change rapidly with respect to ϕ . It was found that even when 216,000 intervals were used in conjunction with Hsu's method, the $\delta x''$ was still approaching but had not reached a fixed value. The subroutine DQDDER in the IMSL library was then used to find the values of $\delta x''$ by numerically differentiating δx .

In synthesizing the cam profile, the equivalent linkage approach (Hall, 1966; Jensen, 1987; Bussell and Hubbart, 1989), which instantaneously duplicates the position, velocity and acceleration of the actual mechanism, was used. Figs. 4 and 5 show the cam with its translating roller follower and the equivalent linkage respectively.

The loop closure equation for loop $O_1 ABO_1$ is

$$R_7 e^{j(\theta_7 + \phi + \pi/2)} + (R_8 + R_f) e^{j(\theta_8 + \pi/2)} - z + Y = 0 \quad (24)$$

where $Y = H - X_t$. After dividing by R_5 and resolving the equation into its imaginary and real components, we have

$$\begin{aligned} r_7 \cos(\theta_7 + \phi) + (r_8 + r_f) \cos \theta_8 - z &= 0 \\ -r_7 \sin(\theta_7 + \phi) - (r_8 + r_f) \sin \theta_8 + y &= 0 \end{aligned} \quad (25)$$

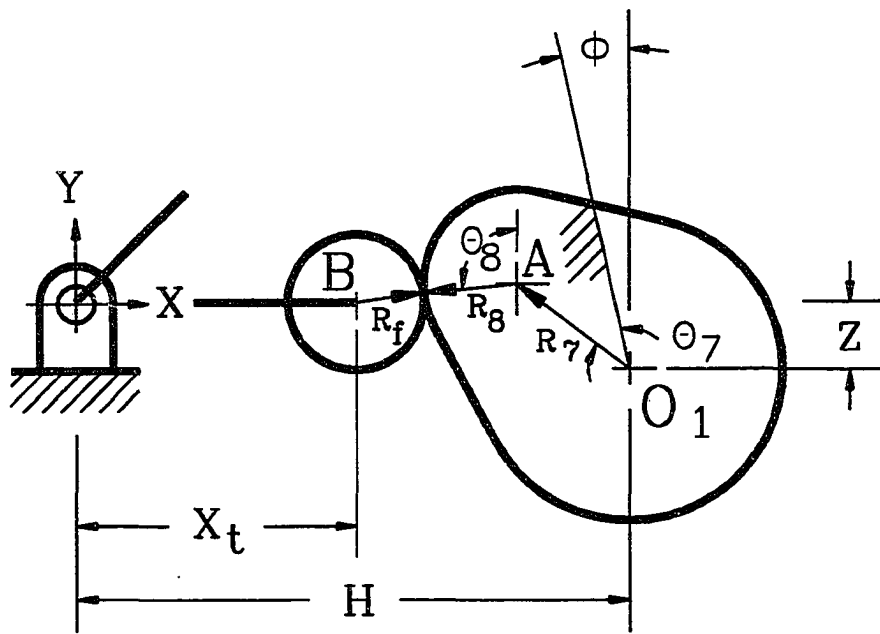


Figure 4: The cam and translating roller follower

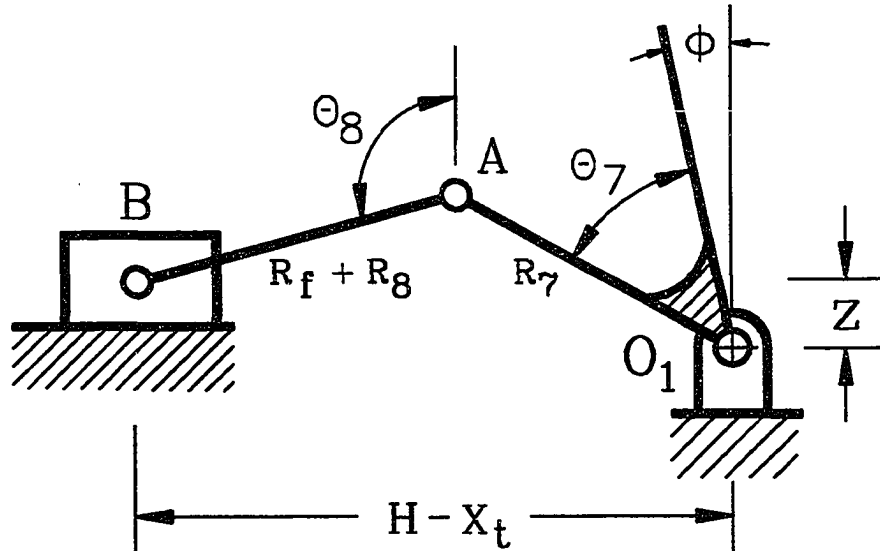


Figure 5: Equivalent linkage for the cam and roller follower

where

$$z = Z/R_5$$

and

$$y = (H - X_t)/R_5 = h - x_t \quad (26)$$

The first and second derivatives for the equivalent linkage can be found by differentiating the above equations. Notice that θ_7 is fixed while θ_8 is changing in the equivalent linkage.

$$\begin{aligned} -r_7 \sin(\theta_7 + \phi) - (r_8 + r_f) \sin \theta_8 \theta'_8 &= 0 \\ -r_7 \cos(\theta_7 + \phi) - (r_8 + r_f) \cos \theta_8 \theta'_8 + y' &= 0 \end{aligned} \quad (27)$$

$$\begin{aligned} -r_7 \cos(\theta_7 + \phi) - (r_8 + r_f) \cos \theta_8 \theta'^2_8 - (r_8 + r_f) \sin \theta_8 \theta''_8 &= 0 \\ r_7 \sin(\theta_7 + \phi) + (r_8 + r_f) \sin \theta_8 \theta'^2_8 - (r_8 + r_f) \cos \theta_8 \theta''_8 + y'' &= 0 \end{aligned} \quad (28)$$

where

$$y' = -x'_t = -x' - \delta x' \quad (29)$$

$$y'' = -x''_t = -x'' - \delta x'' \quad (30)$$

where x' is found by differentiating equations (8),

$$x' = \theta'_5 \sin(\theta_4 - \theta_5) / \cos \theta_4 \quad (31)$$

x'' is obtained in equation (23), and the $\delta x'$ and $\delta x''$ are obtained by differentiating the $\delta x'$ found in solving equation (20). Six unknowns, r_7 , θ_7 , r_8 , θ_8 , θ'_8 , and θ''_8 appear in the above three pairs of nonlinear equations. Due to their unique nature, a closed form solution for these six unknowns can be obtained. The five solutions are

$$\theta'_8 = [yy'' + y'(z - y')] / [y^2 + (z - y')^2] \quad (32)$$

$$r_7 = \{[\theta'_8 y^2 + (\theta'_8 z - \theta'_8)^2]/(\theta'_8 - 1)^2\}^{1/2} \quad (33)$$

$$\theta_7 = \tan^{-1} \{\theta'_8 y / (\theta'_8 z - y')\} - \phi \quad (34)$$

$$r_8 = \{[y^2 + (z - y')^2]/(\theta'_8 - 1)^2\}^{1/2} - r_f \quad (35)$$

$$\theta_8 = \tan^{-1} \{y / (y' - z)\} \quad (36)$$

where ϕ is the cam rotation angle. The synthesized cam profile should be checked for undercutting, i.e., a negative value for r_8 . The above sequence of steps must be repeated for various values of cam rotation angle, ϕ , starting with some initial choice and proceeding with a suitably chosen increment, so that the cam profile coordinates are spaced close enough for accurate manufacture. If an undesirable cam profile is generated, new values of parameters, for example, r_f , h , or z may be used.

Improved synthesis

The rigid body kinematics determined from the cam profile obtained by the initial synthesis provides a better approximation for the rigid body dependent variables θ_4 , and θ_5 . The method for solving the equations by iteration is explained in the following.

Equation (16) has no rigid body dependent coefficients or forcing terms. The θ_5 in equation (16) is really θ_{5t} , the desired value. Thus θ_5 calculated in the initial synthesis can be used as θ_{5t} for iterated synthesis. The θ_4 and θ_5 values in equation (18) are now determined from the initially synthesized cam profile through equations (8), the rigid body constraints, where x is replaced by the sum of the x and δx calculated in the initial synthesis,

$$\theta_5 = \cos^{-1} \left\{ [1 + (x - r_3)^2 - r_4^2] / [2(x - r_3)] \right\}$$

$$\theta_4 = \tan^{-1} \{ \sin \theta_5 / (\cos \theta_5 - x + r_3) \} \quad (37)$$

Unlike the initial synthesis, $\delta\theta_5$ is no longer zero and is equivalent to the difference between θ_{5t} and θ_5 ,

$$\delta\theta_5 = \theta_{5t} - \theta_5 \quad (38)$$

Equation (18) can now be solved for δr_4 with θ_{5t}'' replacing θ_5'' . Equation (19) is then replaced by

$$\delta r_3 = \delta x + \delta r_4 / \cos \theta_4 + \sin(\theta_5 - \theta_4) \delta\theta_5 / \cos \theta_4 \quad (39)$$

Substituting δr_3 , $\delta r'_3$, and $\delta r''_3$ found by differentiating equation (39) into equation (15), one obtains the following equation for the new δx

$$\begin{aligned} \delta x' + [S_3/(2\zeta\Omega D_3)]\delta x &= [1/(2\zeta\Omega D_3)] \left\{ m_c\Omega^2 x'' - (m_c\Omega^2/\cos \theta_4) \delta r_4'' \right. \\ &\quad + (-2\zeta\Omega D_4 \cos \theta_4 - 2m_c\Omega^2 \theta_4' \sin \theta_4 / \cos \theta_4^2 - 2\zeta\Omega D_3 / \cos \theta_4) \delta r_4' \\ &\quad + [-S_4 \cos \theta_4 - m_c\Omega^2 (2\theta_4'^2 \sin^2 \theta_4 / \cos^3 \theta_4 + \theta_4'^2 / \cos \theta_4 \\ &\quad + \theta_4'' \sin \theta_4 / \cos^2 \theta_4) - 2\zeta\Omega D_3 \theta_4' \sin \theta_4 / \cos^2 \theta_4 - S_3 / \cos \theta_4] \delta r_4 \\ &\quad - 2\zeta\Omega D_3 [\sin(\theta_5 - \theta_4) \delta\theta_5' / \cos \theta_4 + \cos(\theta_5 - \theta_4) (\theta_5' - \theta_4') \delta\theta_5 / \cos \theta_4 \\ &\quad + \sin(\theta_5 - \theta_4) \delta\theta_5 \sin \theta_4 \theta_4' / \cos^2 \theta_4] - S_3 \sin(\theta_5 - \theta_4) \delta\theta_5 / \cos \theta_4 \\ &\quad + m_c\Omega^2 [-\cos(\theta_5 - \theta_4) (\theta_5' - \theta_4') \delta\theta_5' / \cos \theta_4 - \sin(\theta_5 - \theta_4) \sin \theta_4 \theta_4' \delta\theta_5' / \cos^2 \theta_4 \\ &\quad - \sin(\theta_5 - \theta_4) \delta\theta_5'' / \cos \theta_4 + \sin(\theta_5 - \theta_4) (\theta_5' - \theta_4')^2 \delta\theta_5 / \cos \theta_4 \\ &\quad - 2\cos(\theta_5 - \theta_4) (\theta_5' - \theta_4') \sin \theta_4 \theta_4' \delta\theta_5 / \cos^2 \theta_4 - \cos(\theta_5 - \theta_4) (\theta_5'' - \theta_4'') \delta\theta_5 / \cos \theta_4 \\ &\quad - \cos(\theta_5 - \theta_4) (\theta_5' - \theta_4') \delta\theta_5' / \cos \theta_4 - 2\sin(\theta_5 - \theta_4) \sin^2 \theta_4 \theta_4'^2 \delta\theta_5 / \cos^3 \theta_4 \\ &\quad \left. - \sin(\theta_5 - \theta_4) \delta\theta_5' \sin \theta_4 \theta_4' / \cos^2 \theta_4 - \sin(\theta_5 - \theta_4) \delta\theta_5 \theta_4'^2 / \cos \theta_4 \right\} \end{aligned}$$

$$-\sin(\theta_5 - \theta_4)\delta\theta_5 \sin \theta_4 \theta_4''/\cos^2 \theta_4] \} \quad (40)$$

The θ'_4 , θ'_5 , θ''_4 , and θ''_5 in equation (40) can be determined by differentiating equations (8), the rigid body constraints,

$$\theta'_4 = \cos \theta_5 x' / [r_4 \sin(\theta_4 - \theta_5)] \quad (41)$$

$$\theta'_5 = \cos \theta_4 x' / \sin(\theta_4 - \theta_5) \quad (42)$$

$$\theta''_4 = [\cos \theta_5 x'' - r_4 \theta_4'^2 \cos(\theta_4 - \theta_5) + \theta_5'^2] / [r_4 \sin(\theta_4 - \theta_5)] \quad (43)$$

$$\theta''_5 = [\cos \theta_4 x'' - r_4 \theta_4'^2 + \theta_5'^2 \cos(\theta_4 - \theta_5)] / \sin(\theta_4 - \theta_5) \quad (44)$$

where x' is the sum of the x' and $\delta x'$, and x'' is the sum of the x'' and $\delta x''$ obtained in the initial synthesis. The $\delta\theta'_5$ and $\delta\theta''_5$ in equation (40) can be determined by differentiating the already calculated $\delta\theta_5$ in equation (38), and the steady state δx can be found by Hsu's method.

For the second iteration, equations (25), (27), and (28) still apply for the synthesis of the cam profile and the x_t in equation (26) becomes the sum of the new x and δx obtained in this second iteration. The cam profile obtained in the second iteration provides the rigid body positions for the third iteration. The above iterative procedure is repeated until the response of the output motion which will be analyzed in the following section is acceptable to the designer or numerical round off errors appear and prevent further refinement as shown in the EXAMPLE. Fig. 6 shows the overall synthesis procedure.

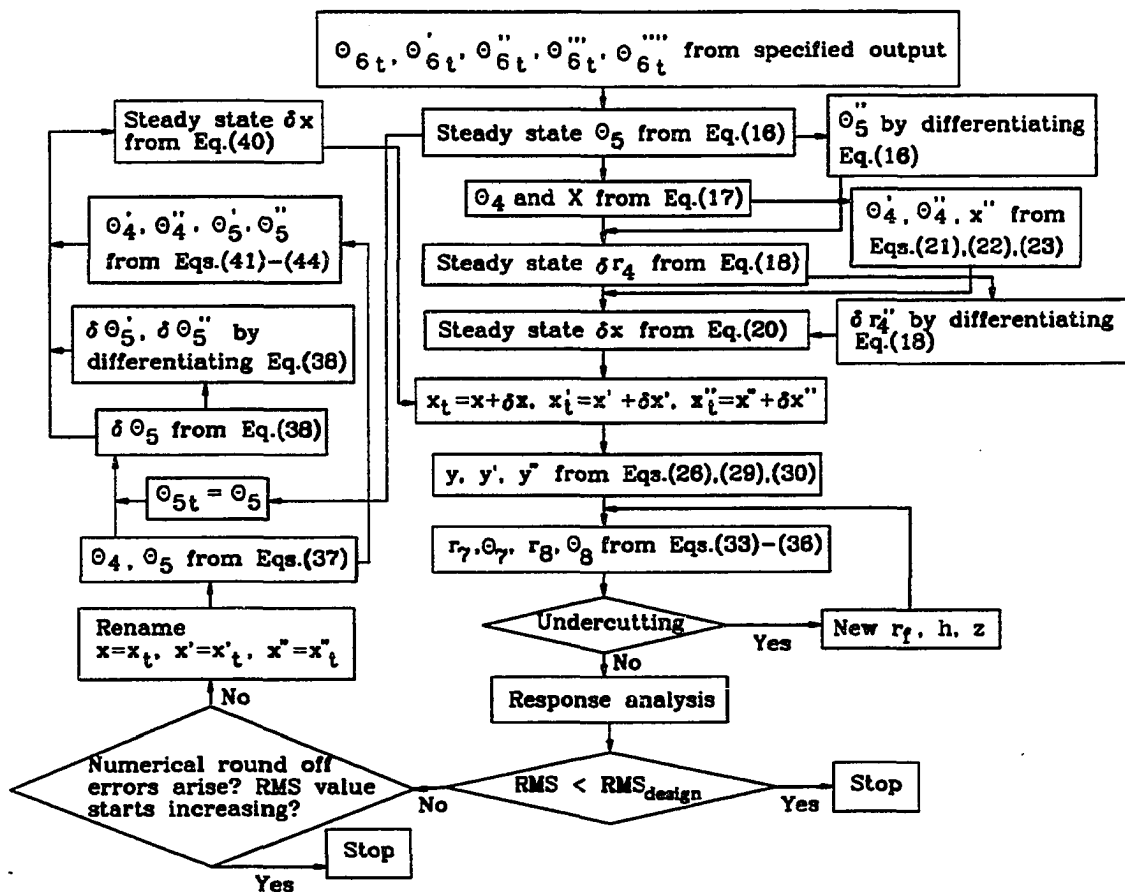


Figure 6: Procedure for cam synthesis

ANALYSIS

After the cam has been synthesized, the profile coordinates are then known as functions of the cam rotation angle, ϕ . The same governing equations used for synthesis still apply for the motion analysis of the linkage, except that δx is set equal to zero since the assumed contact between the follower and the inflexible cam enforced by the follower return spring results in an undeformed distance x . For the rigid cam and its follower, r_7 , θ_7 , r_8 , θ_8 , are now known as functions of the cam rotation angle, ϕ . The x , x' , and x'' replace the x_t , x'_t , and x''_t in equations (26), (29), and (30). Five unknowns y , y' , y'' , θ'_8 , and θ''_8 appear in the governing equations (25), (27), and (28). The x is obtained by considering equations (25) and (26),

$$x = -r_7 \sin(\theta_7 + \phi) - (r_8 + r_f) \sin \theta_8 + h \quad (45)$$

The x' is obtained by considering equations (27) and (29),

$$x' = -r_7 \cos(\theta_7 + \phi) - (r_8 + r_f) \cos \theta_8 \theta'_8 \quad (46)$$

where

$$\theta'_8 = -r_7 \sin(\theta_7 + \phi) / [(r_8 + r_f) \sin \theta_8] \quad (47)$$

The x'' is obtained by considering equations (28) and (30),

$$x'' = r_7 \sin(\theta_7 + \phi) + (r_8 + r_f) \sin \theta_8 \theta'^2_8 - (r_8 + r_f) \cos \theta_8 \theta''_8 \quad (48)$$

where

$$\theta''_8 = \left\{ -r_7 \cos(\theta_7 + \phi) - (r_8 + r_f) \cos \theta_8 \theta'^2_8 \right\} / [(r_8 + r_f) \sin \theta_8] \quad (49)$$

The x , x' , and x'' obtained in equations (45), (46), and (48) are the input for the analysis of the follower linkage. In the seven governing equations for links 3, 4,

5 and 6, two rigid body variables (θ_4 and θ_5) and five elastic deflection variables (θ_{6t} , δr_3 , δr_4 , $\delta\theta_4$, and $\delta\theta_5$) need to be found. Angles θ_4 and θ_5 can be determined from equations (37). The steady state values for the remaining five elastic variables are addressed next. Through the two elastic constraints given by equations (9), δr_4 can be expressed in terms of δr_3 and $\delta\theta_5$,

$$\delta r_4 = \sin(\theta_4 - \theta_5)\delta\theta_5 + \cos\theta_4\delta r_3 \quad (50)$$

The $\delta r'_4$ can be found by differentiating equation (50),

$$\delta r'_4 = \sin(\theta_4 - \theta_5)\delta\theta'_5 + \cos\theta_4\delta r'_3 + (\theta'_4 - \theta'_5)\cos(\theta_4 - \theta_5)\delta\theta_5 \quad (51)$$

Substitution of equations (50) and (51) into the three dynamic equations (equations (7), (14), and (15)) gives

$$\begin{aligned} & \left\{ \begin{array}{l} \theta''_{6t} \\ \delta\theta''_5 \\ \delta r''_3 \end{array} \right\} + \begin{bmatrix} 2\zeta/\Omega & -2\zeta/\Omega & 0 \\ -2\zeta/m_d\Omega & c_{2,2} & c_{2,3} \\ 0 & c_{3,2} & c_{3,3} \end{bmatrix} \left\{ \begin{array}{l} \theta'_{6t} \\ \delta\theta'_5 \\ \delta r'_3 \end{array} \right\} \\ & + \begin{bmatrix} 1/\Omega^2 & -1/\Omega^2 & 0 \\ -1/(m_d\Omega^2) & k_{2,2} & k_{2,3} \\ 0 & k_{3,2} & k_{3,3} \end{bmatrix} \left\{ \begin{array}{l} \theta_{6t} \\ \delta\theta_5 \\ \delta r_3 \end{array} \right\} \\ & = \left\{ \begin{array}{l} 2\zeta\theta'_5/\Omega + \theta_5/\Omega^2 \\ -\theta''_5 - 2\zeta\theta'_5/(m_d\Omega) - \theta_5/(m_d\Omega^2) \\ x'' \end{array} \right\} \end{aligned} \quad (52)$$

where

$$c_{2,2} = 2\zeta[1 + D_4 \sin^2(\theta_4 - \theta_5)]/(m_d\Omega)$$

$$\begin{aligned}
c_{2,3} &= 2\zeta D_4 \cos \theta_4 \sin(\theta_4 - \theta_5) / (m_d \Omega) \\
c_{3,2} &= 2\zeta D_4 \cos \theta_4 \sin(\theta_4 - \theta_5) / (m_c \Omega) \\
c_{3,3} &= 2\zeta [D_3 + D_4 \cos^2 \theta_4] / (m_c \Omega) \\
k_{2,2} &= \left\{ 1 + S_4 \sin^2(\theta_4 - \theta_5) - \zeta \Omega D_4 (\theta'_5 - \theta'_4) \sin[2(\theta_4 - \theta_5)] \right\} / (m_d \Omega^2) \\
k_{2,3} &= S_4 \cos \theta_4 \sin(\theta_4 - \theta_5) / (m_d \Omega^2) \\
k_{3,2} &= \left\{ S_4 \cos \theta_4 \sin(\theta_4 - \theta_5) - 2\zeta \Omega D_4 (\theta'_5 - \theta'_4) \cos \theta_4 \cos(\theta_4 - \theta_5) \right\} / (m_c \Omega^2) \\
k_{3,3} &= \left\{ S_3 + S_4 \cos^2 \theta_4 \right\} / (m_c \Omega^2)
\end{aligned}$$

The θ'_4 , θ'_5 , and θ''_5 in the above equations can be obtained from equations (41), (42), and (44).

Equation (52) is a system of inhomogeneous, linear, ordinary differential equations with periodic coefficients and forcing terms. Hsu's method can be applied after rewriting it as a system of six first order differential equations (see Appendix A).

Fig. 7 shows the analysis procedure.

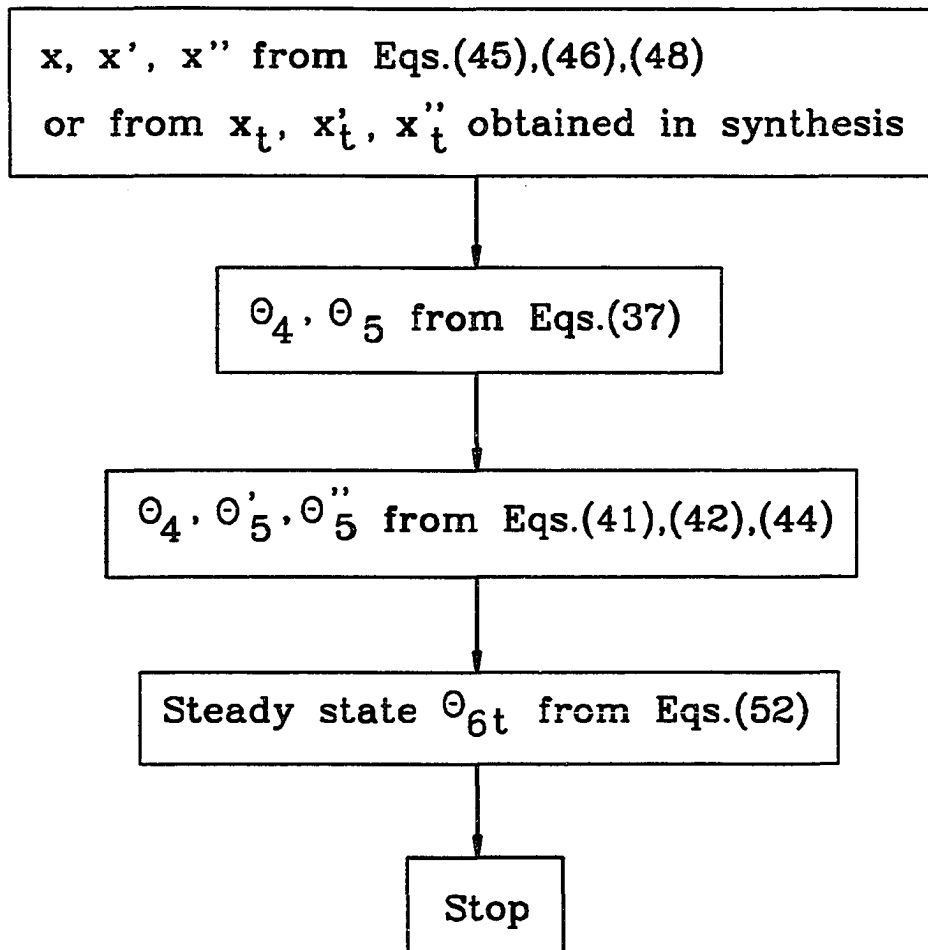


Figure 7: Procedure for cam analysis

EXAMPLE

Methods of the previous sections were used to synthesize cam profiles and then to analyze the motions of the output links at various operating speeds and damping ratios. For the cases considered, $r_3 = 1.0$, $r_4 = 2.0$, $S_3 = 1.0$, $S_4 = 1.0$, $D_3 = 1.0$, $D_4 = 1.0$, $h = 5.5$, $z = 0.0$, $r_f = 0.25$, $m_c = 0.2$, and $m_d = 0.2$.

The desired motion for the output link is shown in Fig. 8. Dwells at the beginning, middle, and end of each cycle lasted for 30, 60, and 30 degrees, respectively. The rise occurred during the 30 degrees of cam rotation. Since the continuity of the fifth derivative of θ_{6t} is required, a 6-7-8-9-10-11 polynomial was used to define the rise and return of the output motions. A few synthesized cam profiles are shown in Fig. 9. Very little difference was observed between the profiles for the design speed ratio of 0.1 with different damping ratios of 0.05 and 0.20.

The Root Mean Squared (RMS) error for the calculated steady state θ_{6t} with reference to the desired θ_{6t} , based upon one degree increments of cam rotation over a full cycle of 360 degrees, was used to investigate the responses for different operating speeds. The objective of synthesis is to obtain the lowest possible RMS value. Fig. 10 shows portions of the cycle possessing the largest differences between the desired output motion and the calculated steady states for iterations 1 to 4, at the design speed ratio of 0.1 and damping ratio of 0.15. The differences for the rigid body positions, $\theta_{6,rigid}$, for different iterations are so small that they coincide in Fig. 10. The RMS values for the first four iterations declined, 0.00262878, 0.00052161, 0.00051628, and 0.00051173 radians, but they increased to 0.00123 and 0.01312 radians for iterations 5 and 6. Fig. 11 shows the corresponding δx calculated in each iteration. As expected, the δx generated in the first iteration was much larger than those generated in the

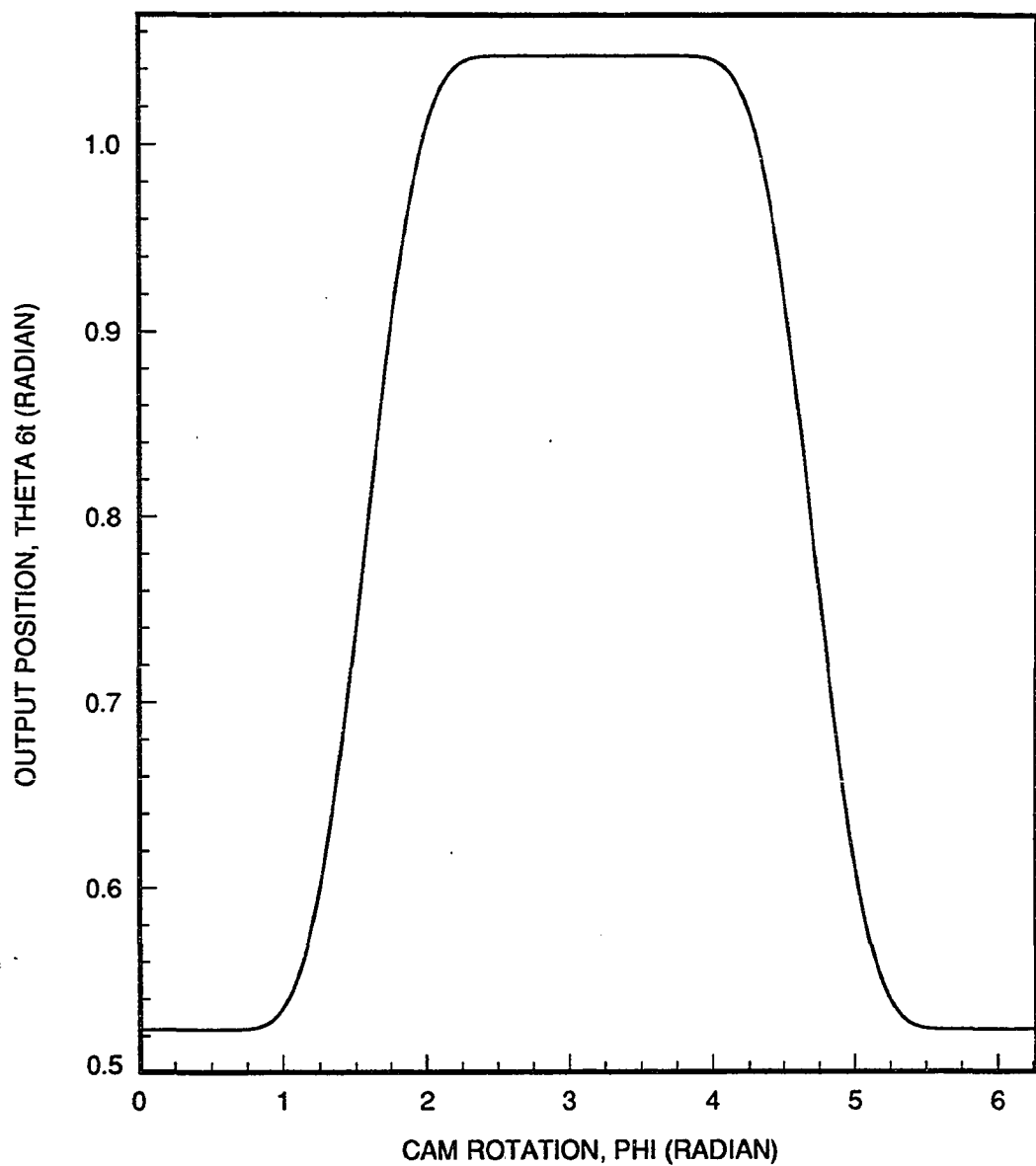


Figure 8: Desired motion for the output link

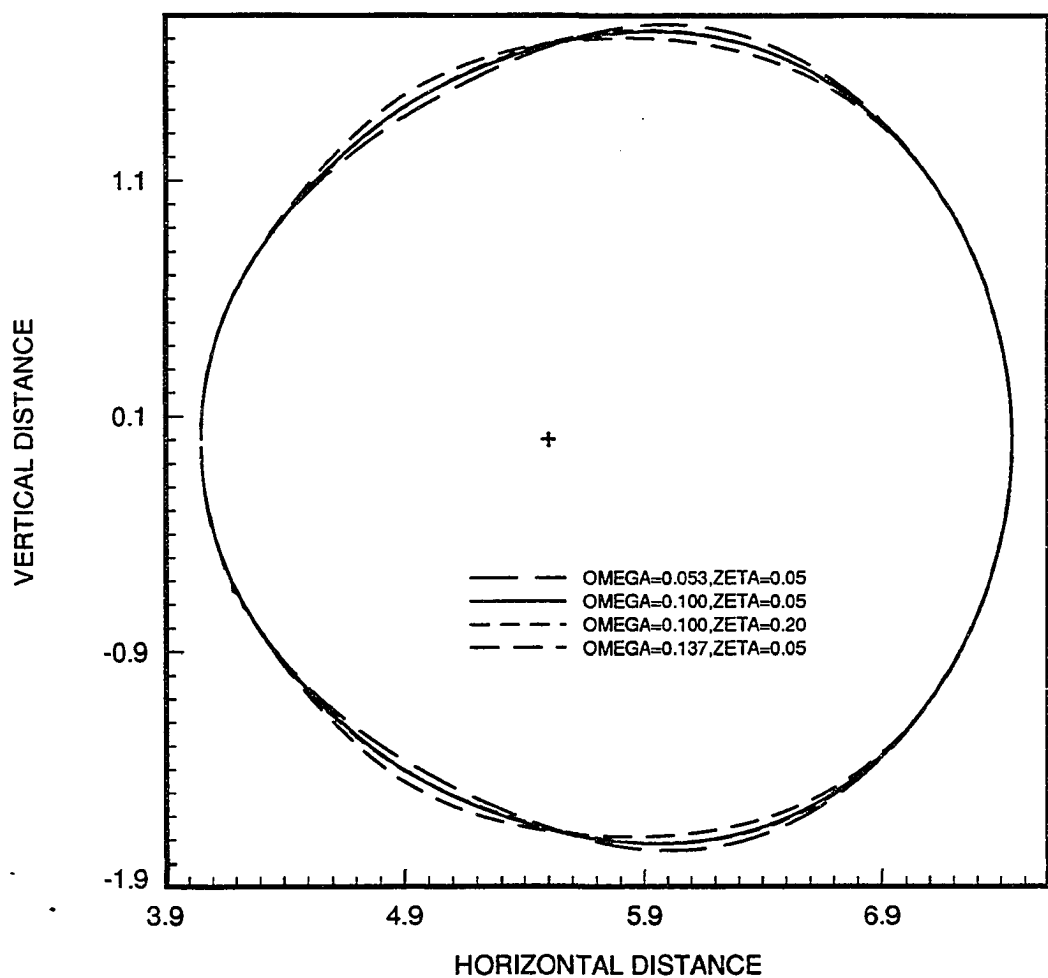
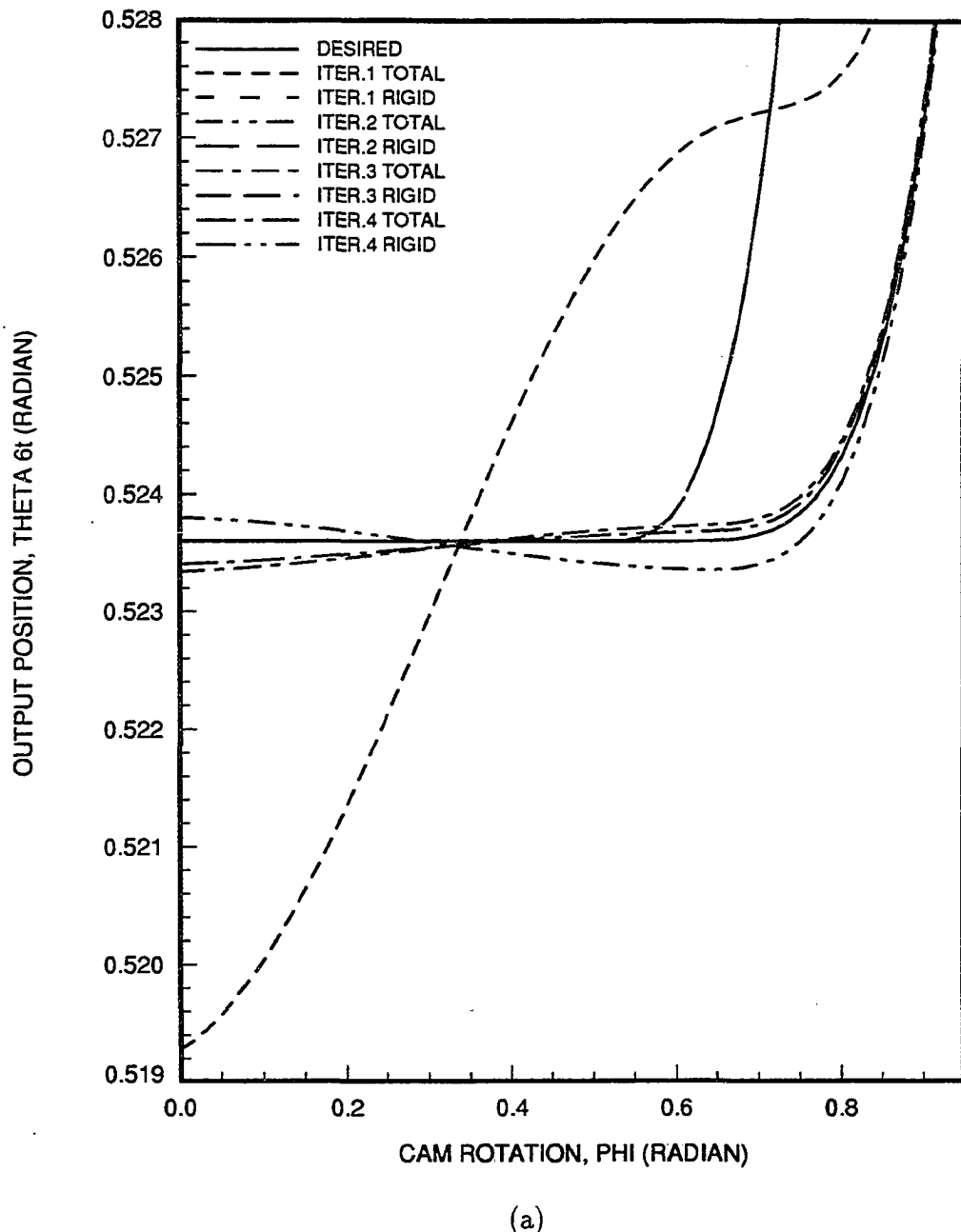


Figure 9: Synthesized cam profiles for different design conditions

following iterations. The values of δx were decreasing as the iteration number was increasing. At iterations 5 and 6, the δx became much smaller compared to the other parameters. The δx generated at iteration 5 were very small (the value with the largest magnitude was $-2.79599509 \times 10^{-6}$) compared to the rigid body displacement x used at iteration 5. Unwanted numerical truncation might occur when δx was added to the rigid body displacement x to form the x_t used for analysis and the following iterated synthesis. The information carried by the much smaller δx might thus be distorted and the increase in RMS value for iteration 5 and oscillations for the δx curve for iteration 6 occurred.

Fig. 12 shows the RMS errors for different iterations for speed ratios of 0.05 to 0.2 with damping ratios of 0.05 and 0.15. Each data point represents the response of the cam system designed and simulated at the same speed ratio. By comparing the RMS values for different iterations at all speed ratios, we found that iteration in synthesis reduced the RMS error. The RMS peaks existing in the initial synthesis either decreased dramatically or disappeared in the following syntheses. However, speeds possessing peaks are not good design speeds as will be discussed in part 2 of this paper. In Fig. 12(b) for the case with damping ratio of 0.05, the RMS value for iteration 4 started to increase at a speed ratio about 0.16. This may be explained by the following. In equation (52) the term x'' comprises the third element of the forcing vector. Ω^2 and Ω appear in the denominators of four other terms of the forcing vector. As the speed ratio increased, the relative influence of the term x'' (containing no Ω) increased. As explained in the last paragraph, after a few iterations the x used for analysis input may not contain all the information carried by the δx calculated in the synthesis due to unwanted truncation. As a result the term x'' may



(a)

Figure 10: Desired and calculated steady state θ_{6t} (labeled TOTAL) and $\theta_{6,rigid}$ for iterations 1 to 4 for the cam system designed at speed ratio of 0.1 and damping ratio of 0.15 at first dwell (a), middle dwell (b), and end dwell (c) of the cycle

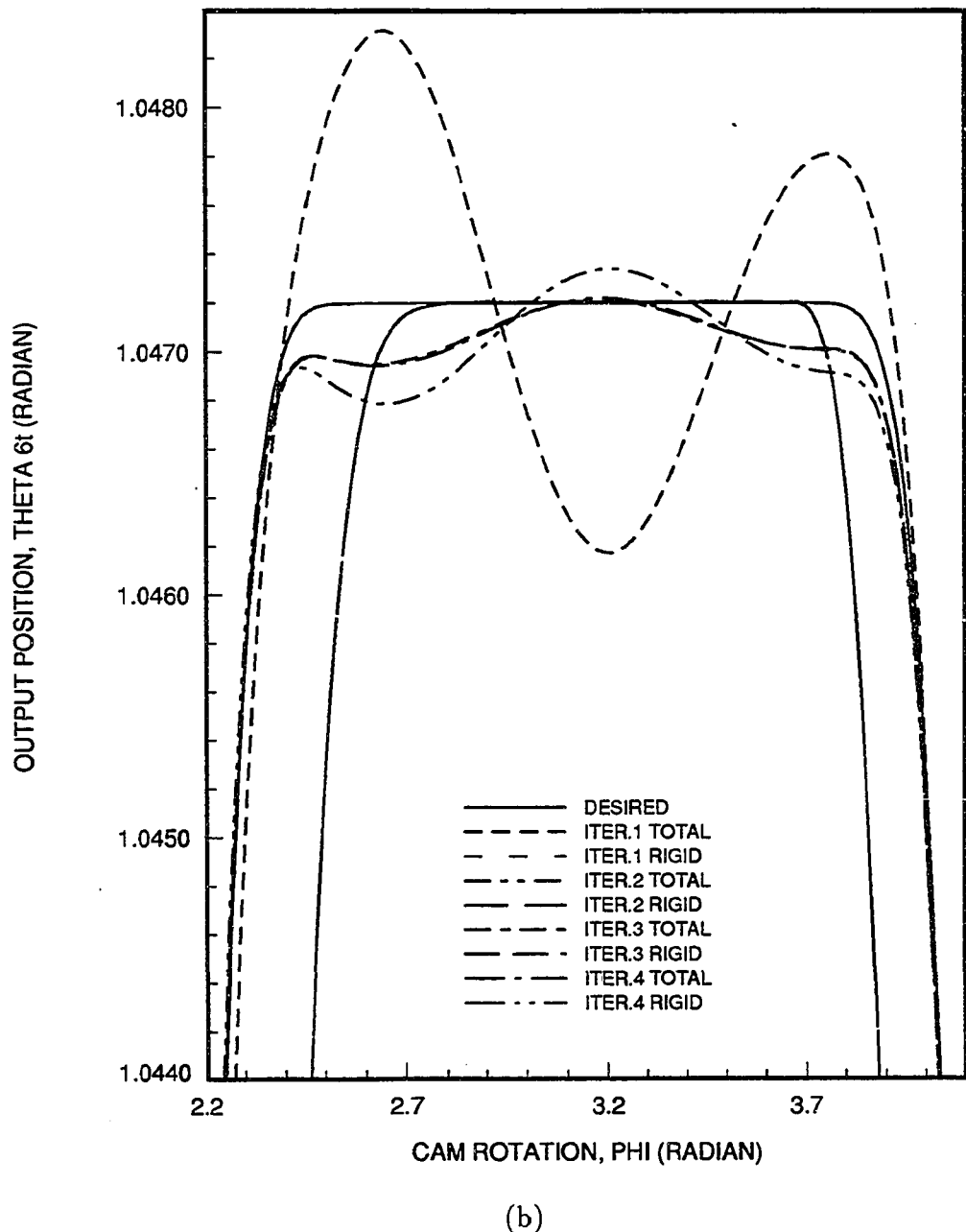
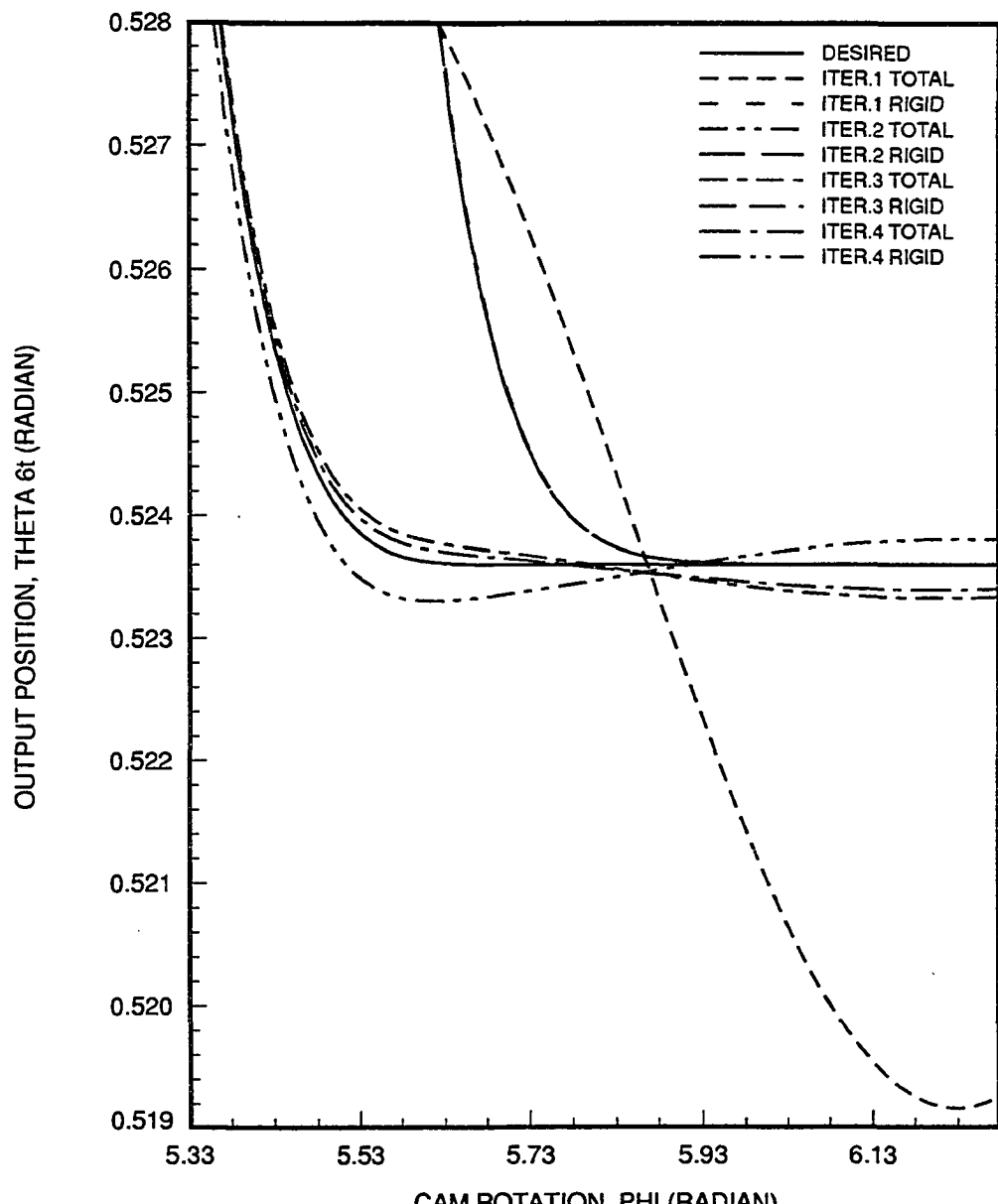


Figure 10 (Continued)



(c)

Figure 10 (Continued)

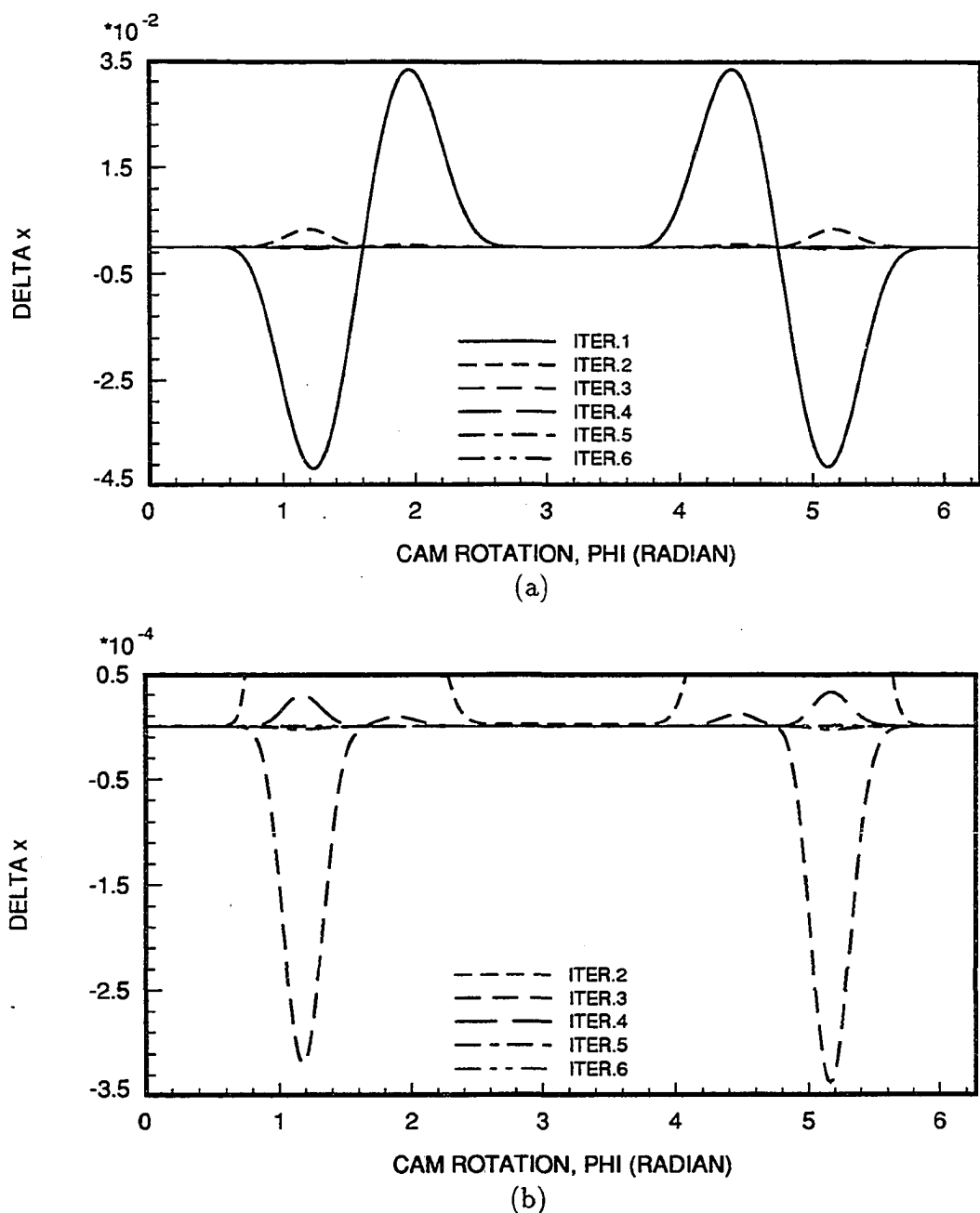
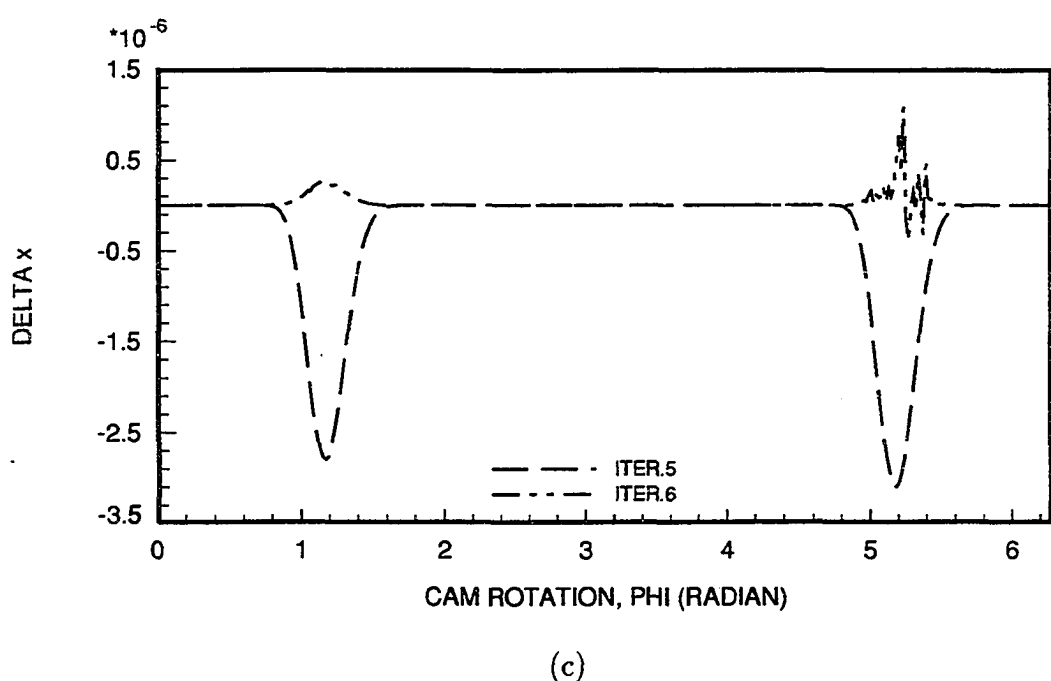


Figure 11: δx for iterations 1 to 6 (a), 2 to 6 (b), and 5 to 6 (c) for the cam system designed at speed ratio of 0.1 and damping ratio of 0.15



(c)

Figure 11 (Continued)

possess inaccurate information at higher speeds and higher iteration numbers. This undesired phenomenon was also observed in Fig. 12(d) for the case with damping ratio of 0.15. But in Fig. 12(d) the increase in RMS value was much less. This may be explained by the presence of the damping ratio, ζ , in the numerators of two terms of the forcing vector in equation (52). Increase in damping increased the influence of these terms and the influence of the term x'' decreased. The round off errors which may be caused by x'' were therefore reduced.

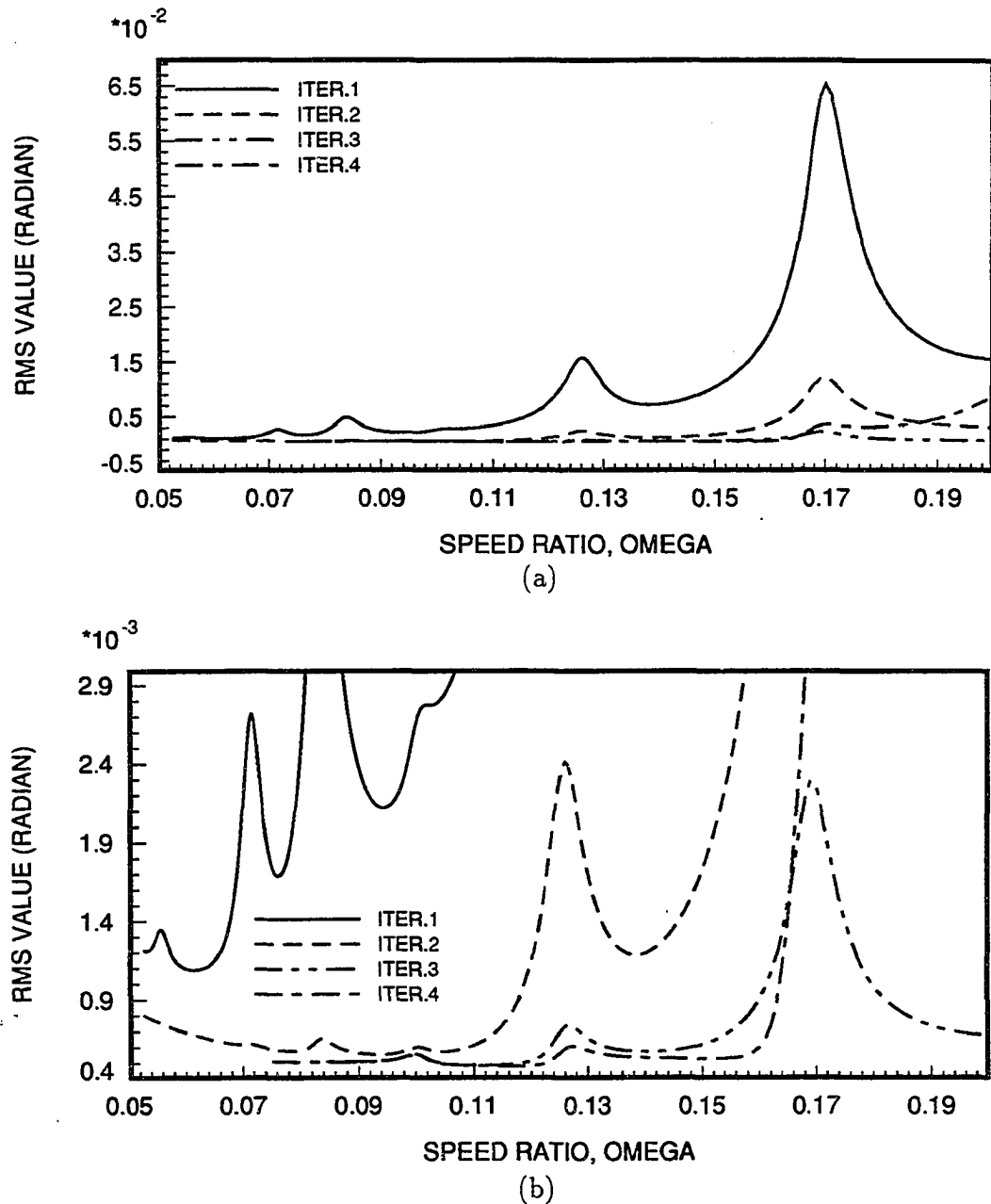


Figure 12: RMS values for different iterations for cam systems designed and simulated at the same speed ratios with damping ratios of 0.05 (a and b) and 0.15 (c and d)

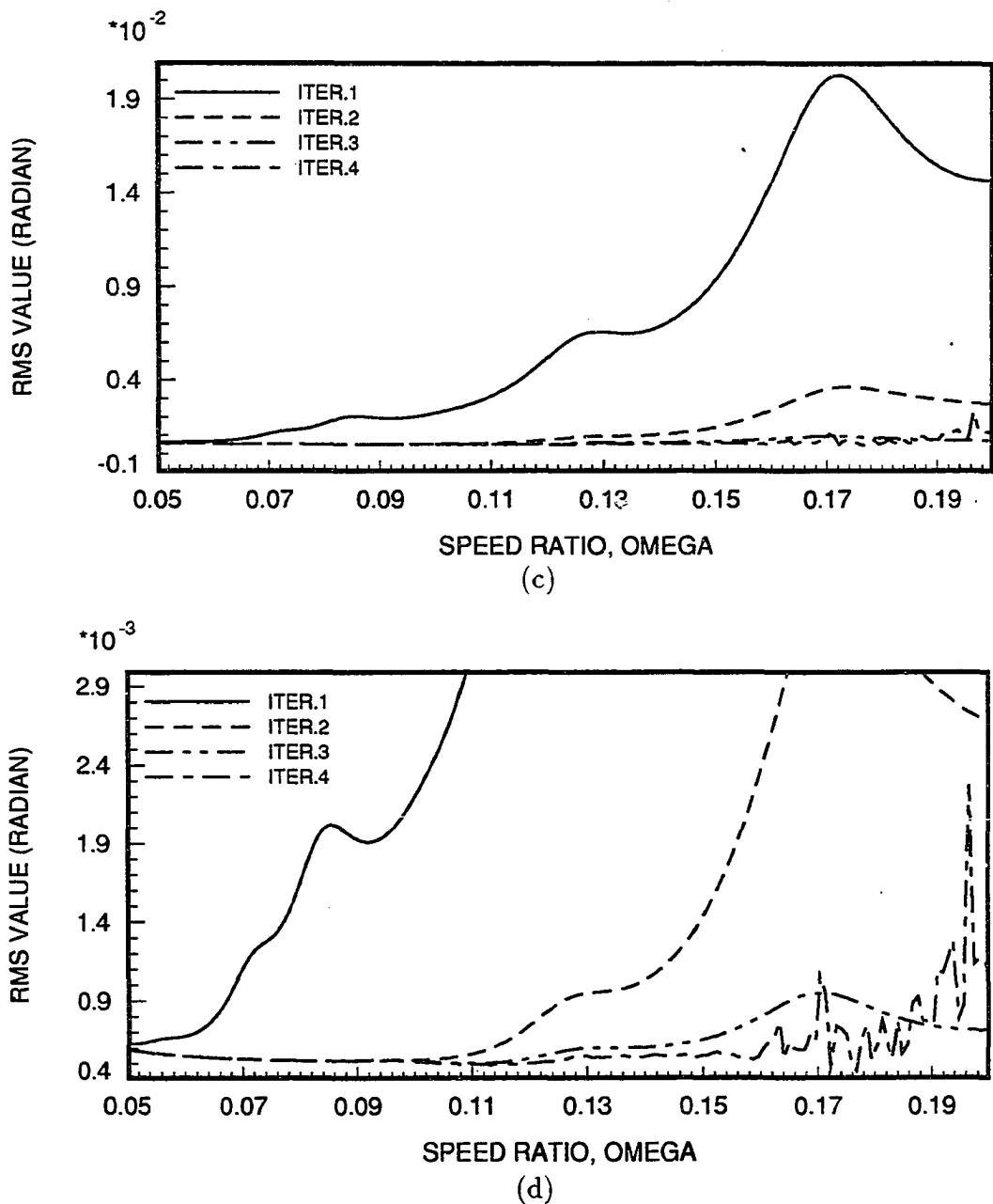


Figure 12 (Continued)

CONCLUSIONS

Synthesis and steady state analysis techniques have been presented for an elastic cam-follower mechanism with concentrated masses. The changing geometry of the linkage during operation resulted in inhomogeneous, periodic, linear, ordinary differential equations which were solved numerically by Hsu's method. Linearization relative to small elastic deformations uncoupled the rigid body and elastic components of motion. The differences in the specified parameters for synthesis and analysis lead to different approaches for solving these equations. One common strategy for both synthesis and analysis is to first solve the rigid body constraint equations since the rigid body motion related variables, which appear in the coefficients and forcing terms of the elastic deflection related equations, will then be known.

Iteration in synthesis lowered the RMS values and produced satisfactory output motions at the design speeds for all speeds simulated. The differences in cam profiles between iterations were very small but the differences in the corresponding RMS values might be significant. This iteration procedure in synthesis may thus serve as a useful tool for design engineers. Part 2 of this paper discusses the selection of design speed based on characteristic multipliers. The double precision data type available on a VAX/11-785 was used throughout this study. The degree to which the lowest RMS values obtained by iteration for different design conditions were limited by round off errors or other numerical problems needs to be investigated further.

REFERENCES

- Bogoliubov, N. N., and Mitropolski, Y. A. 1961. *Asymptotic Methods in the Theory of Nonlinear Oscillations*. Gordon and Breach, New York.
- Bolotin, V. V. 1964. *The Dynamic Stability of Elastic Systems*. English translation. Holden-Day, San Francisco.
- Bussell, W., and Hubbart, T. 1989. "Four Bar Kinematic Analysis As Applied to Slider-Crank and Cams". *First National Applied Mechanisms & Robotics Conference - 1989*, Cincinnati, 89AMR-4B-7.
- Capellen, W. M. 1967. "Torsional Vibrations in the Shafts of Linkage Mechanisms". *Journal of Engineering for Industry*, 89:126-136.
- Capellen, W. M., and Krumm, H. 1971. "Oscillations of an Elastically Suspended Coupler of a Four-Bar-Linkage". *Journal of Mechanisms*, 6:351-365.
- Carnegie, W. D., and Pasricha, M. S. 1974. "Effect of Forcing Terms and General Characteristics of Torsional Vibrations of Marine Engine Systems with Variable Inertia". *Journal of Ship Research*, 18:131-138.
- Chen, F. Y. 1973. "Analysis and Design of Cam-Driven Mechanisms with Nonlinearities". *Journal of Engineering for Industry*, 95:685-694.
- Cleghorn, W. L., Fenton, R. G., and Tabarrok, B. 1984. "Steady-state Vibrational Response of High-speed Flexible Mechanisms". *Mechanism and Machine Theory*, 19, No.4/5:417-423.
- Flugrad, D. R., Jr. 1986. "Cam Synthesis and Analysis for an Elastic Follower Linkage". *Journal of Mechanisms, Transmissions, and Automation in Design*, 108:367-372.
- Flugrad, D. R., Jr., and Liu, H. J. 1988. "Stability analysis by a perturbation method", *Trends and Developments in Mechanisms, Machines, and Robotics - 1988*. ASME, 2:397-405.
- Gao, X., King, Z., and Zhang, Q. 1988. "A Closed-form Linear Multi-step Algorithm for the Steady-state Response of High-speed Flexible Mechanisms". *Mechanism and Machine Theory*, 23, No.5:361-366.

- Gupta, K. C., and Wiederrick, J. L. 1983. "Development of Cam Profiles Using the Convolution Operator". *Journal of Mechanisms, Transmissions, and Automation in Design*, 105:654-657.
- Hall, A. S., Jr. 1966. *Kinematics and linkage design*. Balt Publishers, West Lafayette, Indiana.
- Hsu, C. S. 1963. "On the Parametric Excitation of a Dynamic System Having Multiple Degrees of Freedom". *Journal of Applied Mechanics*, 85, Series E:367-372.
- Hsu, C. S. 1965. "Further Results on the Parametric Excitation of a Dynamic System". *Journal of Applied Mechanics*, 87:373-377.
- Hsu, C. S. 1974. "On Approximating a General Linear Periodic System". *Journal of Mathematical Analysis and Applications*, 45, No.1:234-251.
- Hsu, C. S., and Cheng, W. H. 1973. "Applications of the Theory of Impulsive Parametric Excitation and New Treatments of General Parametric Excitation Problems". *Journal of Applied Mechanics*, 97:78-86.
- Hsu, C. S., and Cheng, W. H. 1974. "Steady State Response of a Dynamical System under Combined Parametric and Forcing Excitations". *Journal of Applied Mechanics*, 98:371-378.
- Jensen, P. W. 1987. *Cam design and manufacture*. 2nd ed. M. Dekker, New York.
- Johnson, R. C. 1959. "Dynamic Analysis and Design of Relatively Flexible Cam Mechanisms Having More Than One Degree of Freedom". *Journal of Engineering for Industry*, 81:323-331.
- Midha, A., and Turcic, D. A. 1980. "On the Periodic Response of Cam Mechanism with Flexible Follower and Camshaft". *Journal of Dynamic Systems, Measurement, and Control*, 102:255-264.
- Midha, A., Erdman, A. G., and Frohrib, D. A. 1979. "A Closed-Form Numerical Algorithm for the Periodic Response of High-Speed Elastic Linkages". *Journal of Mechanical Design*, 101:154-162.
- Müller, P. C., and Schiehlen, W. O. 1985. *Linear Vibrations*. Martinus Nijhoff Publishers, Dordrecht, Holland.

- Nath, P. K., and Ghosh, A. 1980. "Steady State Response of Mechanisms with Elastic Links by Finite Element Methods". *Mechanism and Machine Theory*, 15:199–211.
- Pipes, L. A. 1953. "Matrix Solution of Equations of the Mathieu-Hill Type". *Journal of Applied Physics*, 24:902–910.
- Richards, J. A. 1983. *Analysis of Periodically Time-Varying Systems*. Springer-Verlag, New York.
- Tsay, D. M., and Huey, C. O., Jr. 1989. "Synthesis and Analysis of Cam-Follower Systems with Two Degrees of Freedom". *Advances in Design Automation - 1989*. ASME, 3:281–288.
- Turcic, D. A., and Midha, A. 1984. "Dynamic Analysis of Elastic Mechanism Systems. Part I: Applications". *Journal of Dynamic Systems, Measurements, and Control*, 106:249–254.
- Wiederrick, J. L., and Roth, B. 1975. "Dynamic Synthesis of Cams Using Finite Trigonometric Series". *Journal of Engineering for Industry*, 97:603–618.
- Zodaks, R. I., and Midha, A. 1987a. "Parametric Stability of a Two-Degree-of-Freedom Machine System: Part II – Stability Analysis". *Journal of Mechanisms, Transmissions, and Automation in Design*, 109:216–223.
- Zodaks, R. I., and Midha, A. 1987b. "A Method for Calculating the Steady-State Dynamic Response of Rigid-Body Machine Systems". *Journal of Mechanisms, Transmissions, and Automation in Design*, 109:435–442.

PART II.

**SYNTHESIS AND STEADY STATE ANALYSIS OF HIGH-SPEED
ELASTIC CAM-FOLLOWER LINKAGES WITH CONCENTRATED
MASSES, PART 2: STEADY STATE ANALYSIS**

ABSTRACT

The responses for different design and simulation conditions, including various speed and damping ratios, are investigated for the elastic cam-follower system discussed in Part 1. The location of a single dominant pair of characteristic multipliers of the inhomogeneous periodic linear system is found to have significant influence on the steady state response.

INTRODUCTION

In Part 1 of this paper, synthesis and analysis techniques were presented for an elastic cam-follower mechanism with concentrated masses. The responses for the synthesized mechanisms were satisfactory when simulated at the design conditions. The changing geometry of the rigid body motion, however, results in inhomogeneous, periodic, linear, ordinary differential equations, which give rise to interesting results when the cam follower system is run under conditions other than those used for design.

The existence of the periodic steady state solution is assured if the system is asymptotically stable. As for any linear system, the stability is determined by the homogeneous parts of the equations and can best be judged by Floquet theory in conjunction with a consideration of the magnitudes of the *characteristic multipliers*. These multipliers are the eigenvalues of the discrete transition matrix, $\Phi(T, 0)$, which is the transition matrix for the whole period T . Floquet theory gives the relationship between successive discrete transition matrices for linear periodic systems. The system is asymptotically stable if and only if magnitudes of all the characteristic multipliers are strictly less than one. For a detailed discussion of stability for linear periodic systems, see Müller and Schiehlen (1985) and Reinhard (1986).

Besides stability, the characteristic multipliers are found to have other important effects on steady state responses of the cam systems studied here. Influence of damping on vibration and the effects of the difference in damping ratios used for synthesis and analysis are investigated. Good design speeds may be obtained if the locus of the characteristic multipliers is available. All investigations are based upon the steady states calculated numerically by Hsu's method, as discussed in Part 1.

Richards (1983) explained in detail the concept of a mode as introduced by Keenan (1962). The homogeneous response of a linear periodic system can be written as

$$X(t) = \sum_{j=1}^n \exp(\mu_j t) \Xi(t) \quad (1)$$

where n is the order of the equation, $\Xi(t)$ are bounded and periodic with the same period as the periodically varying parameters. and μ_j are the *characteristic exponents*. Equation (2) shows the relation between the characteristic multipliers and the characteristic exponents:

$$\lambda_j = \exp(\mu_j T) \quad (2)$$

where the characteristic multipliers, λ_j , are the eigenvalues of $\Phi(T, 0)$. When a characteristic multiplier is a positive real number, the corresponding basis solution given in equation (1) is called a *P* type. From equation (2) the characteristic exponent for a *P* type solution is seen to be of the form

$$\mu_j = \alpha_j + \imath(2k\pi/T) \quad (3)$$

where $\imath = \sqrt{-1}$ and k is an integer. The α_j are related to the damping of the system. For an undamped system, all α_j 's are zero. For *C* (complex) and *N* (negative) type solutions, the characteristic exponents are of the forms

$$\mu_j = \alpha_j + \imath\beta_j \quad (4)$$

$$\mu_j = \alpha_j + \imath(2k + 1)\pi/T \quad (5)$$

respectively. *C* type solutions always exist in complex conjugate pairs and exhibit both amplitude and phase modulations. *N* type solutions exist in pairs and are periodic with a period of twice that of the parameter variation. For an undamped

second order system, the only possible modes are $2P$, $2C$ and $2N$ modes, where 2 denotes the number of characteristic multipliers. $2C$ modes are always stable, whereas $2P$ and $2N$ modes are always unstable.

Flugrad and Liu (1988), Hsu and Cheng (1974), as well as Jandrasits and Lowen (1979) noticed that forced resonance for inhomogeneous, periodic, linear systems occurs only at regions close to the even-order instability boundaries ($2P$ modes). No forced resonance was observed at regions close to the odd-order instability boundaries ($2N$ modes).

Kotowski (1943) used Fourier series to obtain forced solutions to second order inhomogeneous Mathieu equations. D'Angelo (1970) and Richards (1983) used Fourier series in conjunction with Sylvester's theorem to derive forced solutions to a sinusoidal forcing function (equation (6)) for general order periodic systems.

$$\mathbf{B}(t) = \mathbf{D} \exp(i\omega_f t) \quad (6)$$

They concluded from the analytical expression that the general steady state response is aperiodic unless ω_p (frequency of the parameter variation) and ω_f (frequency of the forcing term in equation (6)) are commensurate. For example, if $\omega_p = 2\omega_f$, the response will be periodic with fundamental frequency ω_f . The relative amplitudes of the various frequency components in the response depend on the system parameters in a rather complicated fashion. Whether the steady state response can be evaluated analytically depends on the availability of an analytical form for the transition matrix $\Phi(t, t_0)$.

Schmidt and Tondl (1986) investigated the combination effects of the periodic coefficients and forcing terms on the steady state responses of periodic systems. They expressed the periodic coefficients and the forcing terms by Fourier series and used the

integral equation method with generalized Green's function to obtain the expression for periodic steady state solutions. Due to complicated expressions for product terms, the higher terms of the Fourier series were assumed relatively small and discarded. Curves showing the relations between vibration amplitude and system parameters were drawn. They concluded that the interaction between the parametric and forced excitations is too complex to express in a few lines of equations.

For the cam systems studied here, Hsu's method overcomes the problems encountered by the other methods and calculates the steady state response directly.

EXAMPLE

The same parameters used for cam synthesis in Part 1 are used here. The Root Mean Squared (RMS) error for the calculated steady state θ_{6t} with reference to the desired θ_{6t} , based upon one degree increments of cam rotation over a full cycle of 360 degrees, was used to investigate the responses for different operating speeds. The RMS errors for cam systems simulated at speed ratios of 0.05 to 1 with design speed ratio of 0.1 and damping ratios of 0.05, 0.10, and 0.15 are shown in Fig. 1. The lowest RMS errors occurred at the design speed, and the values decreased slightly as damping increased. The RMS errors at the design speed were 0.0006007, 0.0005290, and 0.0005216 radians for the above three design conditions. Apparent in Fig. 1 is the existence of several well-defined peaks at different speed ratios. The magnitudes of these peaks decreased as damping increased.

The location of the characteristic multipliers help explain the existence of these high RMS peaks. Equation (7) below represents the inhomogeneous, periodic, linear, ordinary differential equations to be solved. The periodic initial conditions are given by equation (8) where t_0 can be any instant within the period.

$$\dot{\mathbf{X}} = \mathbf{A}(t)\mathbf{X} + \mathbf{B}(t) \quad (7)$$

$$\mathbf{X}(t_0) = [\mathbf{I} - \Phi(t_0 + T, t_0)]^{-1} \int_{t_0}^{t_0+T} \Phi(t_0 + T, \tau) \mathbf{B}(\tau) d\tau \quad (8)$$

In equation (8), the determinant, $|\mathbf{I} - \Phi(t_0 + T, t_0)|$, appears in the denominator of the inverse ($[\mathbf{I} - \Phi(t_0 + T, t_0)]^{-1}$) of the matrix. Consider the relationship

$$|\mathbf{I} - \Phi(t_0 + T, t_0)| = \prod_{j=1}^n (1 - \lambda_j) \quad (9)$$

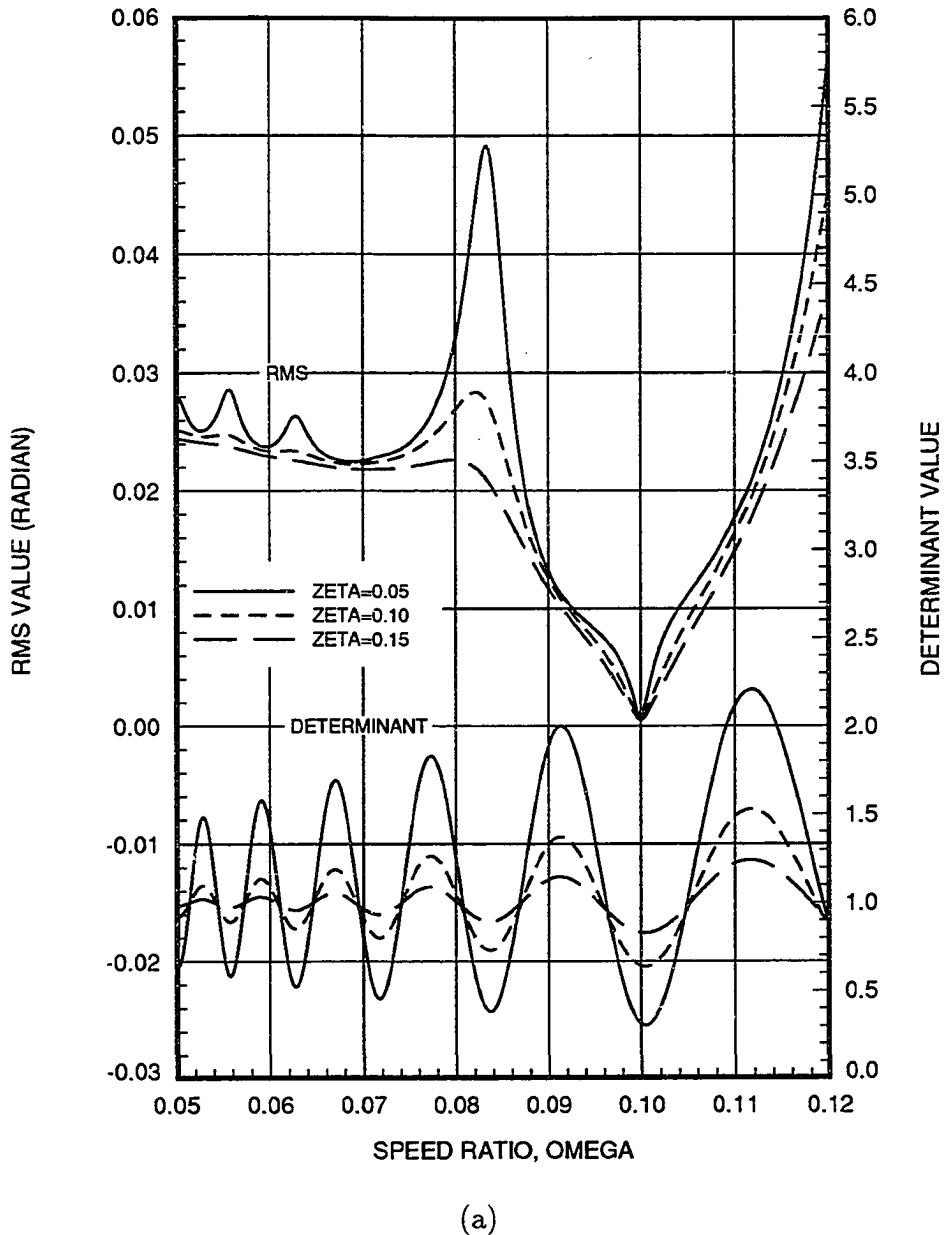
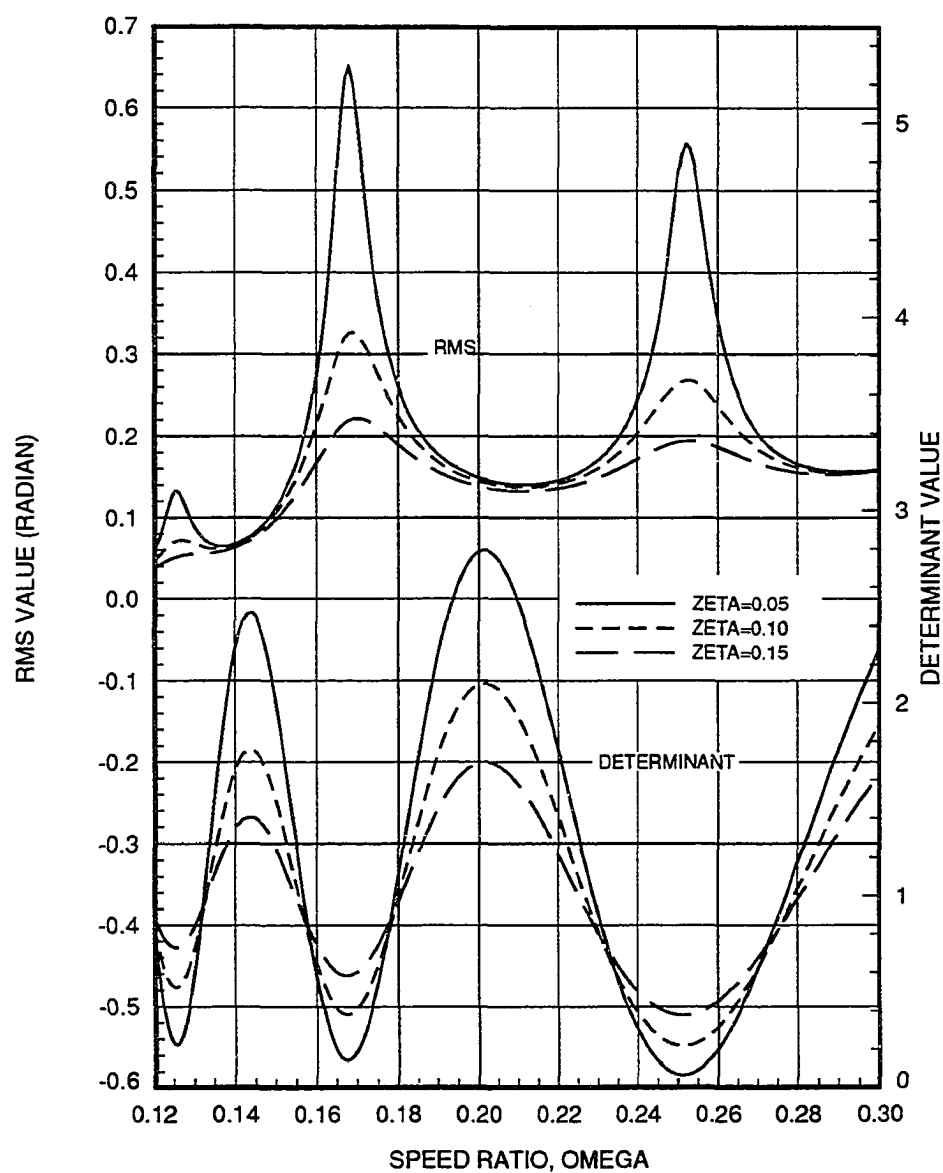
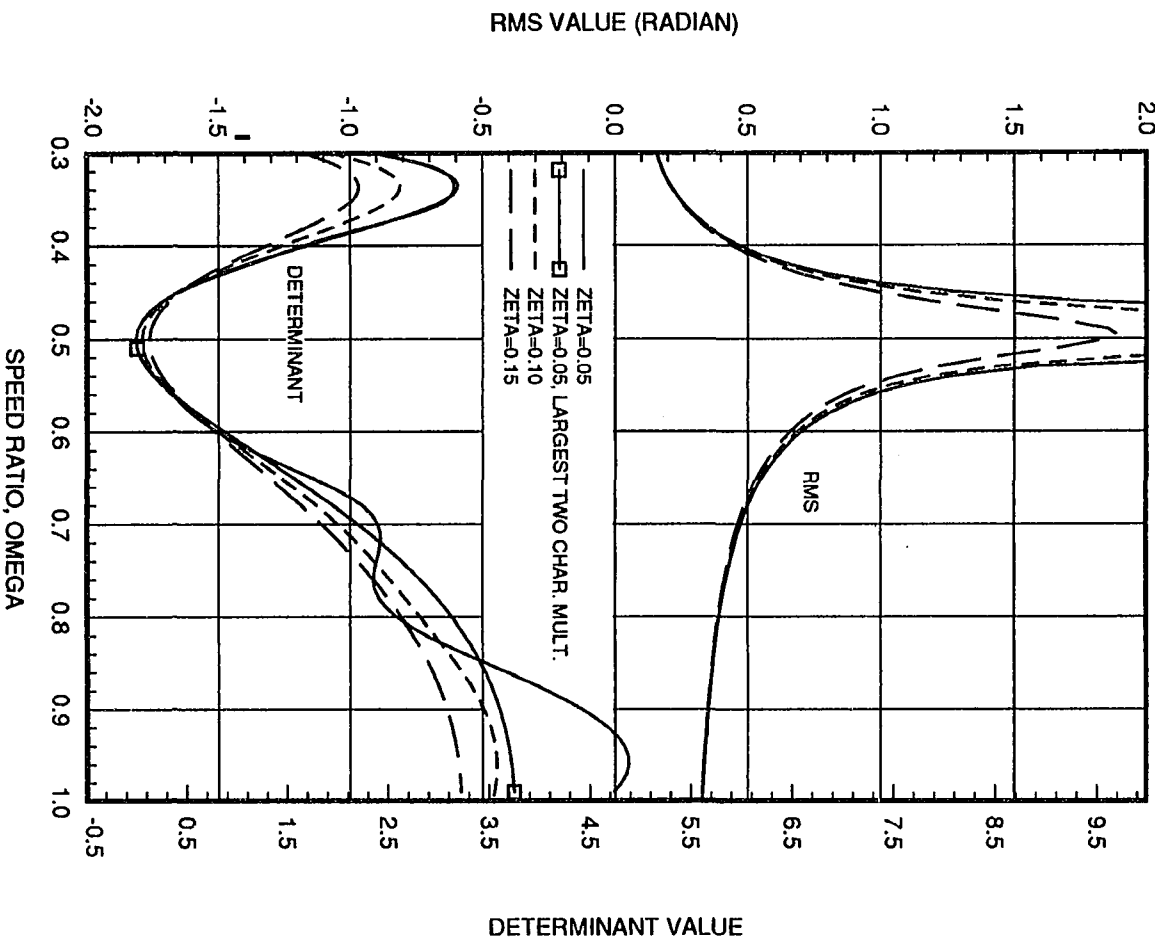


Figure 1: RMS errors and determinants of $[\mathbf{I} - \Phi(t_0 + T, t_0)]$ versus speed ratios for different damping ratios. The design speed ratio is 0.1. The point on the curve with the \square symbol represents approximation of the determinant found by using the single dominant pair of characteristic multipliers in equation (9)



(b)

Figure 1 (Continued)



(c)

Figure 1 (Continued)

where λ_j (characteristic multipliers) are the eigenvalues of $\Phi(t_0 + T, t_0)$. For the present system, the six characteristic multipliers are either three pairs of complex conjugates or complex conjugates and real numbers. If they are complex conjugates, then equation (9) becomes

$$|\mathbf{I} - \Phi(t_0 + T, t_0)| = \prod_{j=1}^3 [(1 - a_j)^2 + b_j^2] \quad (10)$$

where a_j and b_j are the real and imaginary parts of the complex characteristic multipliers. Equation (10) is the product of the square of the distances from point (1,0) to points (a_j, b_j) on the complex plane. If the characteristic multipliers corresponding to a speed ratio are close to (1,0) on the complex plane, the magnitude of the determinant will be close to zero, and the value of $\mathbf{X}(t_0)$ will become very sensitive to the determinant and may deviate significantly from its designed value. If the characteristic multipliers are located far from (1,0), (for example, if their real parts are negative and have large magnitudes) the determinant is not close to zero, and the value of $\mathbf{X}(t_0)$ is less sensitive to the determinant. Besides $|\mathbf{I} - \Phi(t_0 + T, t_0)|$, other terms in equation (8) should also be considered. The related equations are equations (1) and (52) in Part 1. The transition matrix, Φ , is a function of the coefficient matrix \mathbf{A} . Both \mathbf{A} and \mathbf{B} are functions of the rigid body motion and the speed ratio. The speed ratio appears in the denominator in every element of \mathbf{A} and \mathbf{B} either as Ω or Ω^2 . It is easy to see that all individual terms in equation (8) vary smoothly for a speed ratio range. However, the appearance of the term $|\mathbf{I} - \Phi(t_0 + T, t_0)|$ in the denominator produces undesirable sensitivity when it approaches zero.

It was found that magnitudes of all characteristic multipliers increased as the speed ratio increased. For cases with damping ratios larger than 0.05, the magnitudes

of two characteristic multipliers, either two complex conjugates or two real numbers, were much larger than the other four. At low speed ratios in particular, the four smaller characteristic multipliers were almost negligible compared to the larger two. Therefore, the two larger characteristic multipliers dominated $|\mathbf{I} - \Phi(t_0 + T, t_0)|$. At high speed ratios, the four smaller characteristic multipliers were no longer negligible, and they played a role in equation (9). As shown in Fig. 1(c), the curve with the symbol \square representing the values of equation (9) found by neglecting the two smaller pairs of characteristic multipliers did not coincide with the curve representing the real determinant values beyond the speed ratio 0.6. The dependence of locally highest or lowest RMS error on the locally lowest or highest $|\mathbf{I} - \Phi(t_0 + T, t_0)|$ seemed more obvious at low speed ratios. This is because at low speed ratios, the dynamic effect associated with the first and second derivatives of the rigid body variables was relatively small, and the difference in speed ratio between neighboring highest or lowest RMS speeds was less than that at higher speeds. For example, the difference was only 0.0025 between the locally lowest RMS speed ratio 0.05280 and the neighboring highest RMS speed ratio 0.05575.

At higher damping levels, magnitudes of the characteristic multipliers decreased significantly and became close to the $(0,0)$ point on the complex plane. This was more obvious at lower speed ratios, where magnitudes of the characteristic multipliers were so small that they were located in a small neighborhood of the $(0,0)$ point on the complex plane. The determinants, then, only varied slightly from the value 1, and the RMS errors changed very little. This can be explained by the coefficients of the first derivative terms of equations (52) in Part 1, where the damping ratio ζ appeared in the numerator and the speed ratio Ω appeared in the denominator of every nonzero

term. Higher damping ratios or lower speed ratios increased the influence of the first derivative terms, and the α_j in equations (3), (4), and (5) became negative with larger magnitudes which in turn resulted in characteristic multipliers of smaller magnitudes through equation (2).

Fig. 2 shows the locus of one of the largest two characteristic multipliers and the characteristic multipliers corresponding to the locally highest or lowest RMS speed ratios in Fig. 1. As shown the characteristic multiplier spiraled out on the complex plane as speed increased. The two largest characteristic multipliers were positive real or negative real numbers when the corresponding point was located on the real axis in Fig. 2. Otherwise, they were complex conjugates. The characteristic multiplier corresponding to each speed ratio with locally highest RMS value in Fig. 1 was located locally close to the point (1,0) on each revolution of the spiral. The characteristic multiplier was sometimes located on the positive real axis, which means that the largest two characteristic multipliers were two positive real numbers. This confirmed the use of equation (10) to explain the significant deviation of the $\mathbf{X}(t_0)$ in equation (8) from its designed value. And notice that the t_0 can be any instant within the period. At low speed ratios, the characteristic multipliers with locally lowest RMS values were located locally far from (1,0) on each revolution of the spiral.

For the present study, in the unstable cases, the two largest characteristic multipliers were always real numbers ($2P$ or $2N$). The RMS curves inside the unstable zones in Fig. 1 are meaningless since the corresponding solutions diverge and the steady states do not exist even though they can still be calculated (Hsu and Cheng, 1974; Müller and Schiehlen, 1985; Mahyuddin and Midha, 1989). It can be seen from equations (8) and (9) that the steady state $\mathbf{X}(t_0)$ can still be calculated even if a

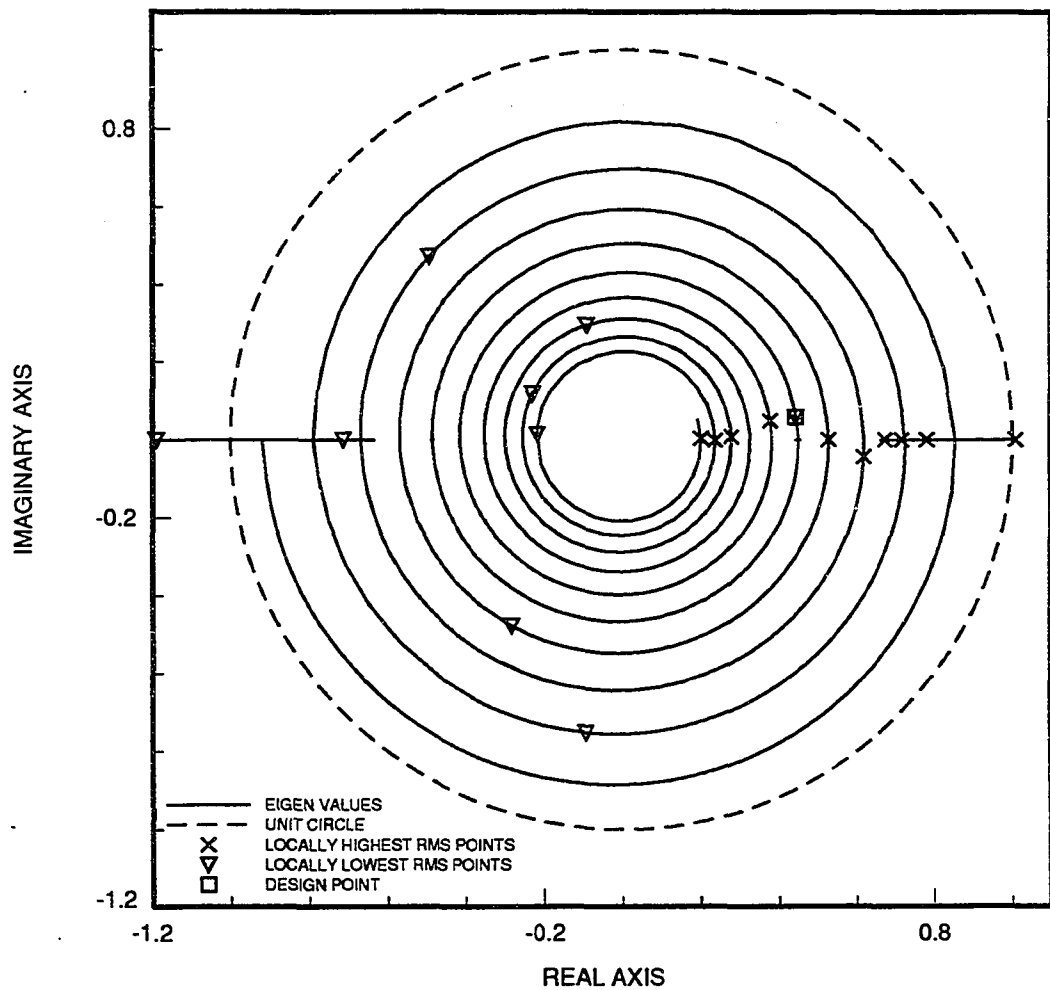


Figure 2: The locus for one of the largest two characteristic multipliers as a function of the speed ratio. The design speed and damping ratios are 0.1 and 0.05, respectively

λ_j is larger than 1 or less than -1 which corresponds to the unstable case. For the case with damping ratio of 0.05, the system was unstable at speed ratios in a small neighborhood of 0.5 where one of the two positive real characteristic multipliers was larger than 1. The RMS errors at speeds close to the boundaries of this unstable interval were extremely large, since the determinant of $[\mathbf{I} - \Phi(t_0 + T, t_0)]$ in equation (8) approached zero as one of the characteristic multipliers got closer to 1. The other unstable interval was located between 0.94 and 1, where one of the two negative real characteristic multipliers was less than -1. Fig. 3 shows the growing vibration for the unstable speed ratio of 0.98 obtained by integrating from time 0 using Runge-Kutta-Verner subroutine DIVPRK in the IMSL library. The RMS curve, however, was continuous and smooth across the instability boundary of 0.94.

After examination of the Fourier series of the periodically varying elements of the 3×3 stiffness matrix (coefficient matrix of the vector $\{\theta_{6t}, \delta\theta_5, \delta r_3\}^T$) in equations (52) in Part 1, the higher terms of the series were found to be relatively smaller than the first term which was the average of the series. Based on the theory of perturbation, if a system is composed of relatively larger and smaller parameters, then the major characteristics of the system may be determined by the larger parameters, and the smaller parameters will contribute only minor modifications. The averages of the Fourier series may thus be treated as elements of the stiffness matrix for systems with constant coefficients, and the square roots of the three eigenvalues of this constant stiffness matrix may be treated as the three natural frequencies. Table 1 lists the quotients of the three natural frequencies divided by 2π when the system was operated at the locally highest RMS speed ratios. The third quotient for each speed ratio was close to an integer and this integer increased regularly from 1, which

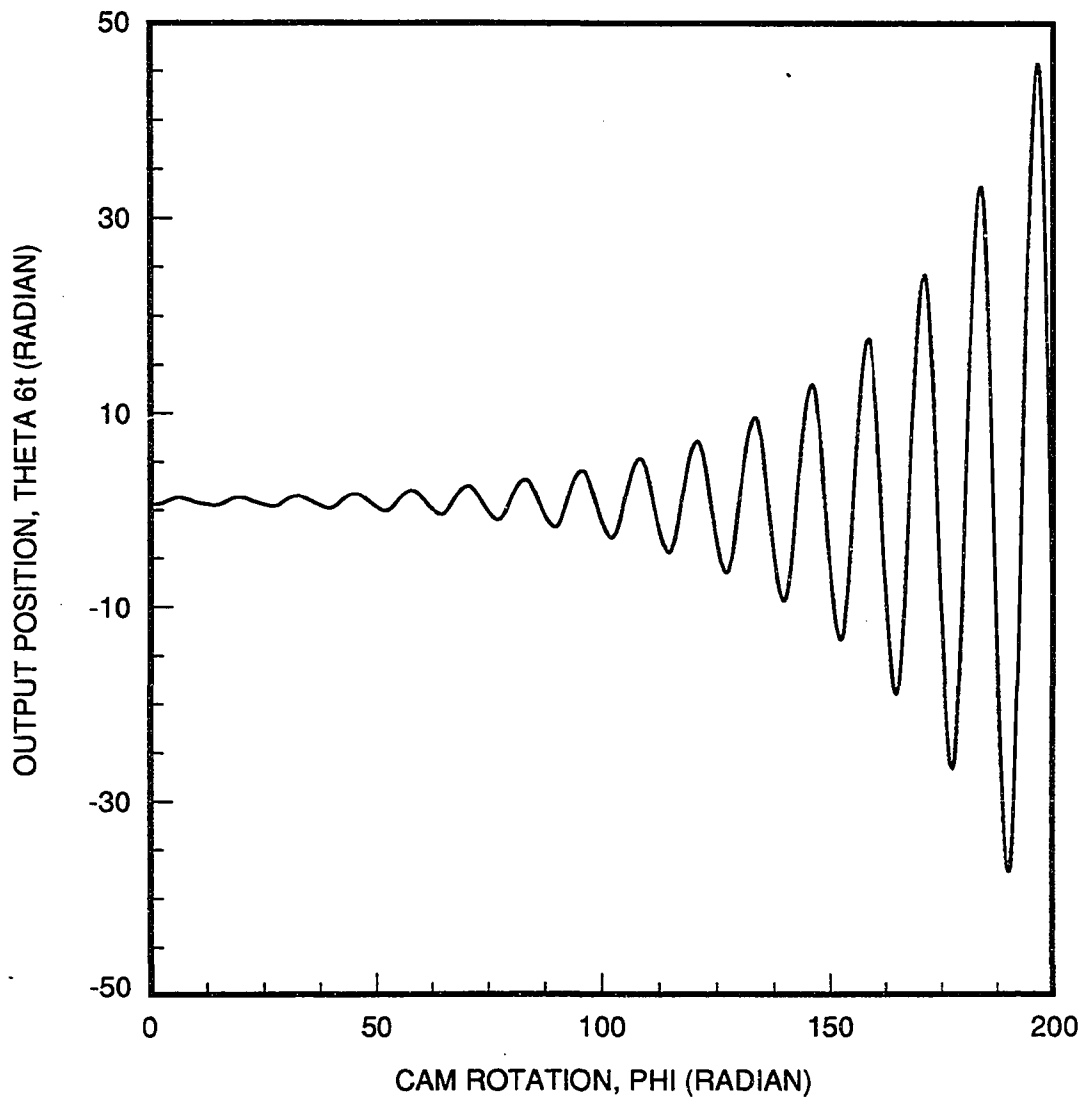


Figure 3: The unstable response integrated from time 0 for the cam system simulated at the speed ratio 0.98. The design speed and damping ratios are 0.1 and 0.05, respectively

corresponded to the speed ratio of 0.49, at the increment of 1. In addition, this third quotient was the number of intersections of the dominant characteristic multiplier locus shown in Fig. 2 and the positive real axis to the right of the point (including the intersection very close to the point) corresponding to the speed ratio. At speed ratios 0.1675 and 0.08336, two of the three quotients were close to integers. This phenomenon of two coordinates vibrating at frequencies close to natural frequencies may explain the unusually strong RMS values associated with these two speeds.

Table 1: Quotients of the three natural frequencies divided by 2π when the system is simulated at the locally highest RMS speed ratios. The design speed and damping ratios are 0.1 and 0.05, respectively

speed ratio, Ω	(natural frequency)/(2π)		
0.05575	0.397	5.97	8.97
0.06275	0.351	5.27	7.93
0.07143	0.309	4.63	6.96
0.08336	0.265	3.97	5.98
0.1000	0.221	3.31	4.98
0.1255	0.180	2.64	3.96
0.1675	0.131	1.97	2.96
0.2520	0.0876	1.31	1.98
0.4900	0.0444	0.662	0.996

The steady state responses for some locally highest and lowest RMS speed ratios with damping ratio of 0.05 are shown in Fig. 4. For the locally highest RMS speeds, the number of waves corresponds to the near integer third quotient in Table 1. No waves were observed for the design speed ratio of 0.1, whose dominant characteristic multiplier was located locally close to the point (1,0). However, waves at this design speed appeared if the simulation damping ratio was less than the design damping

ratio as discussed in the following.

Depending on the location of the dominant characteristic multipliers of the design speed, the uncertainty of damping may have different effects on the response. The speed ratio 0.1, whose dominant characteristic multiplier was located locally close to the point (1,0) in Fig. 2, and the speed ratio 0.091, whose dominant characteristic multiplier was located locally far from (1,0) were chosen as design speeds to demonstrate the damping effects. As shown in Fig. 5(a), undesirably high RMS errors were found for the speed ratio of 0.1 when the system was simulated at speeds close to the design speed with a damping ratio that was 0.05 lower than the design damping ratio of 0.15. The peak occurred at a speed ratio of 0.101 with one of its largest two complex characteristic multipliers located at the point (0.4433, 0.08279), which was locally close to the point (1,0) on a revolution of the spiral. The RMS error at the design speed ratio of 0.091 did not go up high enough to form a locally highest point. This may be explained by the location of the largest two characteristic multipliers on the complex plane as before. Fig. 6 shows the locus of the largest characteristic multipliers for speed ratios in the neighborhood of the design speed ratios 0.1 and 0.091 for different simulation damping ratios used in Fig. 5. Table 2 lists the characteristic multipliers for the design speed ratio of 0.1 with different combinations of design and simulation damping ratios. As shown, the dominant characteristic multipliers were mainly dependent on the simulation damping ratios since the difference in cam profile for different design damping ratios and the same speed ratio was very small. The rigid body motions were thus almost the same, and the simulation damping ratio was the main changing factor for different cases in Table 2. As damping decreased, the magnitudes of the characteristic multipliers increased, and the two

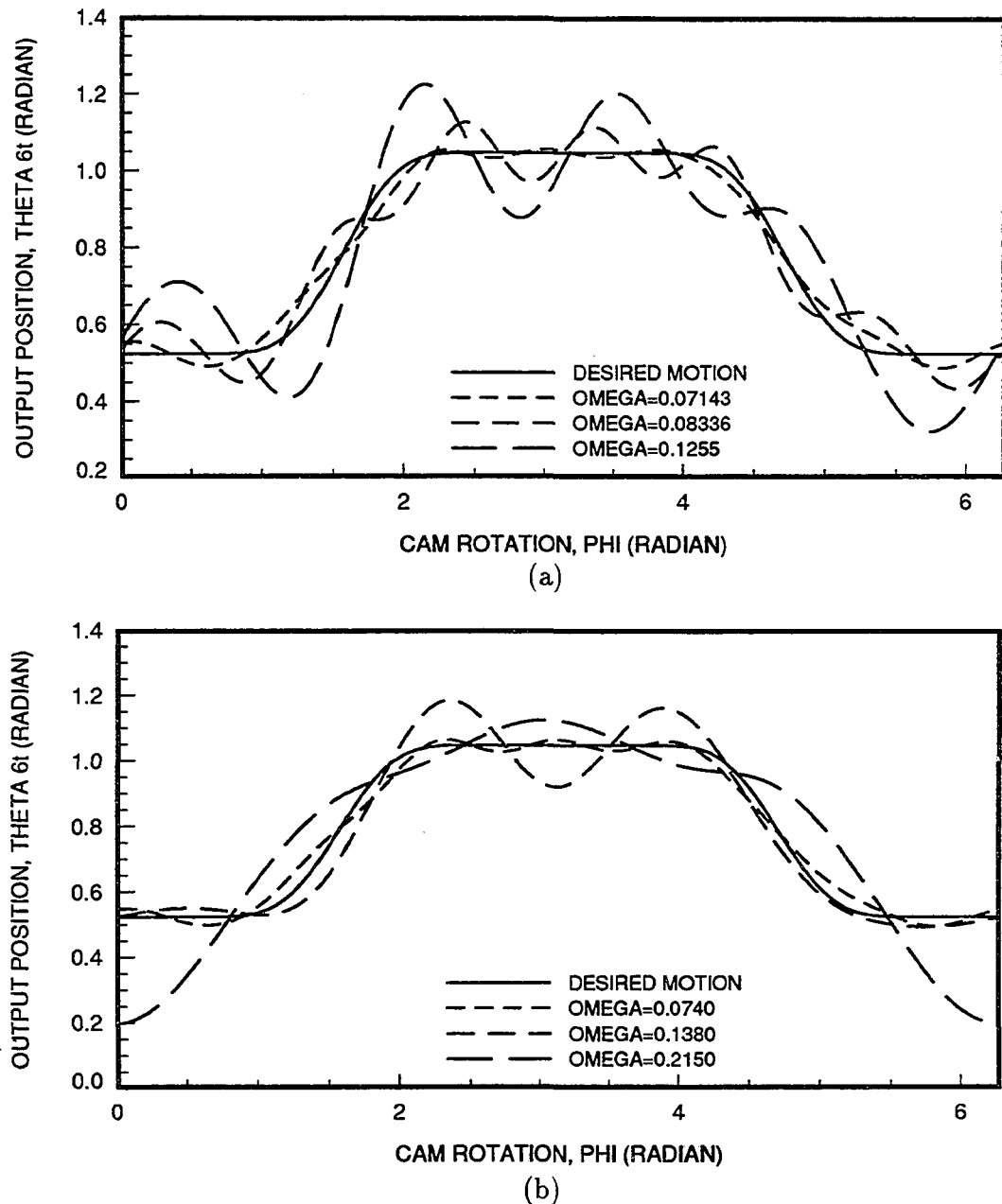


Figure 4: Steady state responses at the speed ratios with locally highest (a) and lowest (b) RMS errors. The design speed ratio (Ω) and damping ratio are 0.1 and 0.05, respectively

largest characteristic multipliers for the speed ratio of 0.1 moved closer to (1,0) while the two largest characteristic multipliers for the speed ratio of 0.091 moved farther from (1,0). This increase in RMS error caused by the difference in damping was not seen at speeds farther away from the design speed. As shown in Fig. 5, at speeds farther from the design speed, the responses were very similar or almost identical to the responses designed and simulated at the same damping ratios. Fig. 7 shows RMS errors for cam systems designed and simulated at the same speed ratios but with different design and simulation damping ratios. As shown the RMS peaks occurred at the same speed ratios as in Figs. 1 and 2. The peaks were higher for the case with design damping ratio of 0.15 and simulation damping ratio of 0.05. Fig. 8 shows the difference in x_t ($= x_{t,\zeta=0.05} - x_{t,\zeta=0.15}$) (see Part 1) for cam systems designed at damping ratios of 0.05 and 0.15 for various design speeds. It is seen that the difference in x_t increased as the design speed increased.

Table 2: Characteristic multipliers when the system is simulated at the design speed ratio of 0.1 with different combinations of design and simulation damping ratios

$\zeta_{simulation}$	$\zeta_{design} = 0.15$	$\zeta_{design} = \zeta_{simulation}$
0.05	$0.4439 \pm 5.590E-02i$ $-2.156E-08 \pm 1.497E-08i$ $-1.457E-18, -6.196E-18$	$0.4435 \pm 5.799E-02i$ $-2.163E-08 \pm 1.479E-08i$ $-2.454E-18 \pm 2.015E-18i$
0.10	$0.1987 \pm 2.140E-02i$ $5.673E-16 \pm 4.142E-16i$ $-3.854E-18 \pm 1.750E-18i$	$0.1987 \pm 2.142E-02i$ $5.669E-16 \pm 3.703E-16i$ $-9.129E-19 \pm 1.775E-18i$
0.20	$3.923E-02, 4.070E-02$ $9.174E-20 \pm 1.082E-18i$ $-2.919E-21, -2.919E-21$	$3.926E-02, 4.068E-02$ $1.253E-18, 3.458E-20$ $-7.224E-19, -1.441E-19$

The Runge-Kutta method was found to be reliable in integrating periodic ordinary differential equations (Carnegie and Pasricha, 1974; Richards, 1983; Mahyuddin

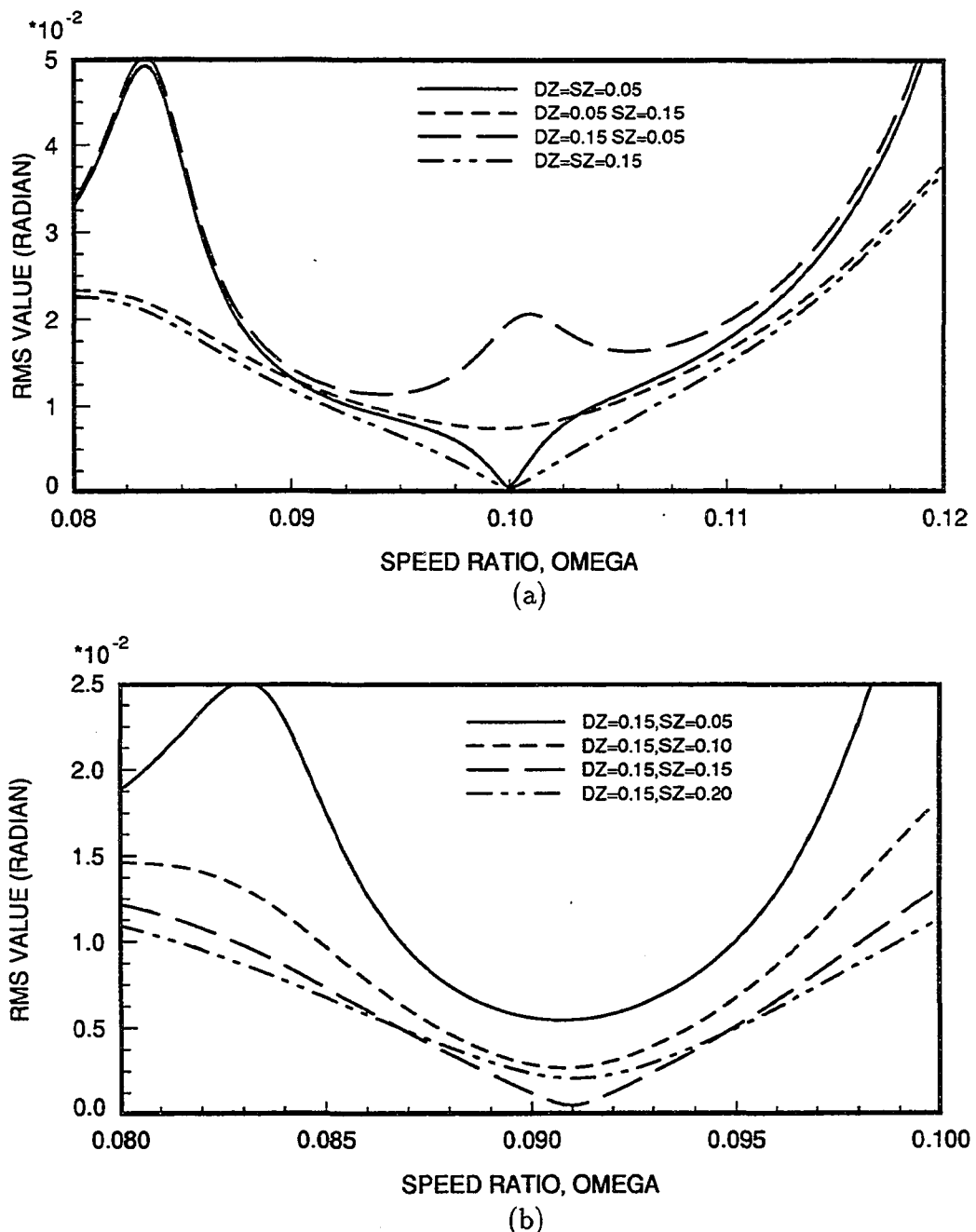


Figure 5: RMS errors for cam systems simulated at various damping ratios. DZ and SZ represent design and simulation damping ratios, respectively. The design speed ratios are 0.1 for (a) and 0.091 for (b)

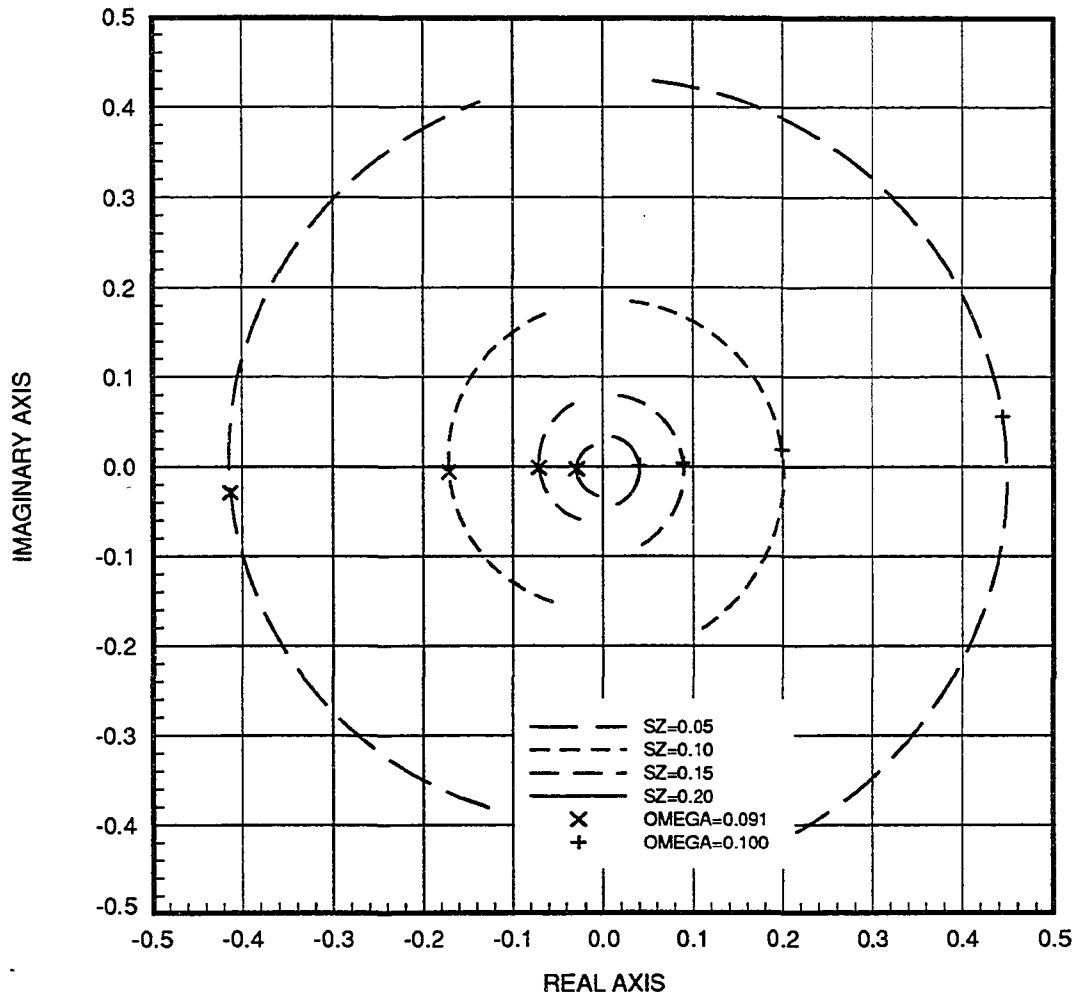


Figure 6: The locus for one of the largest two characteristic multipliers as functions of the speed ratios and simulation damping ratios, for cam systems designed at speed ratios (Ω) 0.091 (left curves, for speed ratio range 0.088 to 0.095), and 0.1 (right curves, for speed ratio range 0.096 to 0.104). The design damping ratio is 0.15 for all cases

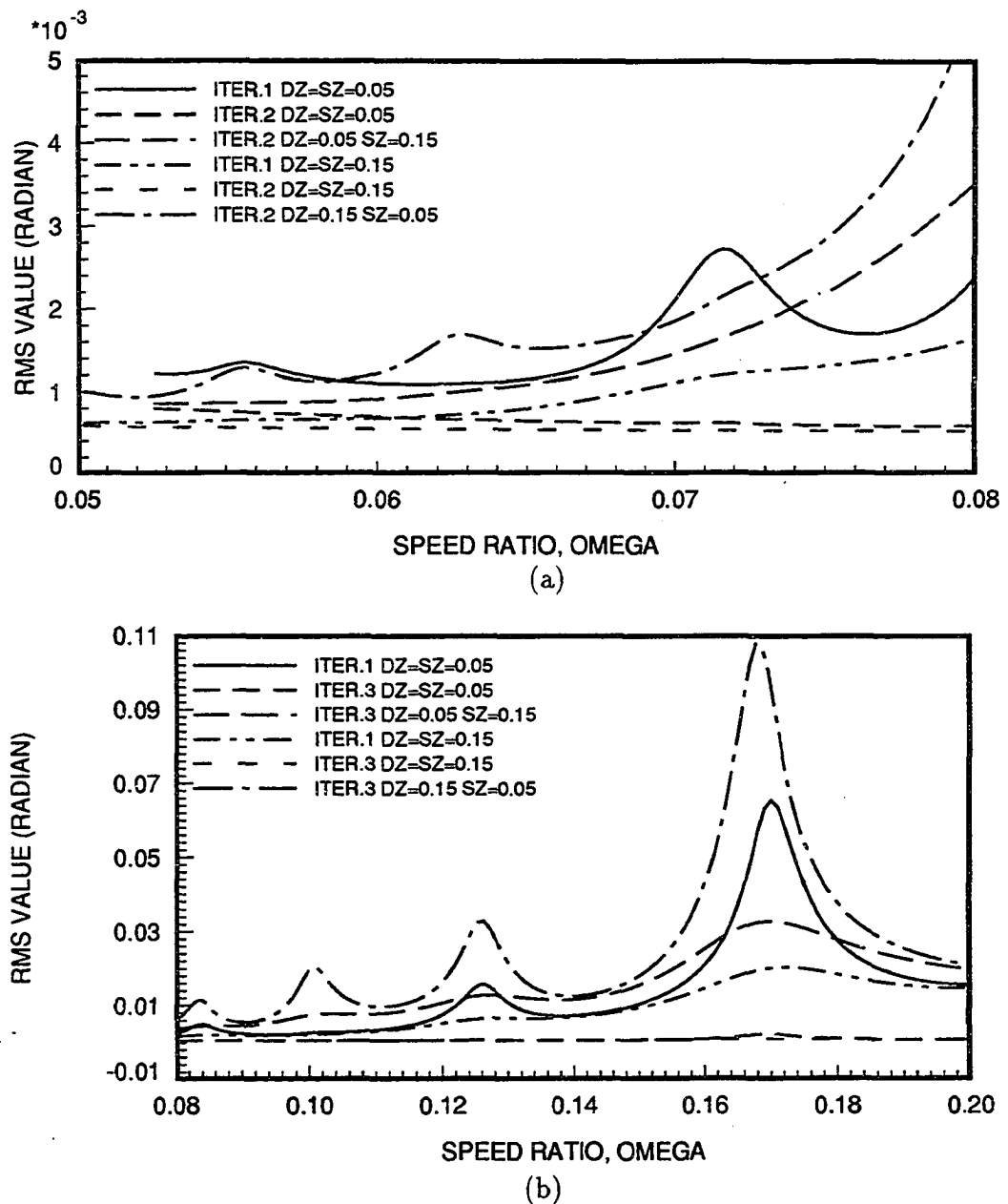


Figure 7: RMS errors for cam systems designed and simulated at the same speed ratios but with different design (DZ) and simulation (SZ) damping ratios of 0.05 and 0.15. The legend ITER. represents the iteration number used for synthesis as explained in Part 1

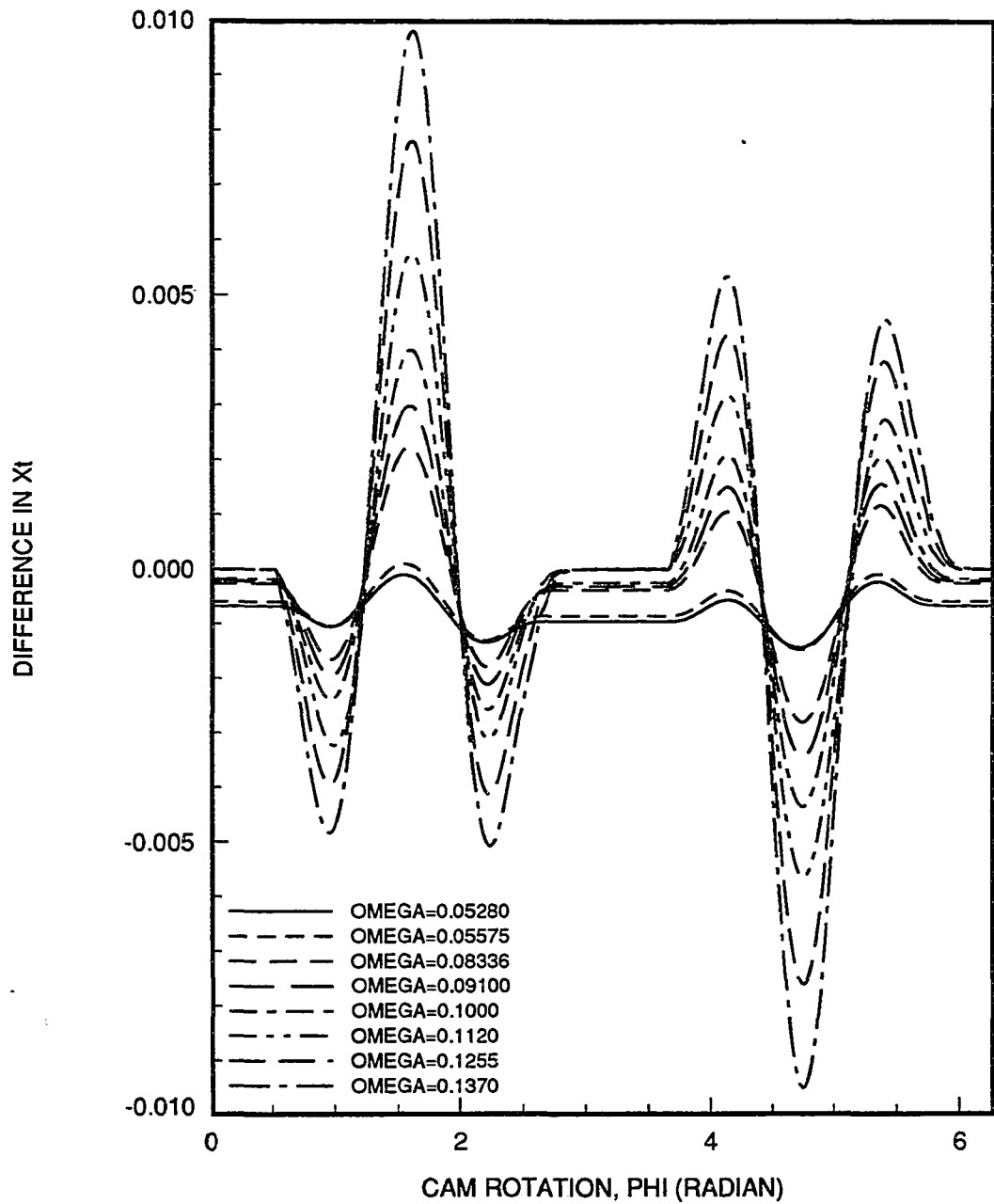


Figure 8: Difference in x_t ($= x_{t,\zeta=0.05} - x_{t,\zeta=0.15}$) for cam systems designed at damping ratios of 0.05 and 0.15 for various design speeds

and Midha, 1989), especially when the system was operated in the neighborhood of the instability boundaries. The double precision fifth-order and sixth-order Runge-Kutta-Verner subroutine DIVPRK in the IMSL library was used to verify the results obtained by Hsu's method. Fig. 9 shows the steady state responses obtained by these two methods for the case with a design speed ratio of 0.1 and a damping ratio of 0.15, simulated at damping ratios of 0.15 and 0.05. The steady state for the design condition was so close to the desired one that they coincide in the figure. Five waves appeared when it was simulated at the lower damping ratio of 0.05. Comparing the two steady states obtained by the two methods, a little difference was found at the ends of the rise and return of the cycle.

Fig. 10 shows the widths of the low RMS operating zones in the neighborhood of various design speeds for damping ratios of 0.05 and 0.15. Speed ratios of 0.05575, 0.08336, 0.1, and 0.1255, were those whose dominant characteristic multipliers were very close to (1,0) and were locally highest RMS points in Fig. 2. Speed ratios 0.091 and 0.112 were very close to the negative real axis, the speed ratio 0.05275 was very close to the negative real axis and was one locally lowest RMS point, and the speed ratio 0.137 was one locally lowest RMS point with one of its largest two complex characteristic multipliers located at the point (-0.2841,0.4772). At the damping ratio of 0.05, the width of the low RMS operating zone was much smaller for speed ratios 0.08336, 0.1, and 0.1255. In Fig. 10(b), however, this phenomenon was not observed for low speed ratios. Fig. 10(b) also shows the wider low RMS operating zone for lower speeds. This may be explained by the location of the largest two characteristic multipliers on the complex plane as before.

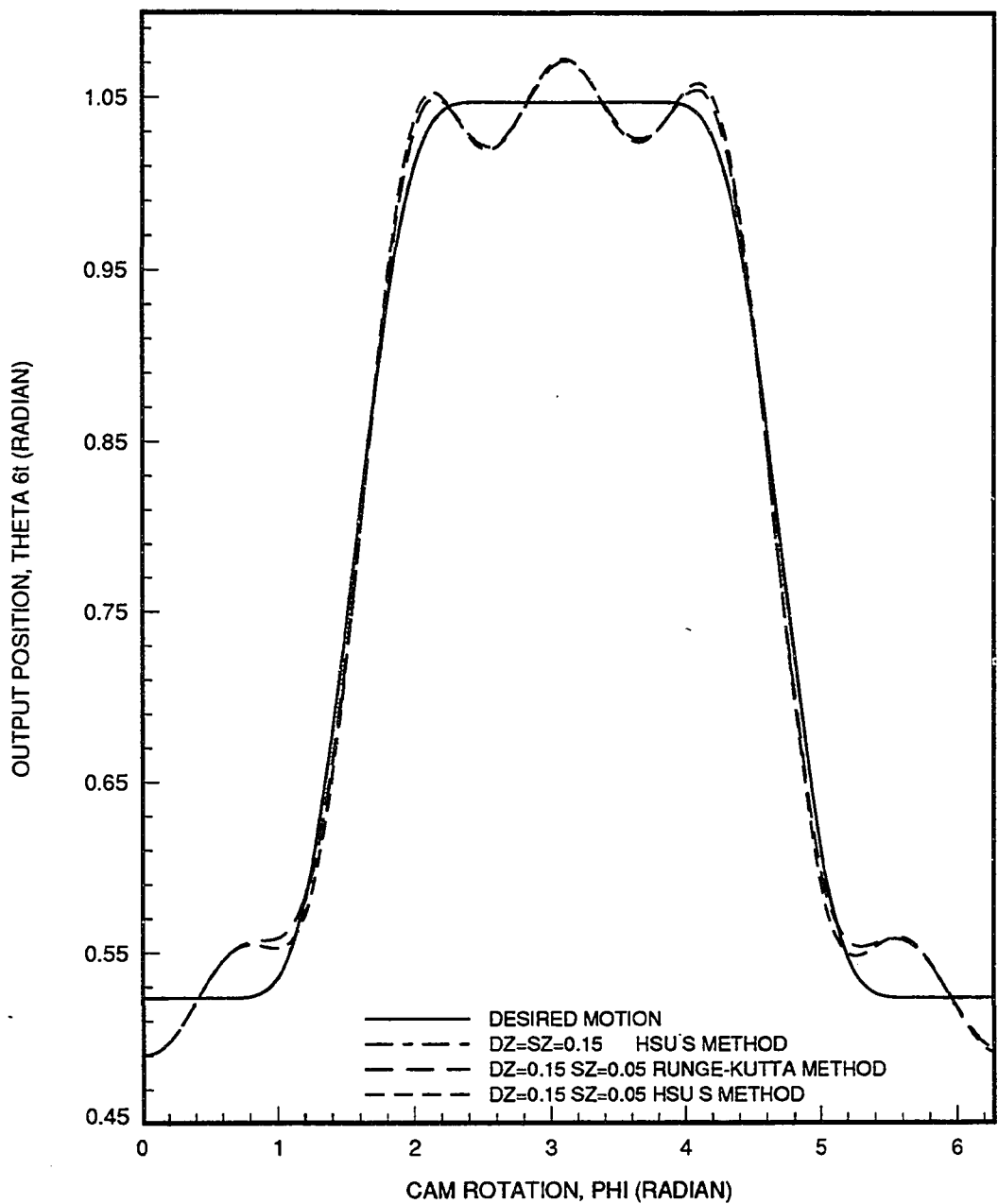
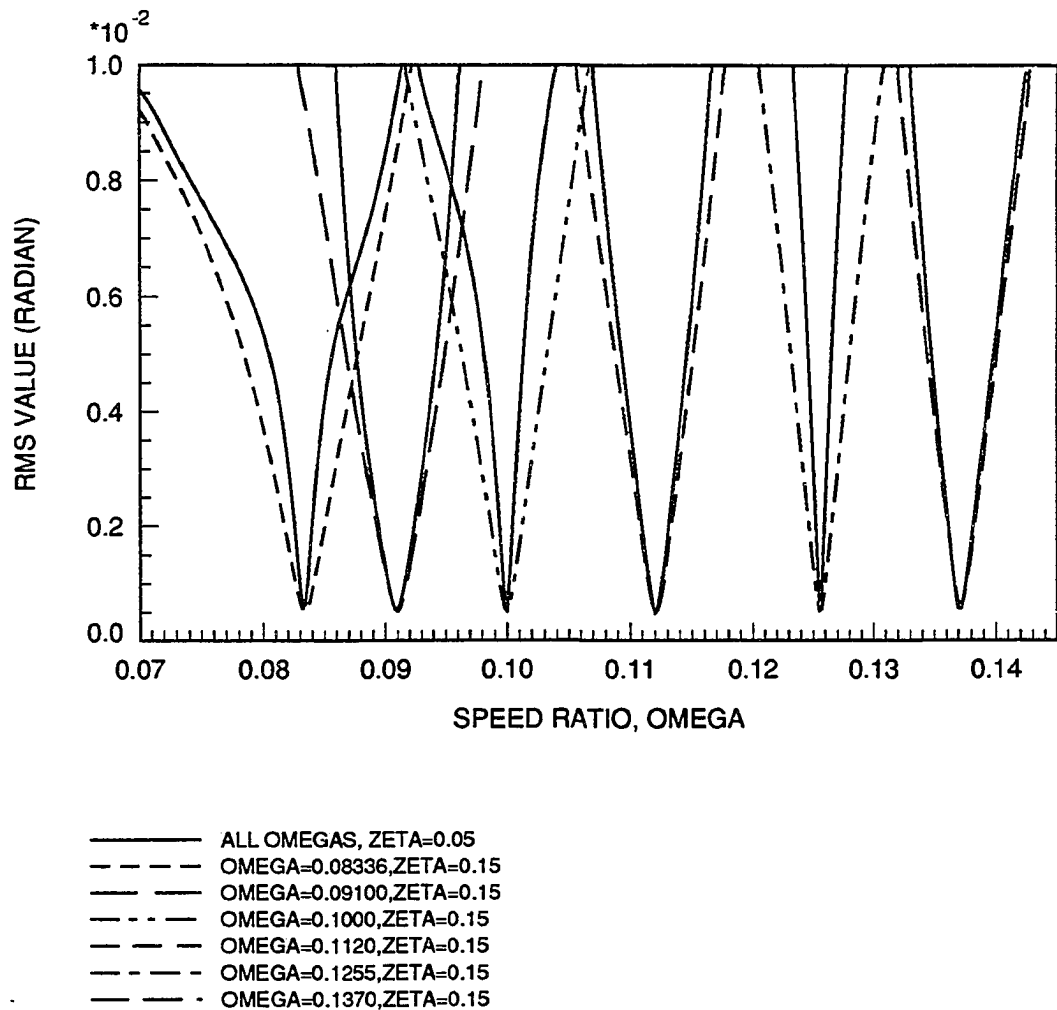
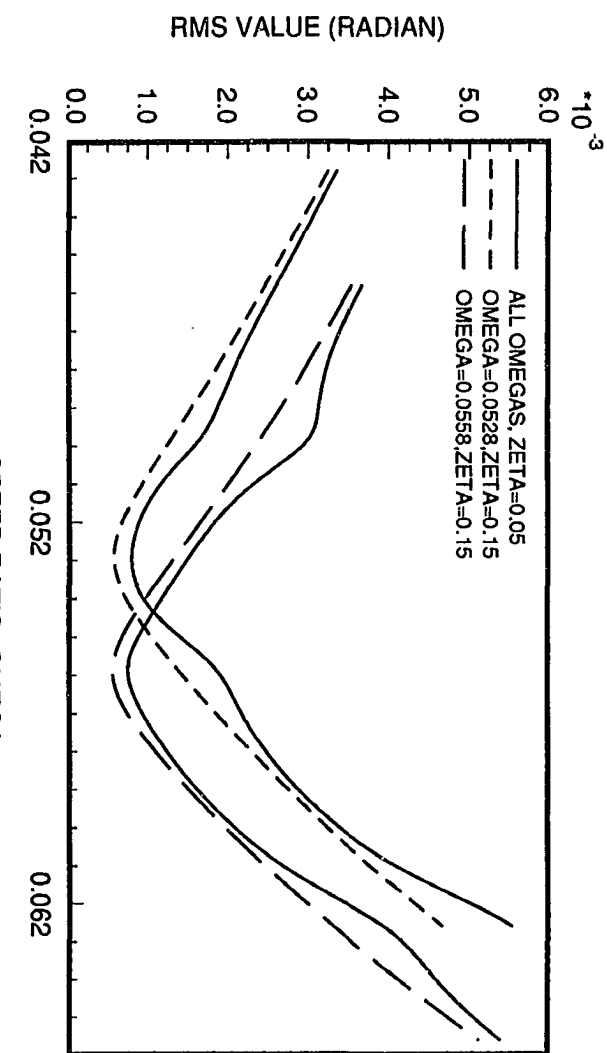


Figure 9: Steady states calculated by Hsu's method and the Runge-Kutta-Verner integration scheme for the design speed ratio of 0.1 and the simulation damping ratios (SZ) of 0.15 and 0.05. The design damping ratio (DZ) is 0.15



(a)

Figure 10: RMS errors for cam systems designed at different speed ratios, the damping ratios are 0.05 and 0.15 for all cases



(b)

Figure 10 (Continued)

CONCLUSIONS

The synthesized mechanisms were simulated over a range of speed ratios, and as expected, the lowest RMS values were found at the design speeds.

For the inhomogeneous, periodic, linear systems studied here, the characteristic multipliers revealed information about the stability and the steady state responses. Multiple high vibration regions caused by the combination effects of the periodic coefficients and the forcing terms were found to occur when the two dominant characteristic multipliers were located close to the point (1,0) on the complex plane.

The difference in the rigid body motion of the linkage for different design speeds and damping ratios was very small since the difference in corresponding cam profiles was very small. Furthermore, the trigonometric terms in the governing equations (equations (52) in part 1) were functions of the rigid body motion. Thus, the relative positions of the dominant characteristic multipliers on the complex plane was intrinsically determined by the rigid body motion of the linkage. Higher or lower damping ratios shrank or enlarged the locus of the dominant characteristic multipliers, but the relative positions of the characteristic multipliers remained the same even though the design speed was different. Considering the vibration induced by inaccurate estimates of damping and the width of the low RMS operating zone, the design speed ratio should be chosen so that the associated dominant characteristic multipliers are not close to the critical point (1,0). The regions close to the point (-1,0) or those with locally lowest RMS regions would be good choices. A locus plot of the dominant characteristic multipliers from the first trial may reveal the speed ratios for a better design.

REFERENCES

- Carnegie, W. D., and Pasricha, M. S. 1974. "Effect of Forcing Terms and General Characteristics of Torsional Vibrations of Marine Engine Systems with Variable Inertia". *Journal of Ship Research*, 18:131-138.
- D'Angelo, H. D. 1970. *Linear time-varying systems: Analysis and synthesis*. Allyn & Bacon, Boston.
- Flugrad, D. R., Jr., and Liu, H. J. 1988. "Stability analysis by a perturbation method". *Trends and Developments in Mechanisms, Machines, and Robotics - 1988*. ASME, 2:397-405.
- Hsu, C. S., and Cheng, W. H. 1974. "Steady State Response of a Dynamical System under Combined Parametric and Forcing Excitations". *Journal of Applied Mechanics*, 98:371-378.
- Jandrasits, W. G., and Lowen, G. G. 1979. "The Elastic-Dynamic Behavior of a Counterweighted Rocker Link with an Overhanging Endmass in a Four-Bar Linkage Part I: Theory, Part II: Application and Experiment". *Journal of Mechanical Design*, 101, No.1:77-98.
- Keenan, R. K. 1962. *An investigation of some problems in periodically parametric systems*. Ph.D. thesis, Monash University, Melbourne.
- Kotowski, G. 1943. "Lösungen der inhomogenen Mathieuschen Differentialgleichung mit periodischer Störfunktion beliebiger Frequenz". *Zeitschrift für angewandte Mathematik und Mechanik*, 23:213-229.
- Mahyuddin, A. I. W., and Midha, A. 1989. "On the Existence of Periodic Response of Flexible Cam-Follower Systems". *First National Applied Mechanisms & Robotics Conference*, Cincinnati, 89AMR-6B-6.
- Müller, P. C., and Schiehlen, W. O. 1985. *Linear Vibrations*. Martinus Nijhoff Publishers, Dordrecht, Holland.
- Reinhard, H. 1986. *Differential Equations: Foundations and applications*. North Oxford Academic Publishers Ltd, London.
- Richards, J. A. 1983. *Analysis of Periodically Time-Varying Systems*. Springer-Verlag, New York.

Schmidt, G., and Tondl, A. 1986. *Nonlinear Vibrations*. Cambridge University Press, New York.

PART III.

**SYNTHESIS AND STEADY STATE ANALYSIS OF HIGH-SPEED
ELASTIC CAM-FOLLOWER LINKAGES WITH A CURVED BEAM
COUPLER BY A FINITE ELEMENT METHOD**

ABSTRACT

A cam driving a lumped inertia through an elastic slider-crank follower linkage with a curved beam coupler is considered. An iterative procedure utilizing the finite element method developed by Midha et al. (1978) is used to synthesize the cam profile to produce a desired output motion at a given design speed and damping coefficient. Nonlinear terms are neglected producing inhomogeneous, periodic, linear, ordinary differential equations. Response of the synthesized linkages are simulated and found to be satisfactory at the design conditions.

INTRODUCTION

Wiederrick and Roth (1975) synthesized high-speed cam profiles by using a finite trigonometric series. The accuracy of the assumed mathematical model was assured and the dynamic performance was improved. Gupta and Wiederrick (1983) used the convolution operator to modify the dynamic properties of the cam motion and developed families for cam profiles having significant zones of near zero vibrations. Tsay and Huey (1989) synthesized a non-rigid cam-follower system based on a linear, lumped, two-degree-of-freedom model. Spline functions were used to define the motions. The finite element spline collocation method and Crank-Nicolson method were used in the synthesis and analysis.

All these and others (Chen, 1973; Johnson, 1959) were concerned with simple followers having straight line motions. Little has been done to synthesize high-speed cams whose elastic follower linkages have significantly changing geometry described by differential equations with periodic coefficients and forcing terms (Flugrad, 1986). Stability and vibration associated with systems described by inhomogeneous linear periodic equations have drawn much attention recently (Nagarajan and Turcic, 1990; Cleghorn et al., 1984; Cronin and LaBouff, 1981; Midha and Turcic, 1980). It is of great interest to know if this vibration can be predicted and reduced at the design stage.

This work demonstrates a systematic procedure using a finite element method to synthesize and analyze a high-speed cam-operated elastic linkage with a curved beam coupler. The elastic deflections induced by the large inertia of the linkage operating at a high speed are taken into account in synthesizing the cam profile.

DERIVATION OF SYSTEM EQUATIONS

As shown in Fig. 1, the cam-driven linkage consists of a lumped output inertia and an elastic slider-crank follower linkage. Links 4, 5 and 6 are made of a curved beam, a straight beam and a circular shaft, respectively. This system is designed to transfer the constant rotation of the cam to output link 7. The slider, which acts as a translating roller follower, is assumed to remain in contact with the cam. Any external load torque that might be applied to link 7 is ignored here. Further, it is assumed that no backlash exists in the joints of the mechanism and that all fixed bearings are rigid.

In finite element analysis, arch problems can be approached by replacing the arch by an assembly of straight beams. The convergence of the solution obtained by this approximation is well established (Yamada and Ezawa, 1977). For this study, the curved coupler beam is approximated by four straight beams of equal length. Fig. 2 illustrates the finite element model of the elastic follower linkage and output shaft. For simplicity the output shaft is considered to be loaded in torsion only. For beam elements Euler-Bernoulli beam theory is used in determining the stiffness properties of the elements. Rotary inertia and shear deformation of the elements are neglected to simplify the problem. The connection between the output shaft and the crank is treated as rigid, i.e., the angular deflection at the joint is the same on both sides.

The finite element approach developed by Midha et al. (1978) to model high-speed elastic linkages is used here. The moving linkage is modeled with consecutive instantaneous structures. In matrix form, the undamped equations of motion are given by

$$\mathbf{M}\ddot{\mathbf{U}}_a + \mathbf{K}\mathbf{U} = \mathbf{F} \quad (1)$$

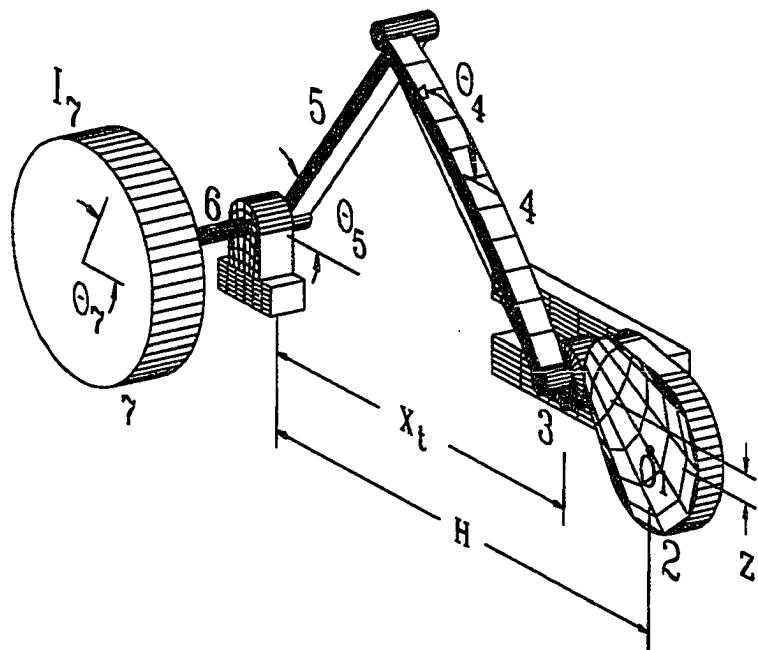


Figure 1: A cam-operated system

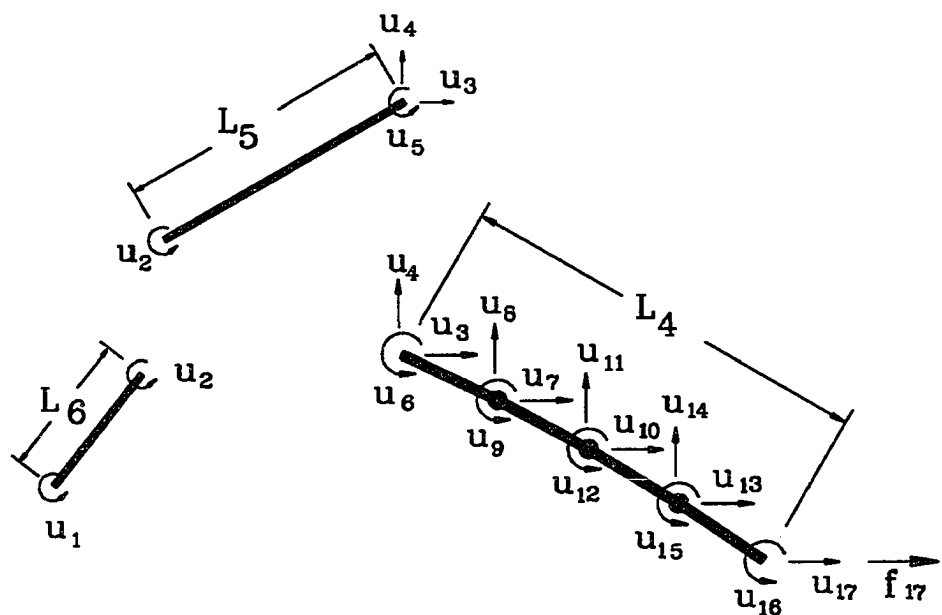


Figure 2: Elastic mechanism model

where $\mathbf{U}_a = \mathbf{U}_r + \mathbf{U}$, i.e., the absolute displacements of the coordinates are the sum of the rigid body and elastic displacements. The coefficient matrices \mathbf{M} and \mathbf{K} are functions of the rigid linkage geometry and vary as the cam rotates. For constant cam rotation, these would be time-periodic. \mathbf{F} is an externally applied load vector.

Fig. 3 shows the rigid body and elastically deformed configurations of a linkage beam element. The mass and stiffness matrices of a beam element expressed in a global coordinate system are

$$\mathbf{m} = \mathbf{R}^T \mathbf{m}^e \mathbf{R}$$

and

$$\mathbf{k} = \mathbf{R}^T \mathbf{k}^e \mathbf{R}$$

where \mathbf{m}^e , \mathbf{k}^e , and \mathbf{R} are element mass, element stiffness, and transformation matrices, respectively, expressed in a local coordinate system,

$$\mathbf{m}^e = \rho A L \begin{bmatrix} 1/3 & 0 & 0 & 1/6 & 0 & 0 \\ 0 & 13/35 & 11L/210 & 0 & 9/70 & -13L/420 \\ 0 & 11L/210 & L^2/105 & 0 & 13L/420 & -L^2/140 \\ 1/6 & 0 & 0 & 1/3 & 0 & 0 \\ 0 & 9/70 & 13L/420 & 0 & 13/35 & -11L/210 \\ 0 & -13L/420 & -L^2/140 & 0 & -11L/210 & L^2/105 \end{bmatrix}$$

$$\mathbf{k}^e = \begin{bmatrix} EA/L & 0 & 0 & -EA/L & 0 & 0 \\ 0 & 12EI/L^3 & 6EI/L^2 & 0 & -12EI/L^3 & 6EI/L^2 \\ 0 & 6EI/L^2 & 4EI/L & 0 & -6EI/L^2 & 2EI/L \\ -EA/L & 0 & 0 & EA/L & 0 & 0 \\ 0 & -12EI/L^3 & -6EI/L^2 & 0 & 12EI/L^3 & -6EI/L^2 \\ 0 & 6EI/L^2 & 2EI/L & 0 & -6EI/L^2 & 4EI/L \end{bmatrix}$$

$$\mathbf{R} = \begin{bmatrix} \cos \theta & \sin \theta & 0 & 0 & 0 & 0 \\ -\sin \theta & \cos \theta & 0 & 0 & 0 & 0 \\ 0 & 0 & 1 & 0 & 0 & 0 \\ 0 & 0 & 0 & \cos \theta & \sin \theta & 0 \\ 0 & 0 & 0 & -\sin \theta & \cos \theta & 0 \\ 0 & 0 & 0 & 0 & 0 & 1 \end{bmatrix}$$

where L is the length of the element, E is modulus of elasticity, A is the cross sectional area, I is the cross sectional area moment of inertia, ρ is the mass density, and θ is the angle between the local \bar{X} and global X axes. As shown in Fig. 3 the corresponding generalized displacement vector, expressed in a local coordinate system is

$$\{x_1 \ y_1 \ \alpha_1 \ x_2 \ y_2 \ \alpha_2\}^T$$

After substitution of the dimensionless speed ratio, Ω (operating speed divided by the natural frequency of the combination of links 6 and 7), equation (1) becomes

$$\Omega^2 \mathbf{M} \mathbf{U}_a'' + \mathbf{K} \mathbf{U} = \mathbf{F} \quad (2)$$

where primes denote differentiation with respect to cam rotation angle, ϕ .

For small elastic displacements, the coupling terms between the rigid body velocities and accelerations and the elastic displacements and velocities are small when

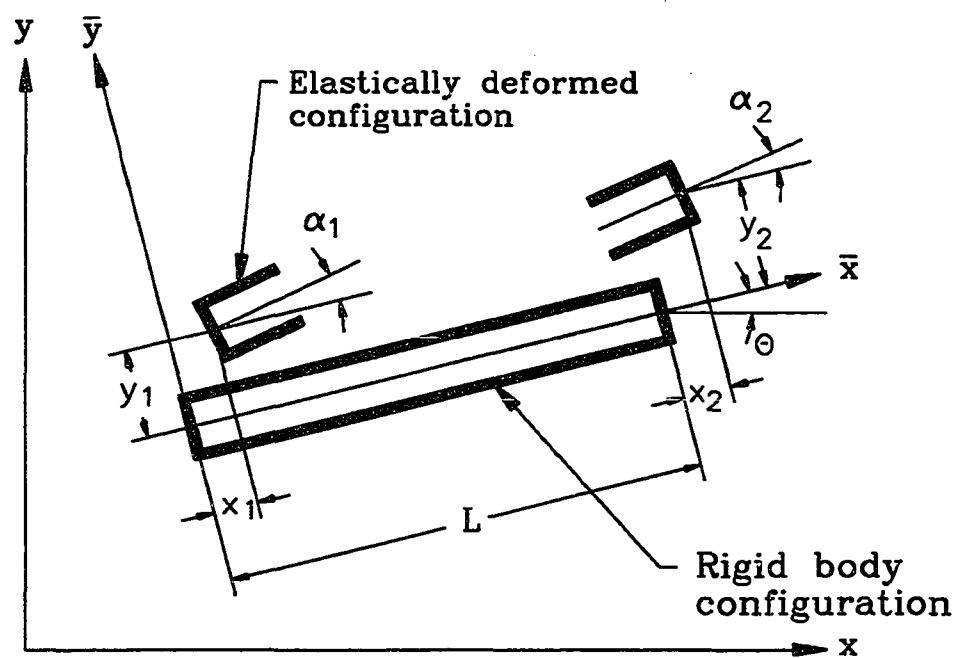


Figure 3: Rigid body and elastically deformed configurations of a beam element

compared with other terms and have generally been neglected by most investigators (Alexander and Lawrence, 1974; Turcic and Midha, 1984). Thus, the Coriolis, normal and tangential components of \mathbf{U}_a can be neglected (Midha et al., 1978). Only the rigid body and elastic components remain

$$\mathbf{U}_a'' = \mathbf{U}_r'' + \mathbf{U}''$$

SYNTHESIS

Initial synthesis

The objective of synthesis is to accurately determine the profile of the cam needed to produce the desired motion of the output member at a given operating speed and damping coefficient. The approach used here is to solve the governing equations developed in the last section by imposing known quantities and valid assumptions. For synthesis, the rigid body positions generating the desired total output motion are unknown. Since the mass and stiffness matrices in equation (1) depend on the unknown rigid body positions, an iterative procedure is developed.

For synthesis, the motion of the output member, $u_{1,a}$, is specified as a function of the cam rotation angle, ϕ . $u''_{1,a}$ can be found by differentiating $u_{1,a}$. For initial synthesis, the rigid body positions can be approximated by making u_1 zero, i.e., by imposing

$$u_{1,r} = u_{1,a} \quad (3)$$

Equation (2) then becomes:

$$\Omega^2 \begin{bmatrix} m_{1,1} & m_{1,2} & \cdots & m_{1,17} \\ m_{2,1} & m_{2,2} & \cdots & m_{2,17} \\ \vdots & \vdots & \ddots & \vdots \\ m_{17,1} & m_{17,2} & \cdots & m_{17,17} \end{bmatrix} \begin{Bmatrix} u''_{1,a} \\ u''_{2,r} + u''_2 \\ \vdots \\ u''_{17,r} + u''_{17} \end{Bmatrix}$$

$$+ \begin{bmatrix} k_{1,1} & k_{1,2} & \cdots & k_{1,17} \\ k_{2,1} & k_{2,2} & \cdots & k_{2,17} \\ \vdots & \vdots & \ddots & \vdots \\ k_{17,1} & k_{17,2} & \cdots & k_{17,17} \end{bmatrix} \begin{Bmatrix} 0 \\ u_2 \\ \vdots \\ u_{17} \end{Bmatrix} = \begin{Bmatrix} 0 \\ \vdots \\ 0 \\ f_{17} \end{Bmatrix} \quad (4)$$

where $m_{i,j}$ and $k_{i,j}$ are elements of the global system mass (\mathbf{M}) and stiffness (\mathbf{K}) matrices respectively, u_i , $u_{i,r}$, and $u_{i,a}$, are elements of \mathbf{U} , \mathbf{U}_r , and \mathbf{U}_a , respectively, and the double primes stand for second derivatives with respect to cam rotation angle, ϕ . The unknown contact force f_{17} between the cam and the follower in equations (4) does not cause difficulty for synthesis because the elastic component, u_{17} , of the distance, X_t , needed for synthesizing the cam profile can be found without considering the last equation in equations (4) as demonstrated in the following. After moving terms generated by the multiplication of the first column of the mass matrix and the known acceleration terms ($u''_{1,a}, u''_{2,r}, \dots, u''_{17,r}$) to the right hand side and eliminating the first column and the last row of the matrices, we have from equations (4),

$$\Omega^2 \begin{bmatrix} m_{1,2} & m_{1,3} & \cdots & m_{1,17} \\ m_{2,2} & m_{2,3} & \cdots & m_{2,17} \\ \vdots & \vdots & \ddots & \vdots \\ m_{16,2} & m_{16,3} & \cdots & m_{16,17} \end{bmatrix} \begin{Bmatrix} u''_2 \\ u''_3 \\ \vdots \\ u''_{17} \end{Bmatrix} + \begin{bmatrix} k_{1,2} & k_{1,3} & \cdots & k_{1,17} \\ k_{2,2} & k_{2,3} & \cdots & k_{2,17} \\ \vdots & \vdots & \ddots & \vdots \\ k_{16,2} & k_{16,3} & \cdots & k_{16,17} \end{bmatrix} \begin{Bmatrix} u_2 \\ u_3 \\ \vdots \\ u_{17} \end{Bmatrix} = -\Omega^2 \left\{ \begin{array}{l} m_{1,1}u''_{1,a} + m_{1,2}u''_{2,r} + m_{1,3}u''_{3,r} + \cdots + m_{1,17}u''_{17,r} \\ m_{2,1}u''_{1,a} + m_{2,2}u''_{2,r} + m_{2,3}u''_{3,r} + \cdots + m_{2,17}u''_{17,r} \\ \cdots \\ m_{16,1}u''_{1,a} + m_{16,2}u''_{2,r} + m_{16,3}u''_{3,r} + \cdots + m_{16,17}u''_{17,r} \end{array} \right\} \quad (5)$$

Rayleigh structural damping (Midha et al., 1978; Yang and Sadler, 1990) may be introduced by the following relationship

$$\mathbf{C} \begin{Bmatrix} u'_2 \\ u'_3 \\ \cdot \\ u'_{17} \end{Bmatrix} = \beta \mathbf{K} \begin{Bmatrix} u'_2 \\ u'_3 \\ \cdot \\ u'_{17} \end{Bmatrix} \quad (6)$$

where \mathbf{K} is the stiffness matrix of equations (5). The stiffness damping coefficient, β , is defined as $\beta = 2\zeta/\omega_1$ where ζ is the damping ratio and ω_1 is the average of the lowest natural frequency (one for every small time interval) for one cycle. The final system of equations is generated by adding equations (6) to the left hand side of equations (5).

The above system is comprised of linear ordinary differential equations with periodic coefficients and forcing terms. Their analytical expressions are so complicated that the analytical solution is hardly possible. Numerically, however, the continuous system may be approximated by successive systems with constant system parameters (Sandor and Zhuang, 1985; Midha and Turcic, 1980; Hsu and Cheng, 1974). The time period T is divided into N equal intervals, Δt , for convenience. Within each interval, the system parameters are considered constant. In this study, two numbers of intervals, 360 and 720, were used for some cases, and the results were identical for five to six digits beyond the decimal point. Thus 360 was used to solve the equations.

After imposition of the condition that the steady state solution is periodic, the problem becomes a boundary value problem in time. Finite difference methods (Sandor and Zhuang, 1985) are, therefore, applicable to solve the governing equations. With the central finite difference scheme, the first and second derivatives are approx-

imated by:

$$u'^k = (u^{k+1} - u^{k-1})/(2\Delta t) \quad (7)$$

and

$$u''^k = (u^{k+1} - 2u^k + u^{k-1})/(\Delta t)^2 \quad (8)$$

where $k-1$, k , and $k+1$ denote the time step numbers. Substitution of equations (7) and (8) into the final governing equations yields the following system of equations for time step k .

$$[2M - C\Delta t]^k U^{k-1} + [-4M + 2(\Delta t)^2 K]^k U^k + [2M + C\Delta t]^k U^{k+1} = 2(\Delta t)^2 Q^k \quad (9)$$

where M , C , and K are mass, damping, and stiffness coefficients in equations (5) and (6), and Q and U are the forcing and elastic displacement vectors in equations (5). With the periodic condition, the N sets of equations (one set for each time step) can be written in matrix form and solved efficiently (see Appendix B).

Improved synthesis

Instead of imposing the restriction on $u_{1,r}$ represented by equation (3) we can determine the rigid body positions generating the desired output motion more accurately by the following,

$$u_{17,r}^{(2)} = u_{17,r}^{(1)} + u_{17}^{(1)} \quad (10)$$

where $u_{17,r}^{(1)}$ is the rigid body displacement for coordinate 17 and $u_{17}^{(1)}$ is the elastic displacement for coordinate 17 obtained in the initial synthesis. The superscripts in the parentheses in equation (10) represent the iteration numbers. The mass and stiffness matrices which are dependent on the rigid body positions can thus be more

accurately approximated. The desired $u''_{1,a}$ is used repeatedly for consecutive synthesis as for the initial synthesis. The rigid displacement for coordinate 1, $u^{(2)}_{1,r}$, can be determined through rigid body kinematics using the rigid displacement for coordinate 17, $u^{(2)}_{17,r}$, calculated in equation (10). The approximate elastic displacement for coordinate 1, $u^{(2)}_1$, can thus be found by

$$u^{(2)}_1 = u_{1,a} - u^{(2)}_{1,r} \quad (11)$$

A system of equations similar to equations (4), except that the zero elastic displacement for coordinate 1 is replaced by the $u^{(2)}_1$ calculated in equation (11), can be formed. After moving the product of the mass matrix and the known acceleration components and the product of the first column of the stiffness matrix and the first element of the elastic deflection vector to the right hand side and then upon eliminating the first column and the last row of the matrices, we arrive at a new system of equations,

$$\Omega^2 \left[\begin{array}{ccc} m_{1,2}^{(2)} & m_{1,3}^{(2)} & \cdot & m_{1,17}^{(2)} \\ m_{2,2}^{(2)} & m_{2,3}^{(2)} & \cdot & m_{2,17}^{(2)} \\ \cdot & \cdot & \cdot & \cdot \\ m_{16,2}^{(2)} & m_{16,3}^{(2)} & \cdot & m_{16,17}^{(2)} \end{array} \right] \left\{ \begin{array}{c} u_2^{(2)''} \\ u_3^{(2)''} \\ \cdot \\ u_{17}^{(2)''} \end{array} \right\} + \left[\begin{array}{ccc} k_{1,2}^{(2)} & k_{1,3}^{(2)} & \cdot & k_{1,17}^{(2)} \\ k_{2,2}^{(2)} & k_{2,3}^{(2)} & \cdot & k_{2,17}^{(2)} \\ \cdot & \cdot & \cdot & \cdot \\ k_{16,2}^{(2)} & k_{16,3}^{(2)} & \cdot & k_{16,17}^{(2)} \end{array} \right] \left\{ \begin{array}{c} u_2^{(2)} \\ u_3^{(2)} \\ \cdot \\ u_{17}^{(2)} \end{array} \right\}$$

$$= - \left\{ \begin{array}{l} \Omega^2 [m_{1,1}^{(2)} u_{1,a}^{(2)} + m_{1,2}^{(2)} u_{2,r}^{(2)''} + \dots + m_{1,17}^{(2)} u_{17,r}^{(2)''}] + k_{1,1}^{(2)} u_1^{(2)} \\ \Omega^2 [m_{2,1}^{(2)} u_{1,a}^{(2)} + m_{2,2}^{(2)} u_{2,r}^{(2)''} + \dots + m_{2,17}^{(2)} u_{17,r}^{(2)''}] + k_{2,1}^{(2)} u_1^{(2)} \\ \dots \\ \Omega^2 [m_{16,1}^{(2)} u_{1,a}^{(2)} + m_{16,2}^{(2)} u_{2,r}^{(2)''} + \dots + m_{16,17}^{(2)} u_{17,r}^{(2)''}] + k_{16,1}^{(2)} u_1^{(2)} \end{array} \right\} \quad (12)$$

where all superscripts in parentheses denote the iteration number. The final governing equations are formed after adding the Rayleigh structural damping to the left hand

side of equations (12) as in the initial synthesis. The same central finite difference scheme used for the initial synthesis is then applied to solve the governing equations. The unknown elastic displacement, $u_{17}^{(2)}$, in equations (12) is used for the following third iteration. For the third iteration, the rigid displacement, $u_{17,r}^{(3)}$, needed in determining the rigid body positions can be found by

$$u_{17,r}^{(3)} = u_{17,r}^{(2)} + u_{17}^{(2)} = u_{17,r}^{(1)} + u_{17}^{(1)} + u_{17}^{(2)} \quad (13)$$

and the elastic displacement, $u_1^{(3)}$, is approximated by

$$u_1^{(3)} = u_{1,a} - u_{1,r}^{(3)}$$

where the rigid displacement, $u_{1,r}^{(3)}$, is determined through rigid body kinematics from the rigid displacement, $u_{17,r}^{(3)}$, calculated in equation (13). The same steps used in the second iteration are used to form the new governing equations which are again solved by the same central finite difference scheme. The above iterative procedure can be repeated until the response of the output motion is acceptable to the designer or numerical round off errors appear and prevent further refinement.

After the distance X_t ($= u_{17,r} + u_{17}$ obtained in the final iteration) is calculated, the cam profile can be determined through rigid body kinematics, since the cam itself is considered rigid in this study. The equivalent linkage approach, (Hall, 1966; Jensen, 1987; Bussell and Hubbart, 1989) which instantaneously duplicates the position, velocity, and acceleration of the actual mechanism, was used. The synthesized cam profile should be checked for undercutting. If an undesirable cam profile is generated, new values of parameters, for example, r_f , H , or Z may be used.

ANALYSIS

After the cam profile has been synthesized, the profile coordinates are known as functions of the cam rotation angle, ϕ . The same system of equations (equations (4)) is used for analysis after appropriate boundary conditions are applied. For analysis, the rigid body positions are determined by X_t . The elastic displacement, u_{17} , is set to 0, due to the assumed contact between the cam and the follower. The system of equations is formed by moving the known quantities to the right hand side and eliminating the last row and last column of the matrices,

$$\Omega^2 \begin{bmatrix} m_{1,1} & m_{1,2} & \cdots & m_{1,16} \\ m_{2,1} & m_{2,2} & \cdots & m_{2,16} \\ \vdots & \vdots & \ddots & \vdots \\ m_{16,1} & m_{16,2} & \cdots & m_{16,16} \end{bmatrix} \begin{Bmatrix} u_1'' \\ u_2'' \\ \vdots \\ u_{16}'' \end{Bmatrix} + \begin{bmatrix} k_{1,1} & k_{1,2} & \cdots & k_{1,16} \\ k_{2,1} & k_{2,2} & \cdots & k_{2,16} \\ \vdots & \vdots & \ddots & \vdots \\ k_{16,1} & k_{16,2} & \cdots & k_{16,16} \end{bmatrix} \begin{Bmatrix} u_1 \\ u_2 \\ \vdots \\ u_{16} \end{Bmatrix} = -\Omega^2 \begin{Bmatrix} m_{1,1}u_{1,r}'' + m_{1,2}u_{2,r}'' + m_{1,3}u_{3,r}'' + \cdots + m_{1,17}u_{17,r}'' \\ m_{2,1}u_{1,r}'' + m_{2,2}u_{2,r}'' + m_{2,3}u_{3,r}'' + \cdots + m_{2,17}u_{17,r}'' \\ \vdots \\ m_{16,1}u_{1,r}'' + m_{16,2}u_{2,r}'' + m_{16,3}u_{3,r}'' + \cdots + m_{16,17}u_{17,r}'' \end{Bmatrix} \quad (14)$$

The mass matrix, stiffness matrix, and second derivatives (U''_r) of the rigid displacements in equations (14) are dependent on the rigid body positions and can be determined by the known quantities X_t and X_t'' . The final governing equations are formed after introducing the Rayleigh structural damping as in the synthesis. The central finite difference scheme can again be used to solve the equations. The output response is the sum of the rigid and elastic displacements for coordinate 1,

$$u_{1,a} = u_{1,r} + u_1$$

EXAMPLE

Methods of the previous sections were used to synthesize cam profiles and then to analyze motions of the output links at various operating speeds and damping coefficients. Parameters defining the mechanisms are listed in Table 1. The total

Table 1: Cam mechanism parameters

Parameter	Output shaft	Crank	Curved coupler
Length	10.16 cm	12.70 cm	12.70 cm (L_4)
Cross-section area	2.027 cm^2	1.936 cm^2	1.293 cm^2
Cross-section height	0.5080 cm (diameter)	0.7620 cm	0.508 cm
Horizontal distance between ground pivots, H	30.48 cm		
Vertical distance between ground pivots, Z	20.32 cm		
Modulus of elasticity, E		$6.89 \times 10^7 \text{ kPa}$	
Poisson ratio, μ		0.30	
Weight density		$2.71 \times 10^3 \text{ kg/m}^3$	
Moment of inertia of output shaft, I_6		$1.843 \times 10^{-9} \text{ kg} \cdot \text{m} \cdot \text{s}^2$	
Moment of inertia of imposed mass, I_7		$120 I_6 = 2.211 \times 10^{-7} \text{ kg} \cdot \text{m} \cdot \text{s}^2$	
Radius of roller follower, r_f		1.27 cm	

degrees of freedom for the finite element model was 17. Two damping coefficients 0.00023 and 0.00075 corresponding to damping ratios of approximately 0.06 and 0.18 were used in the syntheses and analyses. The desired motion for the output link was defined in the following way: dwells at the beginning, middle, and end of each cycle lasting for 30, 60, and 30 degrees, respectively. The rise between the beginning and middle dwells was 30 degrees. A 4-5-6-7 polynomial was used to define the rise and return of the output motions. A few synthesized cam profiles are shown in Fig. 4. some differences were observed among the profiles for different speed ratios. However, the difference in profiles for damping coefficients of 0.00023 and 0.00075,

for the design speed ratio of 0.113235, for instance, was very small.

Fig. 5 shows the steady state output motion, $\theta_{7,a}$ ($= u_{1,a}$), and the synthesized rigid displacement, $\theta_{7,r}$ ($= u_{1,r}$), for the initial synthesis and iterated syntheses for the design speed ratio of 0.105757 and the damping coefficient of 0.00023 at regions possessing the largest differences between desired and simulated responses. The differences in the synthesized $\theta_{7,r}$ after the second iteration are barely observable in the figure.

The Root Mean Squared (RMS) error for the calculated steady state $\theta_{7,a}$, with reference to the desired $\theta_{7,a}$, based upon one degree increments of cam rotation over a full cycle of 360 degrees, was used to investigate the responses for different operating speeds. Fig. 6 shows the RMS values for cams designed and simulated at the same speeds for different damping coefficients. The data points were generated at the increment of 1 radian per second of cam rotation speed. As shown in Fig. 6, the responses for iterated syntheses were better than for the initial synthesis. To reach the lowest RMS values at higher speeds, more iterations were needed. This may be due to the larger differences in the rigid body positions used in the initial synthesis as compared to the true values. Generally speaking, at higher speeds the lowest RMS values were higher than those at lower speeds. After reaching the lowest RMS values, further iterations may lead to slightly higher RMS values because of computing round off errors. Since the new unknown, u_{17} , which decreases in magnitude at each iteration, may become a much smaller number compared to the other unknown coordinates as shown in Fig. 7.

As observed in Fig. 6, RMS results for those cams simulated at damping coefficients different from the design conditions generally were higher than those simulated

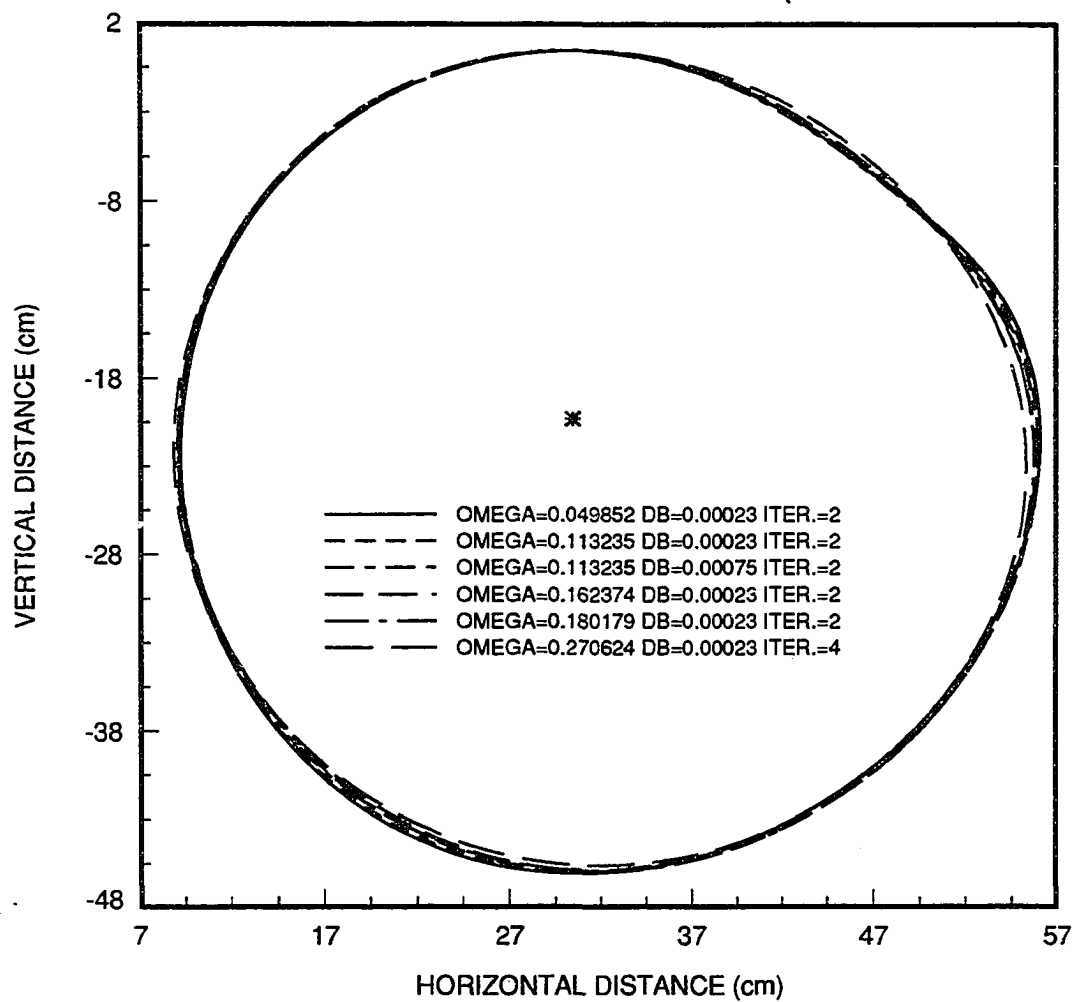


Figure 4: Synthesized cam profiles for the iterations generating lowest RMS values for different design conditions. DB stands for design damping coefficient

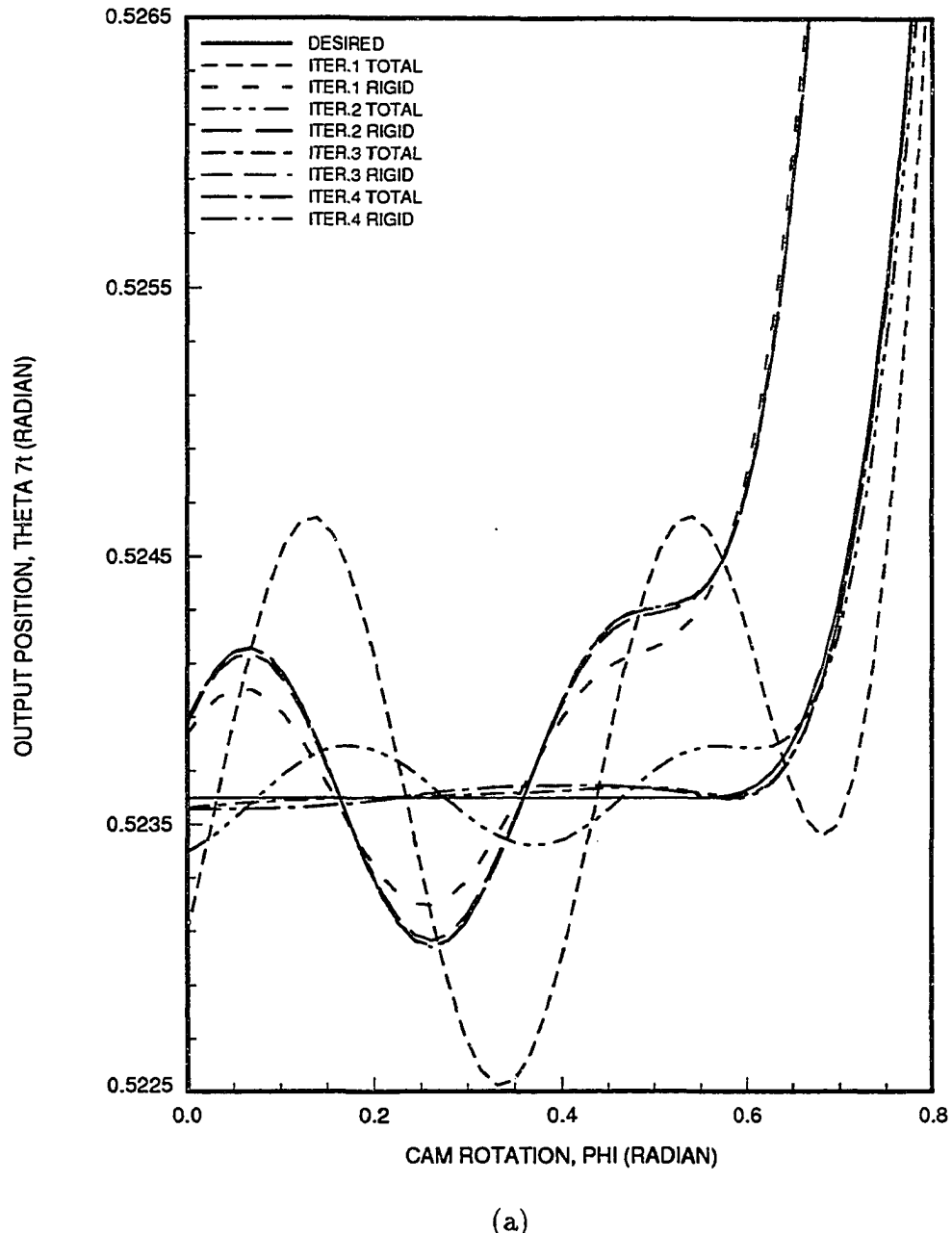
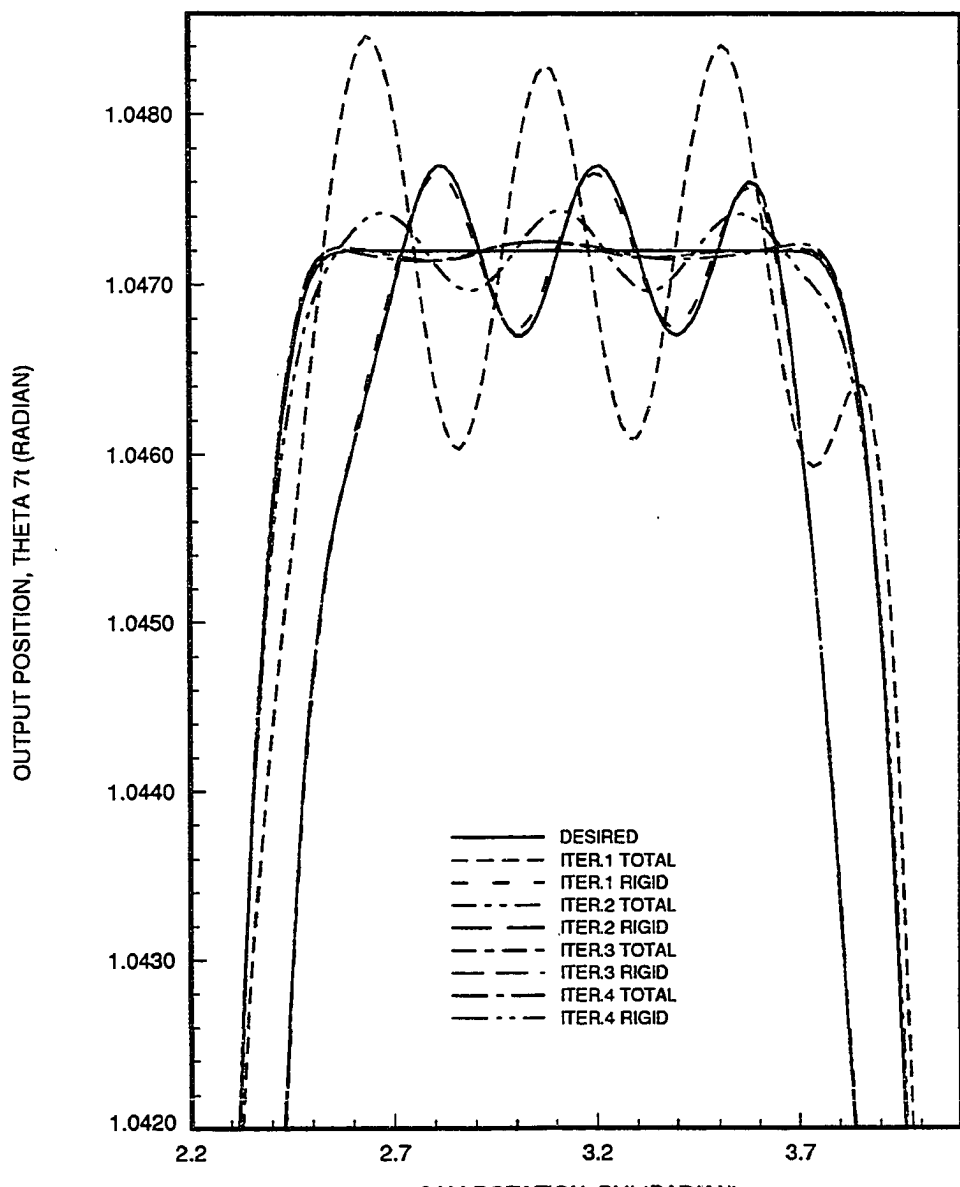
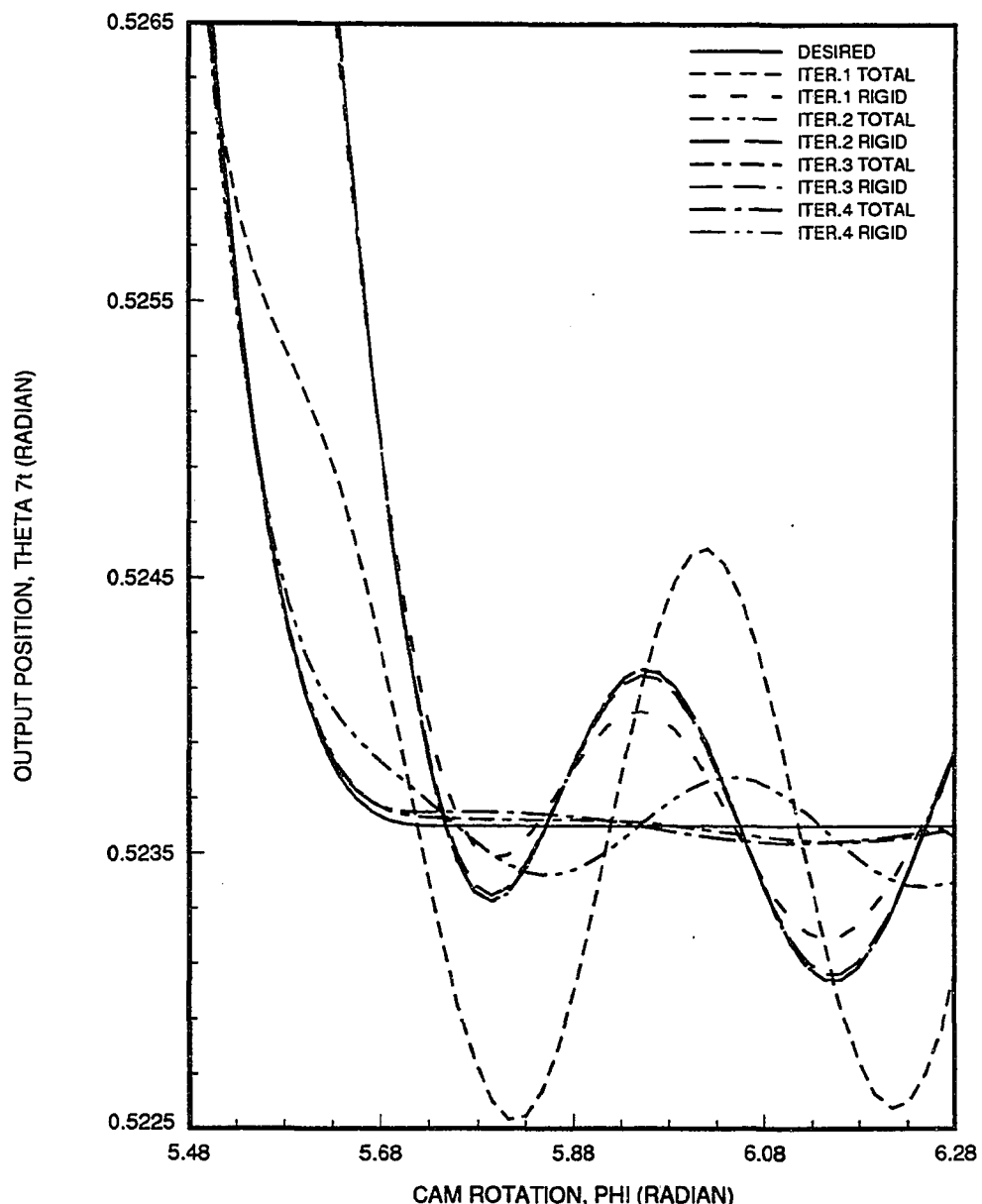


Figure 5: Desired and calculated steady state $\theta_{7,a}$ (labeled TOTAL) and $\theta_{7,r}$ for iterations 1 to 4 for the design speed ratio 0.105757 and damping coefficient 0.00023 at first dwell (a), middle dwell (b) and end dwell (c) of the cycle. The radius of curvature is 63.5 cm



(b)

Figure 5 (Continued)



(c)

Figure 5 (Continued)

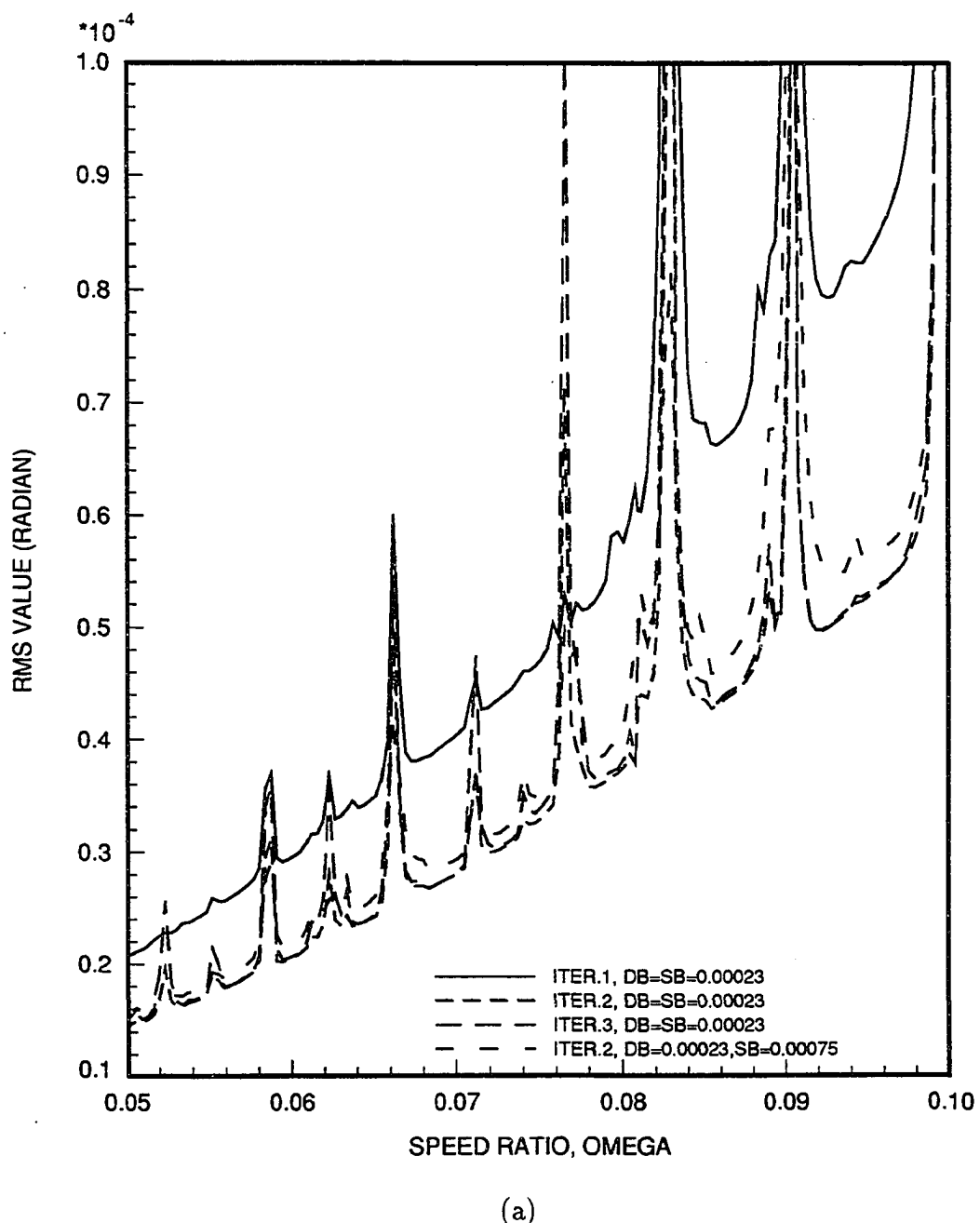


Figure 6: RMS values for different iterations for cam systems designed and simulated at the same speed ratios with design β (DB) values 0.00023 (a to e) and 0.00075 (f and g). SB stands for simulation β . The radius of curvature is 63.5 cm

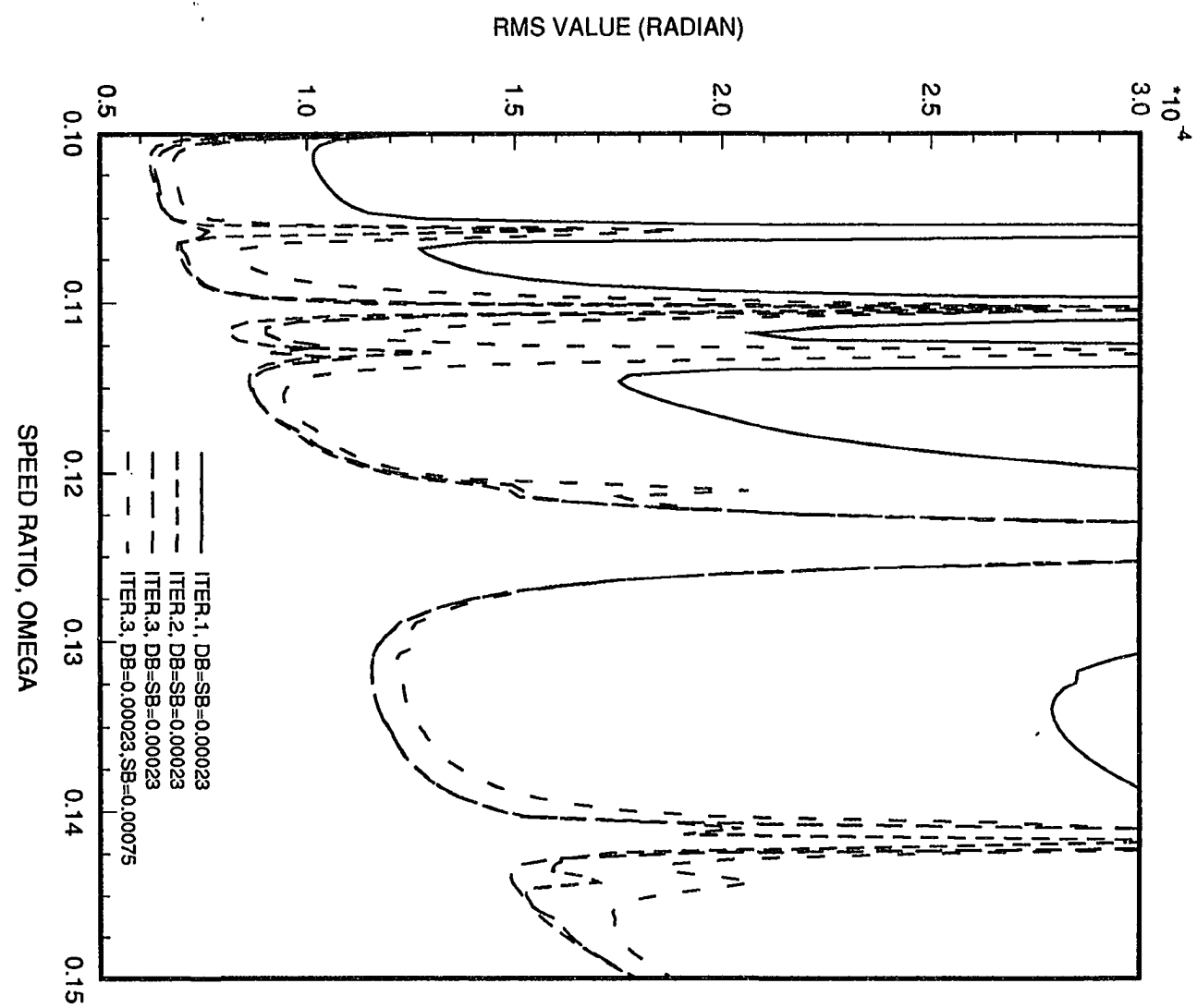
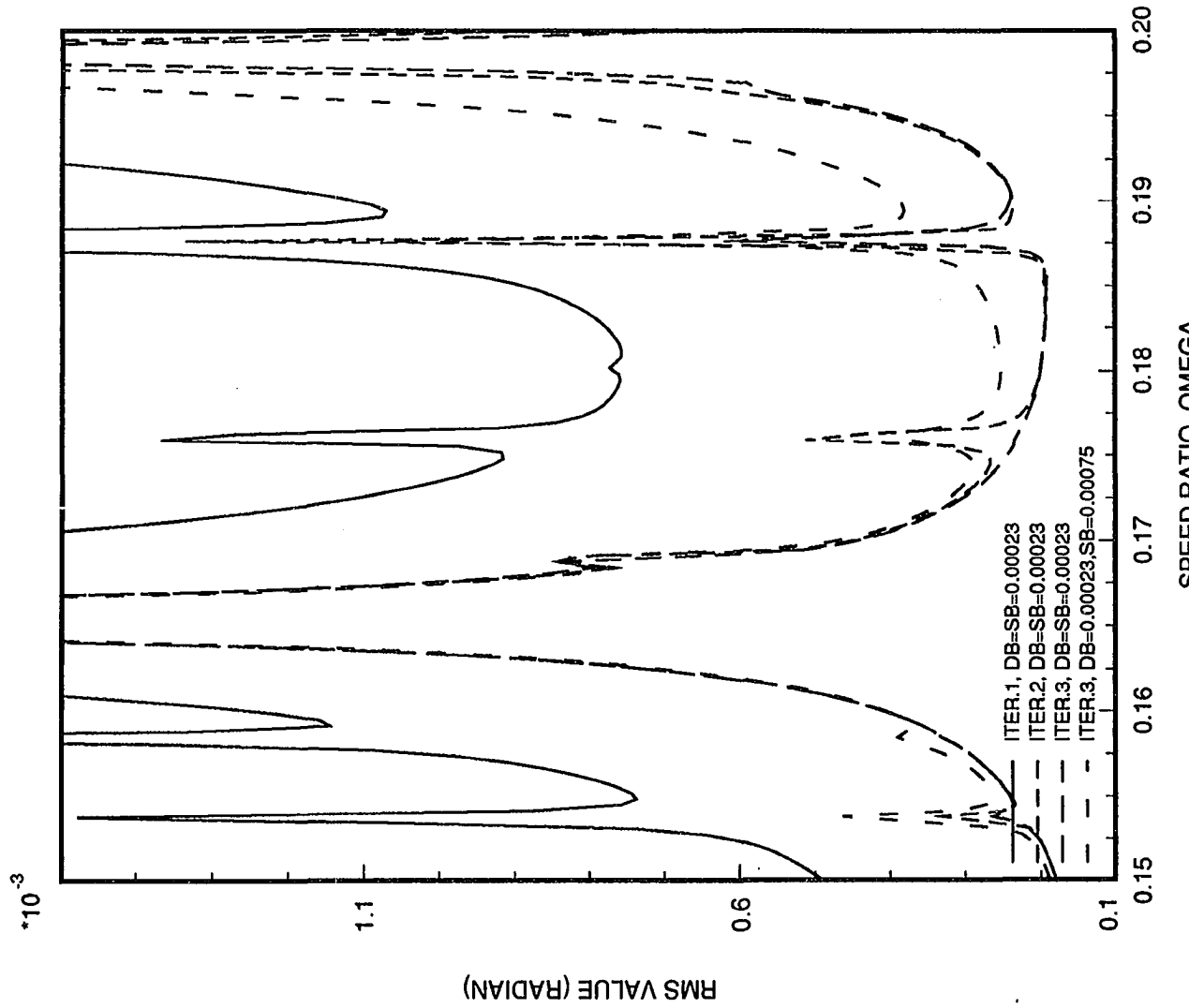
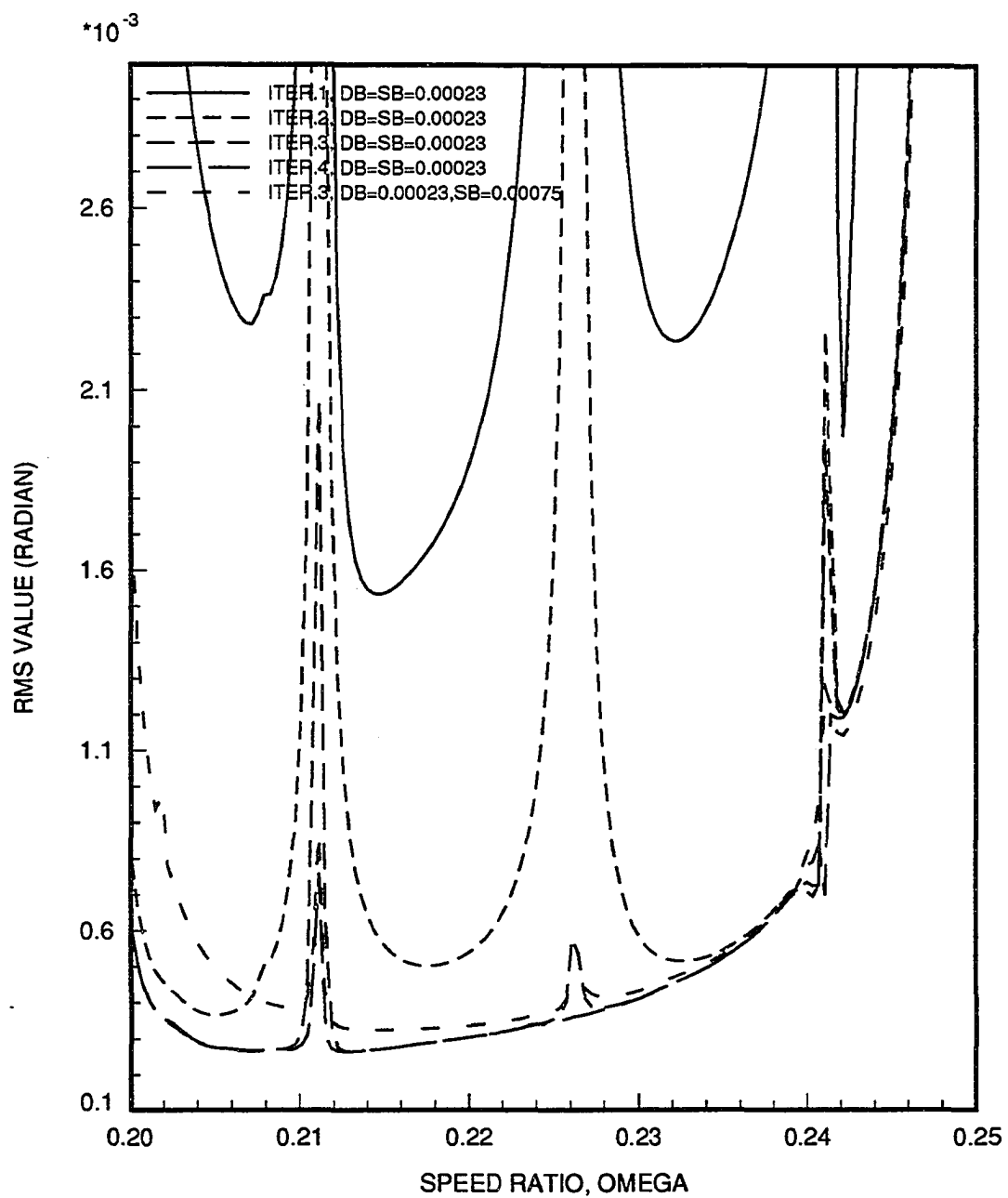


Figure 6 (Continued)



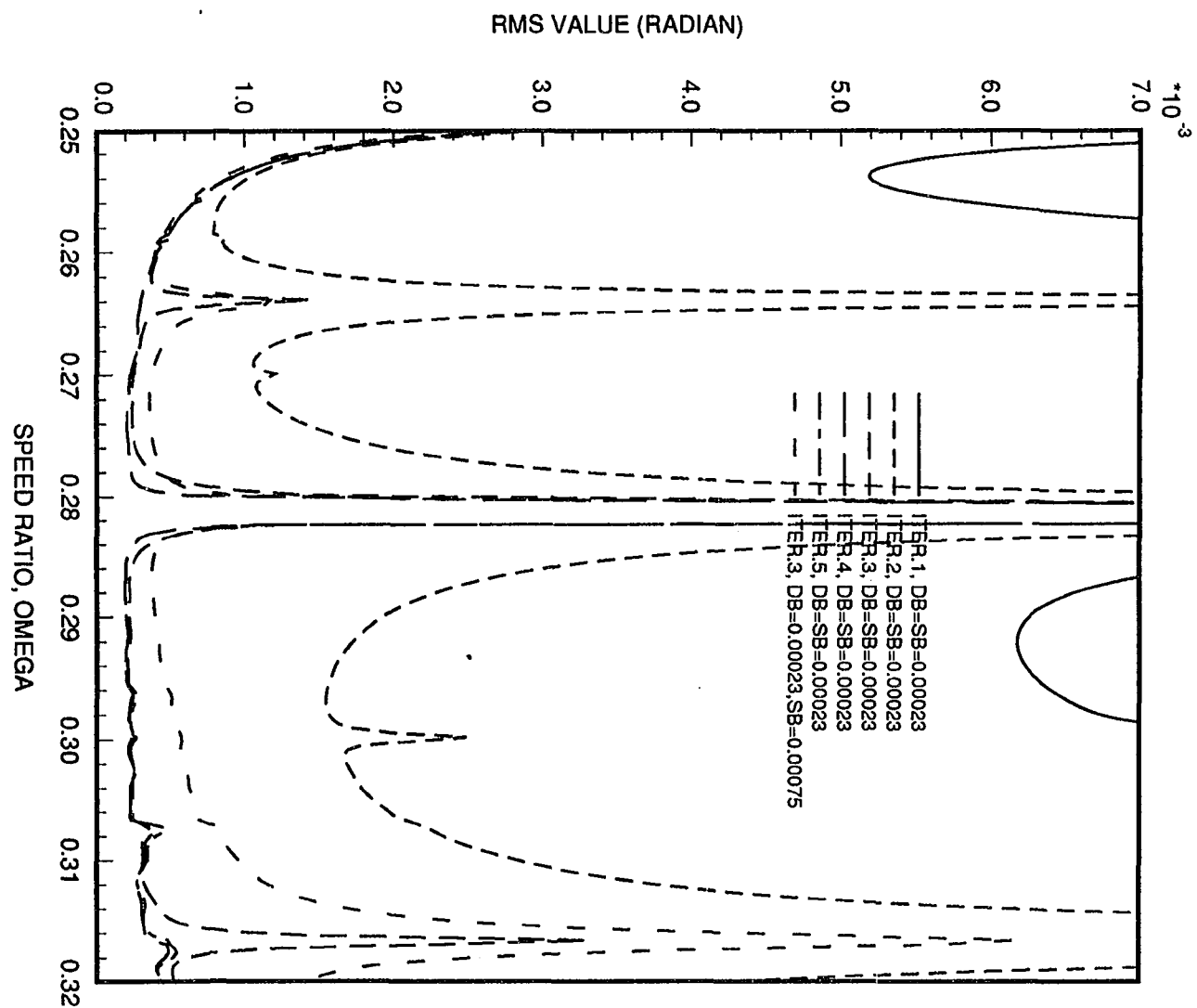
(c)

Figure 6 (Continued)



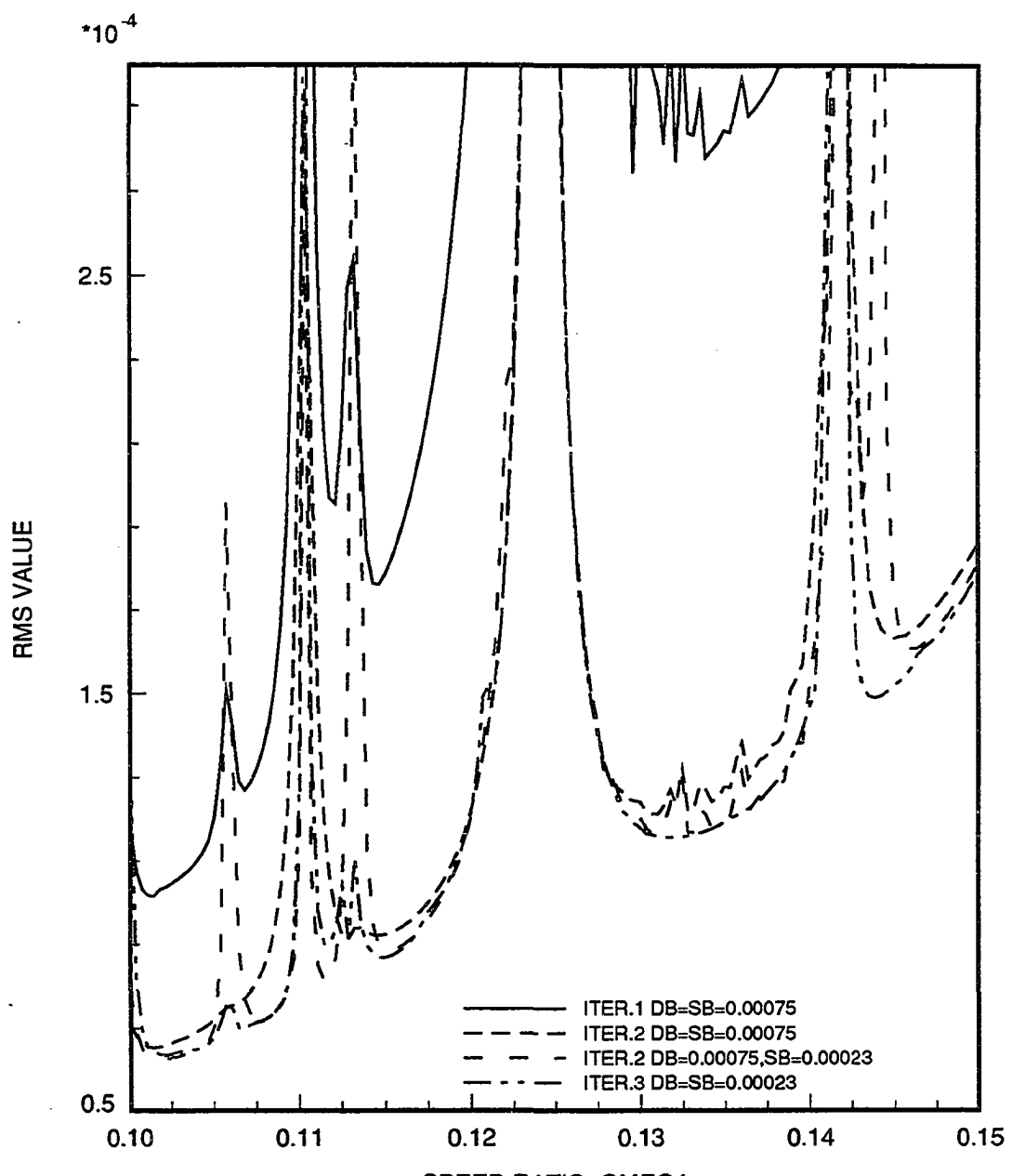
(d)

Figure 6 (Continued)



(e)

Figure 6 (Continued)



(f)

Figure 6 (Continued)

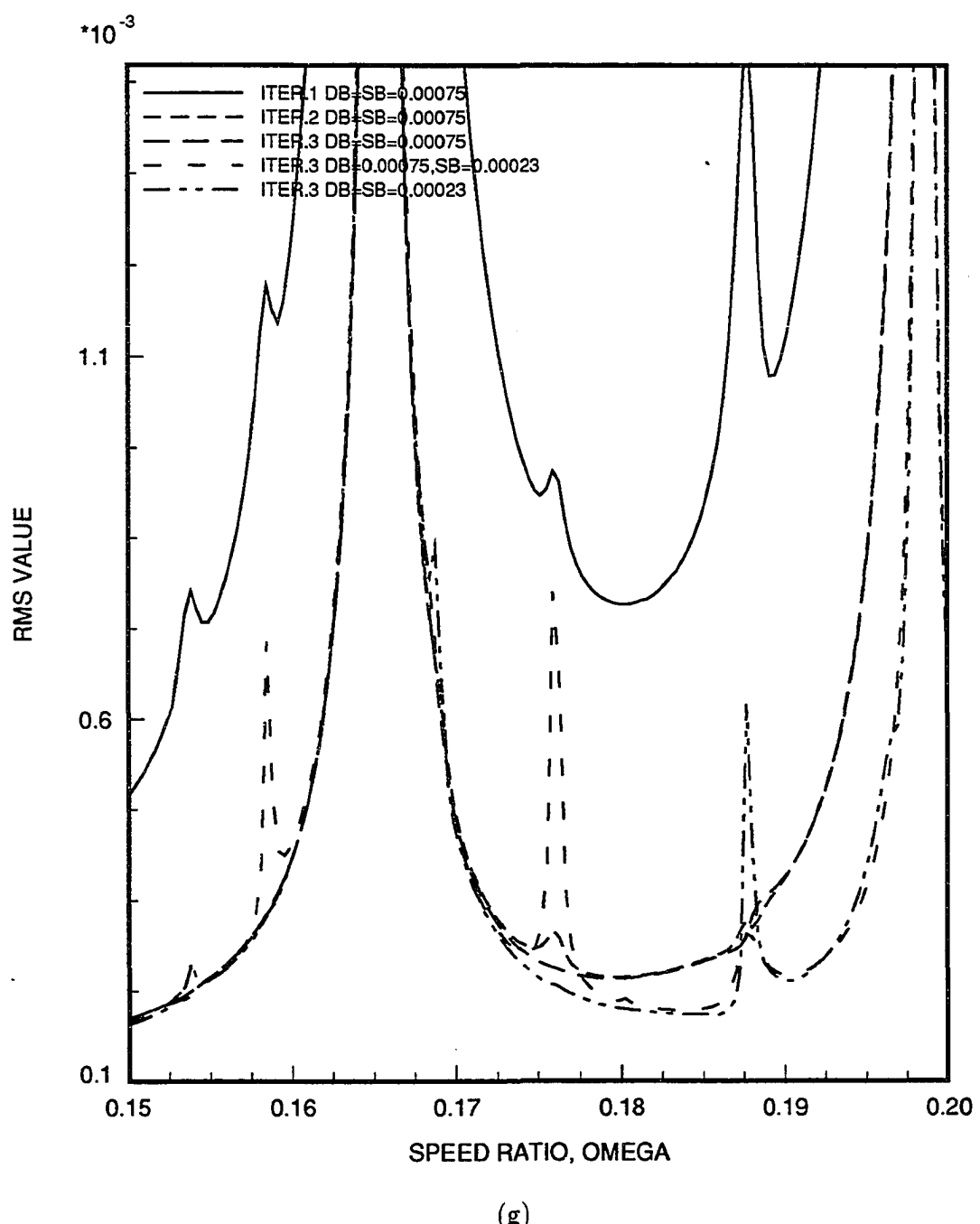


Figure 6 (Continued)

at the designed values. However, if the RMS peak was very strong, then the RMS values in the neighborhood of the peak were almost the same when simulated at the two damping coefficients shown in the figure. In the speed ratio ranges 0.130 to 0.141 and 0.178 to 0.198, the simulation damping coefficients seemed to dominate the RMS values.

A number of high RMS peaks appear in Fig. 6. Iteration in synthesis lowered some RMS peaks, which implied that in these regions the cam profiles need to be carefully designed since the difference in the cam profile between iterations was usually very little as shown in Fig. 7. Fig. 7 shows the δX_t ($= u_{17}$) derived in each iteration for the cam system discussed in Fig. 5. As expected, the δX_t generated in the first iteration was much larger than those generated in the following iterations. As shown in Fig. 5, the third iteration gave the lowest RMS error. The δX_t for the fourth and fifth iterations seemed more random than the first three iterations and may be due to numerical round off errors.

Fig. 8 shows the difference in X_t ($= X_{t,\beta=0.00023} - X_{t,\beta=0.00075}$) between cam systems designed at damping coefficients of 0.00023 and 0.00075 for various speeds. The speeds 0.113235 and 0.175906 resulted in RMS peaks in Fig. 6. The difference in X_t for the speed 0.113235 was much larger than for 0.175906.

Fig. 9 shows the RMS errors for systems designed at speed ratios of 0.106826, 0.113235, 0.180179, and 0.2706249 with damping coefficients of 0.00023 and 0.00075. The lowest RMS errors occurred at the design conditions. For the above four design speed ratios, the RMS values were 0.000068924, 0.000099029, 0.00020068, and 0.00022789 radians for the damping coefficient 0.00023; and 0.000077927, 0.000093965, 0.00024391, and 0.00032256 radians for the damping coefficient 0.00075, respectively.

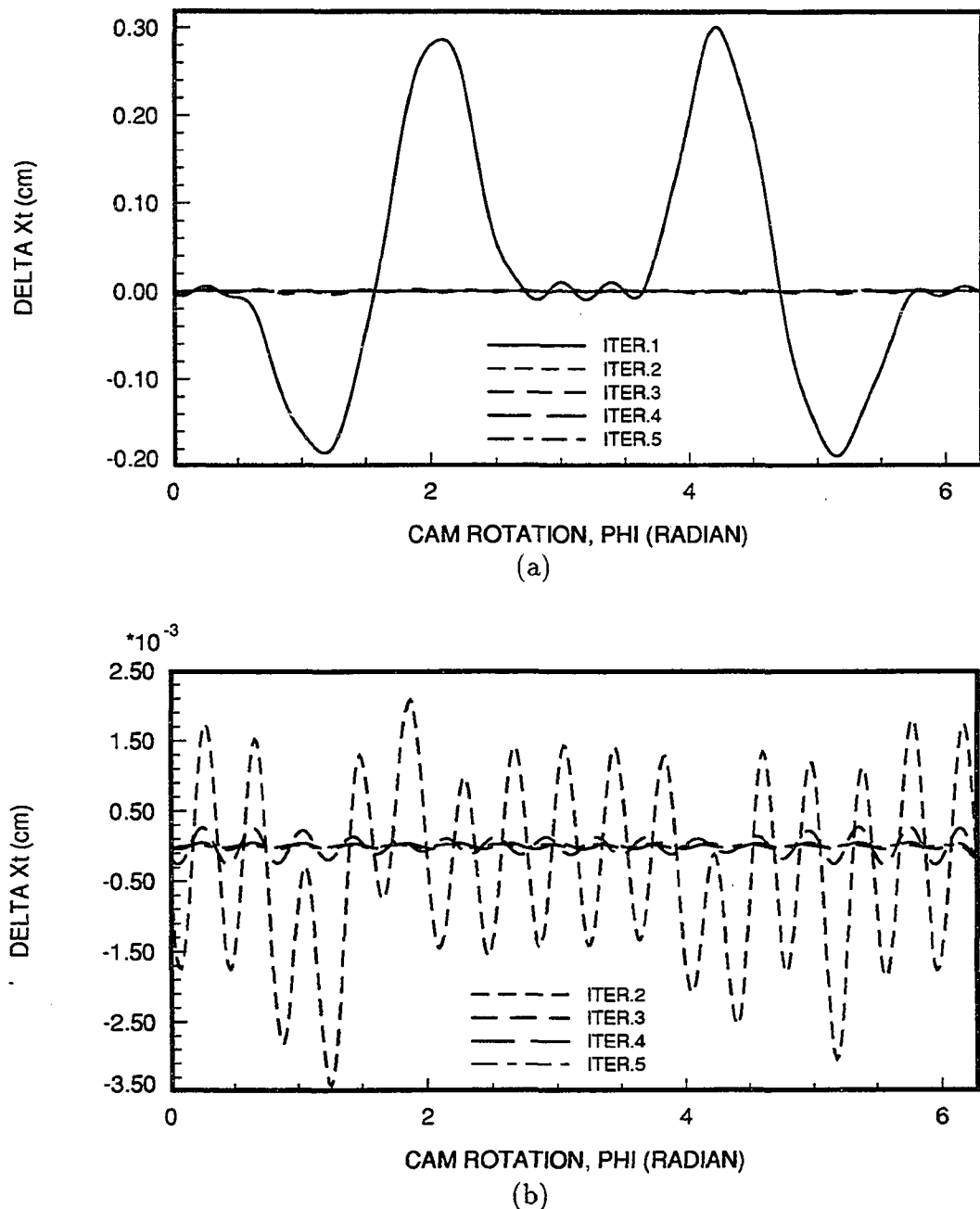


Figure 7: δX_t ($= u_{17}$) for iterations 1 to 6, for a cam system designed and simulated at the design speed ratio 0.105757 and damping coefficient 0.00023. The radius of curvature is 63.5 cm

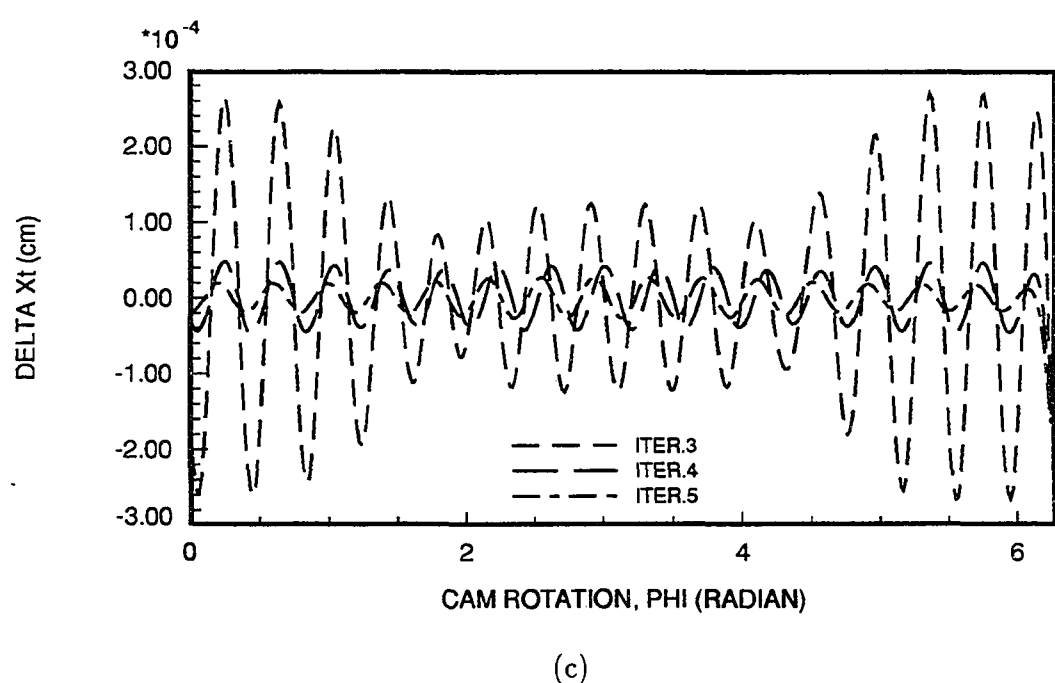


Figure 7 (Continued)

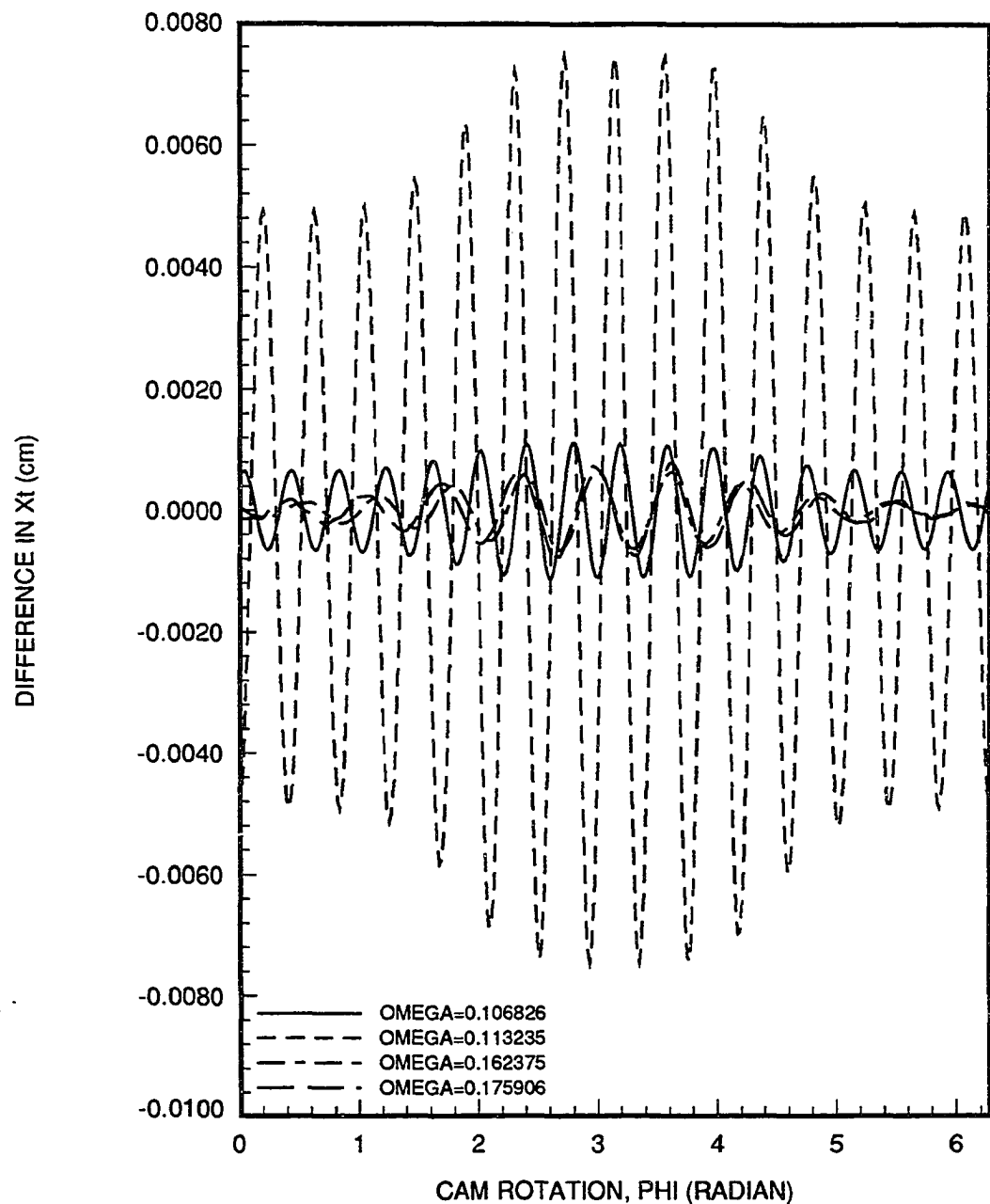
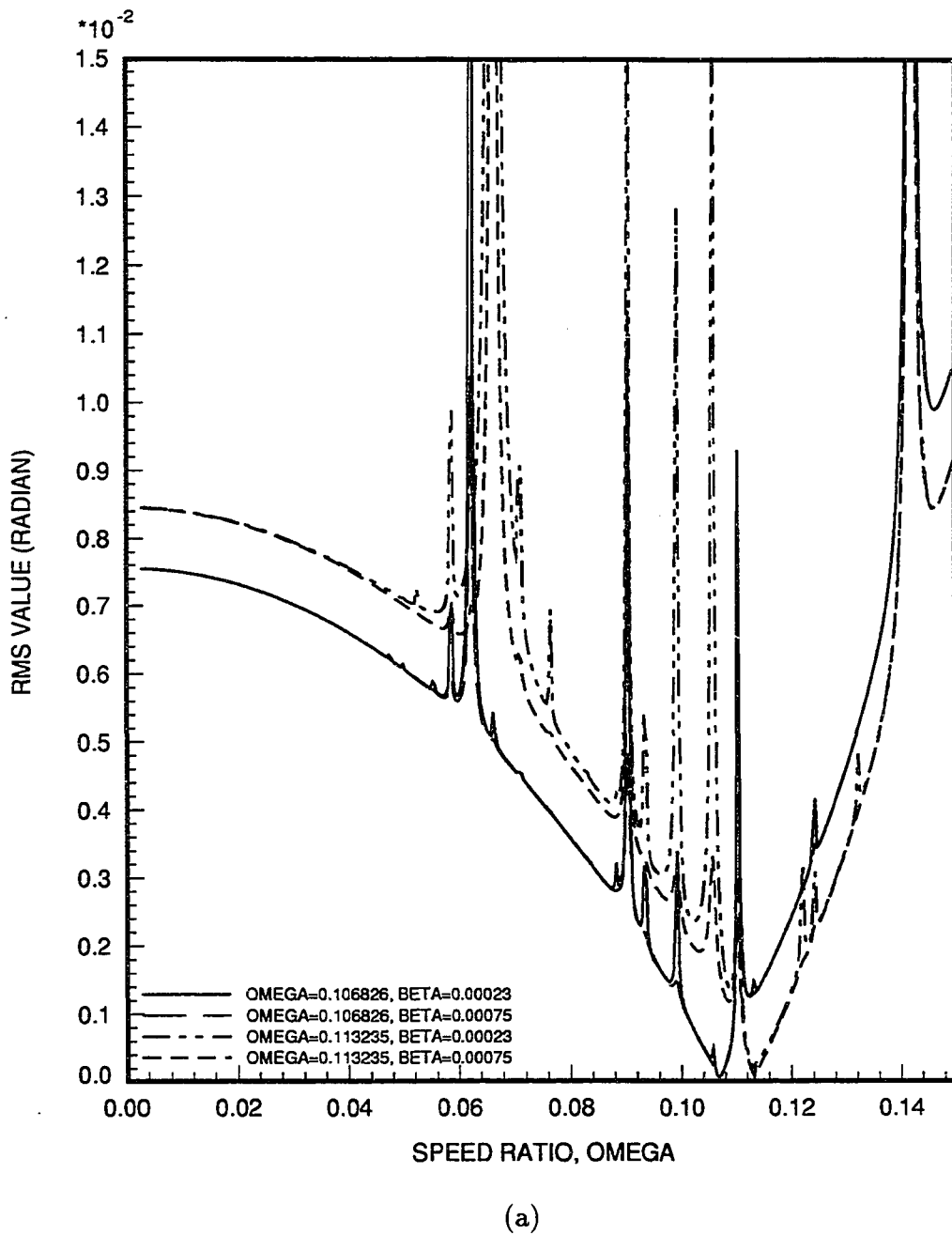


Figure 8: Difference in X_t ($=X_{t,\beta=0.00023}-X_{t,\beta=0.00075}$) between cam systems designed at damping coefficients of 0.00023 and 0.00075 for various speeds. The radius of curvature is 63.5 cm

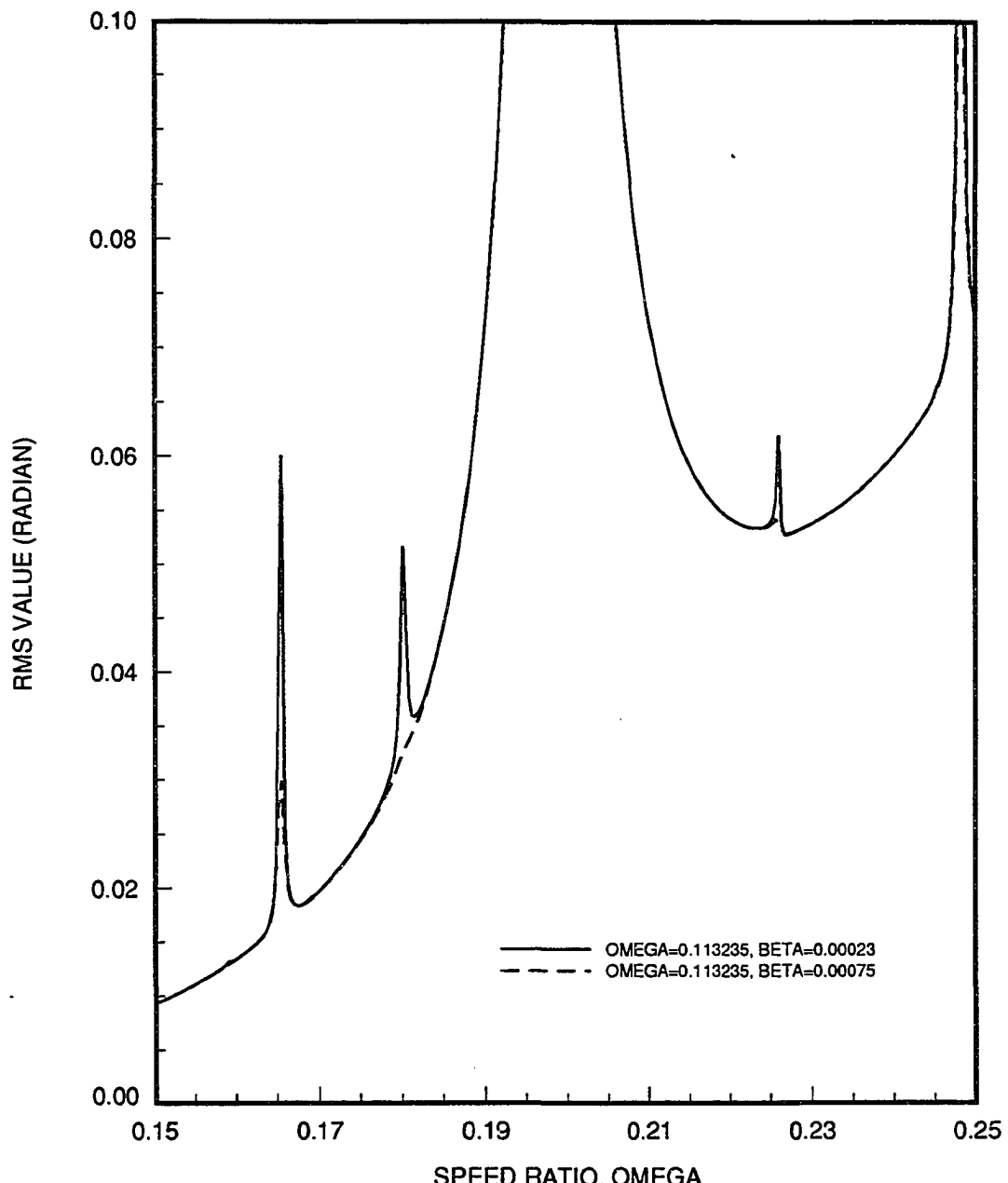
The RMS errors increased as the operating speeds moved away from the design speed, and the rate of increase was higher for systems designed at higher speeds. As shown in Fig. 9(e), for the higher design speed ratio 0.2706249, the two curves for the two different damping coefficients coincide.

Characteristic multipliers (eigenvalues of the discrete transition matrix for a whole period) determine the stability of the linear periodic systems (Müller and Schiehlen, 1985; Richards, 1983). The approximate characteristic multipliers for the cam system (Fig. 9(a)) designed at a speed ratio of 0.113235 and a damping coefficient of 0.00023 were numerically calculated by Hsu's method (Hsu and Cheng, 1973) (see Appendix C) for the speed ratio range from 0.026 to 0.35. Magnitudes of six pairs of complex characteristic multipliers were much larger than the other ten pairs. None of the magnitudes of the characteristic multipliers was larger than 1, which means that all responses were stable.



(a)

Figure 9: RMS values for cam systems designed at speed ratios 0.106826 (a), 0.113235 (a-c), 0.180179 (d), and 0.2706249 (e) with damping coefficients 0.00023 and 0.00075 and simulated at these damping coefficients. The radius of curvature is 63.5 cm



(b)

Figure 9 (Continued)

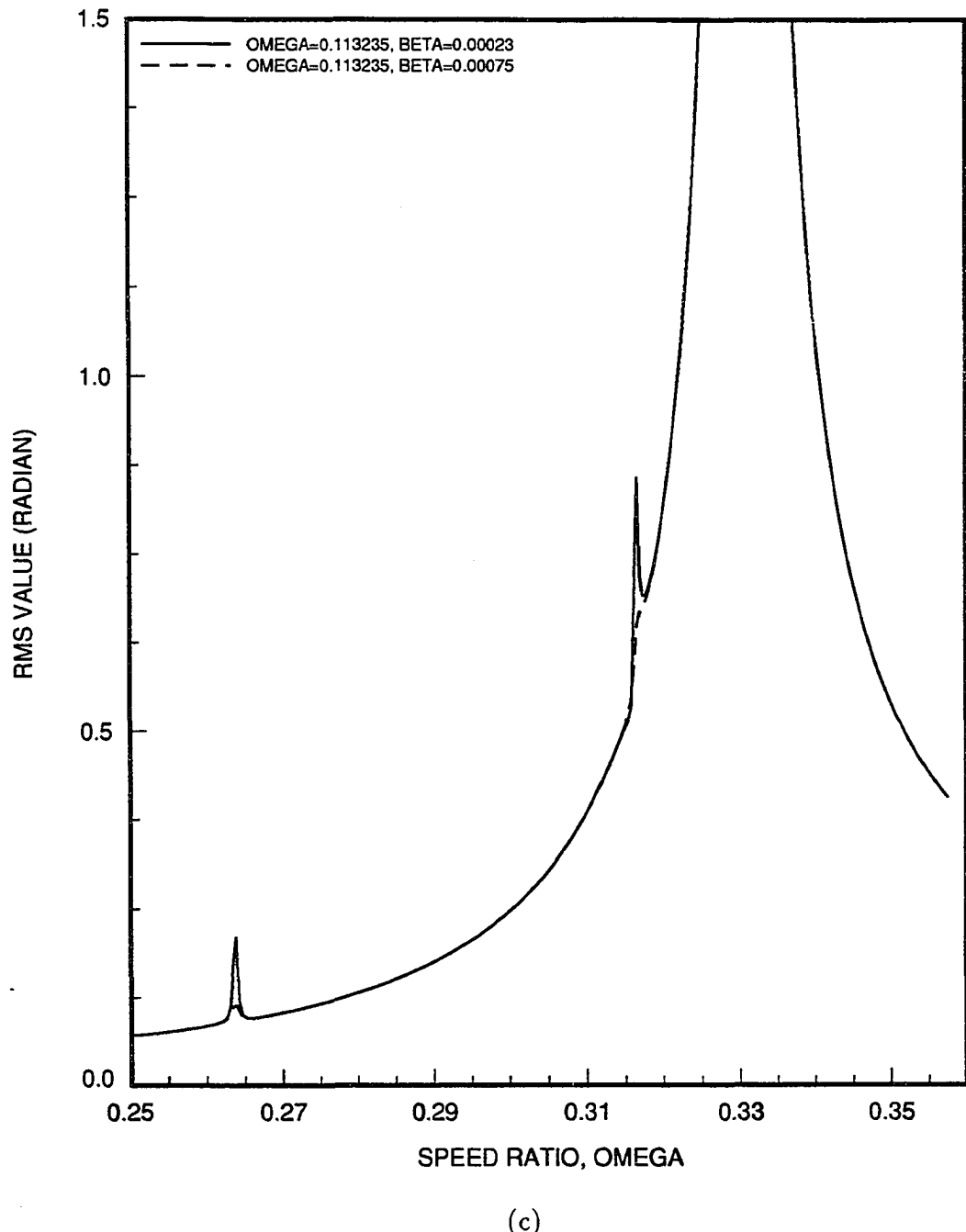


Figure 9 (Continued)

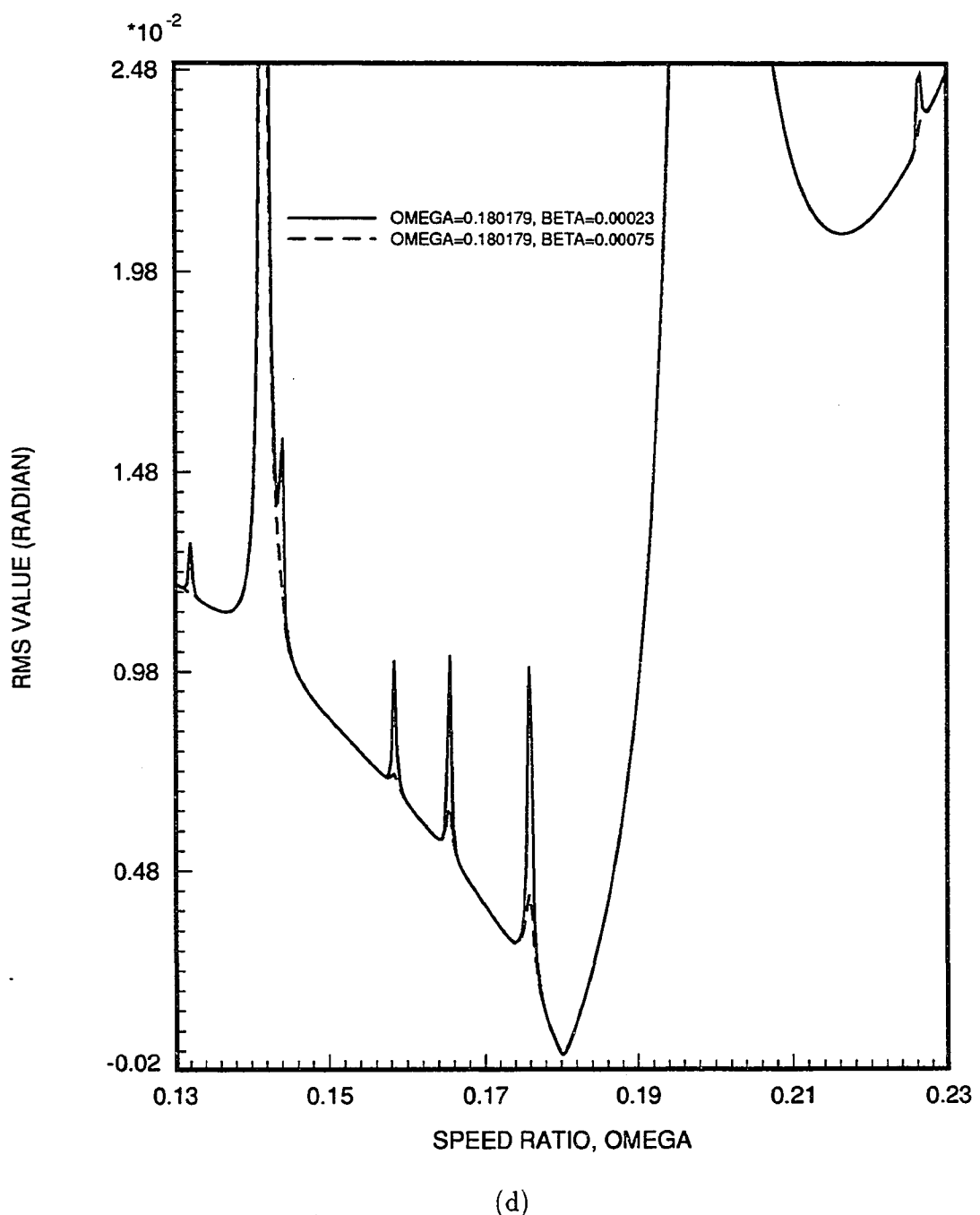
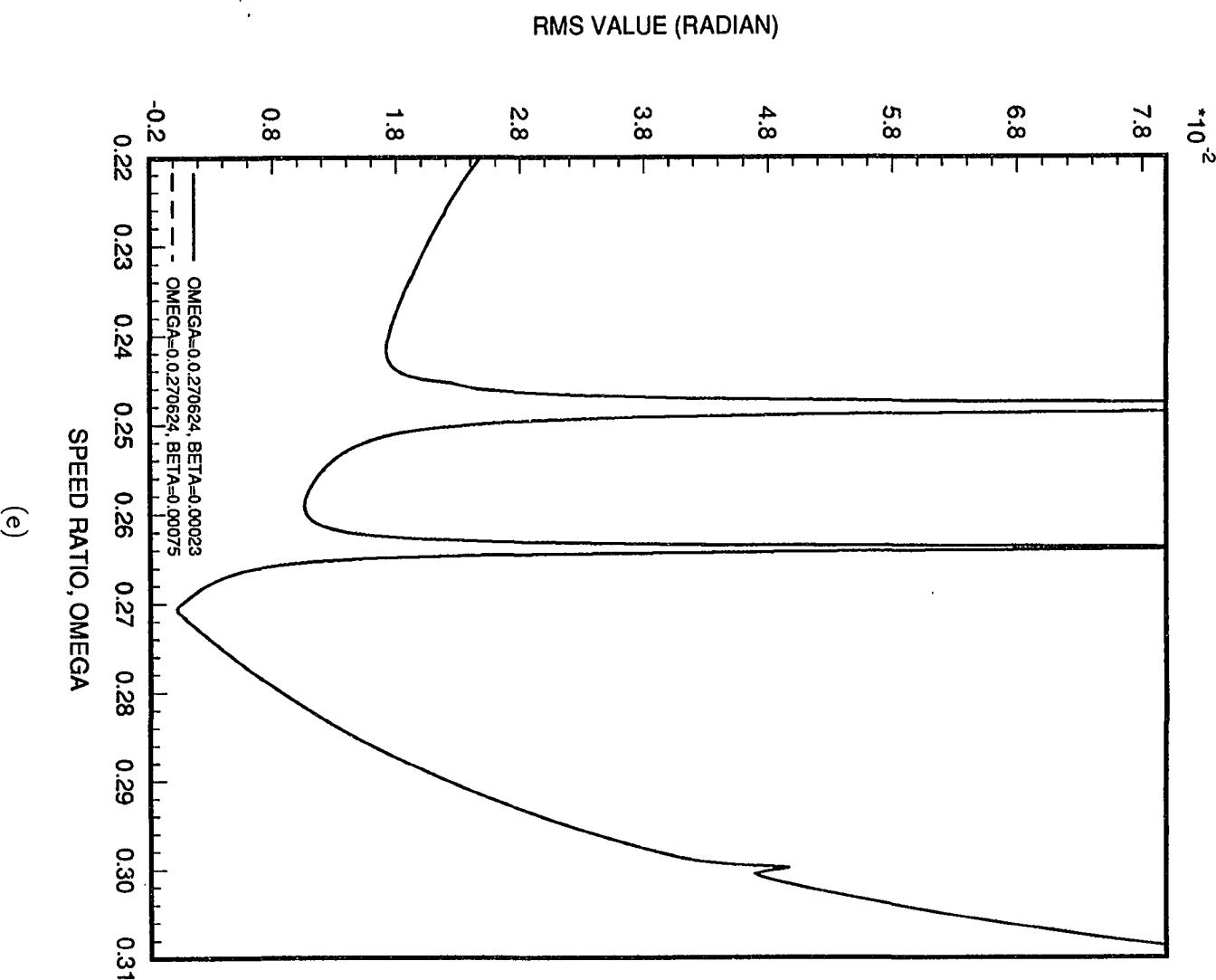


Figure 9 (Continued)



(e)

Figure 9 (Continued)

CONCLUSIONS

This work demonstrates a systematic procedure using a finite element method to synthesize and analyze a high-speed cam-operated elastic linkage. The elastic deflections induced by the large inertia of the linkage operating at a high speed were taken into account in synthesizing the cam profile. Iteration was used to generate more accurate coefficient matrices and forcing terms for the governing equations. This gave more accurate elastic deflections, u_{17} . The u_{17} produced a more accurate cam profile, and the RMS value decreased as the iteration proceeded. Since the finite element method is particularly useful for modeling objects of complex shapes, the approach is expected to be useful for more general designs.

Because of the changing geometry of the linkage, synthesized cam profiles for speeds in some zones possessed poor performance. This indicates that good or bad design speeds may be intrinsically determined by the changing geometry of the linkage. Numerical simulations may help to find good design speeds. Incorrect estimates of damping in design showed different effects on the response depending on operation speed. For the two damping coefficients used, the effects generally were not significant. The double precision data type available on a VAX/11-785 computer was used throughout this study. Whether the lowest RMS values obtained through iterations at different design conditions were limited by the round off errors or other numerical problems may need further investigation.

REFERENCES

- Alexander, R. M., and Lawrence, K. L. 1974. "An Experimental Investigation of the Dynamic Response of an Elastic Mechanism". *Journal of Engineering for Industry*, 96, No.1:268-274.
- Bussell, W., and Hubbart, T. 1989. "Four Bar Kinematic Analysis As Applied to Slider-Crank and Cams". *First National Applied Mechanisms & Robotics Conference - 1989*, Cincinnati, 89AMR-4B-7.
- Chen, F. Y. 1973. "Analysis and Design of Cam-Driven Mechanisms with Nonlinearities". *Journal of Engineering for Industry*, 95:685-694.
- Cleghorn, W. L., Tabarrok, B., and Fenton, R. G. 1984. "Critical Running Speeds and Stability of High-speed Flexible Mechanisms". *Mechanism and Machine Theory*, 19, No.3:307-317.
- Cronin, D. L., and LaBouff, G. A. 1981. "Resonances and Instabilities in Dynamic Systems Incorporating a Cam". *Journal of Mechanical Design*, 103:914-921.
- Flugrad, D. R., Jr. 1986. "Cam Synthesis and Analysis for an Elastic Follower Linkage". *Journal of Mechanisms, Transmissions, and Automation in Design*, 108:367-372.
- Gupta, K. C., and Wiederrick, J. L. 1983. "Development of Cam Profiles Using the Convolution Operator". *Journal of Mechanisms, Transmissions, and Automation in Design*, 105:654-657.
- Hall, A. S., Jr. 1966. *Kinematics and linkage design*. Balt Publishers, West Lafayette, Indiana.
- Hsu, C. S., and Cheng, W. H. 1973. "Applications of the Theory of Impulsive Parametric Excitation and New Treatments of General Parametric Excitation Problems". *Journal of Applied Mechanics*, 97:78-86.
- Hsu, C. S., and Cheng, W. H. 1974. "Steady State Response of a Dynamical System under Combined Parametric and Forcing Excitations". *Journal of Applied Mechanics*, 98:371-378.
- Jensen, P. W. 1987. *Cam design and manufacture*. 2nd ed. M. Dekker, New York.

- Johnson, R. C. 1959. "Dynamic Analysis and Design of Relatively Flexible Cam Mechanisms Having More Than One Degree of Freedom". *Journal of Engineering for Industry*, 81:323–331.
- Midha, A., and Turcic, D. A. 1980. "On the Periodic Response of Cam Mechanism with Flexible Follower and Camshaft". *Journal of Dynamic Systems, Measurement, and Control*, 102:255–264.
- Midha, A., Erdman, A. G., and Frohrib, D. A. 1978. "Finite Element Approach to Mathematical Modelling of High-Speed Elastic Linkages". *Mechanism and Machine Theory*, 13:603–618.
- Müller, P. C., and Schiehlen, W. O. 1985. *Linear Vibrations*. Martinus Nijhoff Publishers, Dordrecht, Holland.
- Nagarajan, S., and Turcic, D. 1990. "General Methods of Determining Stability and Critical Speeds for Elastic Mechanism Systems". *Mechanism and Machine Theory*, 25:209–223.
- Richards, J. A. 1983. *Analysis of Periodically Time-Varying Systems*. Springer-Verlag, New York.
- Sandor, G., and Zhuang, X. 1985. "A Linearized Lumped Parameter Approach to Vibration and Stress Analysis of Elastic Linkages". *Mechanism and Machine Theory*, 20, No.5:427–437.
- Tsay, D. M., and Huey, C. O., Jr. 1989. "Synthesis and Analysis of Cam-Follower Systems with Two Degrees of Freedom". *Advances in Design Automation - 1989*. ASME, 3:281–288.
- Turcic, D. A., and Midha, A. 1984. "Dynamic Analysis of Elastic Mechanism Systems. Part I: Applications". *Journal of Dynamic Systems, Measurements, and Control*, 106:249–254.
- Wiederrick, J. L., and Roth, B. 1975. "Dynamic Synthesis of Cams Using Finite Trigonometric Series". *Journal of Engineering for Industry*, 97:603–618.
- Yamada, Y. L., and Ezawa, Y. 1977. "On Curved Finite Elements for the Analysis of Circular Arches". *International Journal for Numerical Methods in Engineering*, 11:1735–1751.

Yang, Z., and Sadler, J. P. 1990. "Large-Displacement Finite Element Analysis of Flexible Linkages". *Journal of Mechanical Design*, 112:175–182.

GENERAL CONCLUSIONS

For both the cam-follower linkage with an output inertia, massless links and concentrated masses located at the pin joints considered in Parts I and II, and the cam-follower linkage with an output inertia and a curved beam coupler modeled with finite elements in Part III, the responses for the synthesized mechanisms were satisfactory, and they gave the lowest RMS values when simulated at the design conditions. Iteration proved to be useful in lowering RMS values, especially for speeds at or near RMS peaks. However, these high RMS speeds should not be considered as design speeds because the difference in profiles between iterations is usually very little and may require high precision manufacturing and careful maintenance. These high RMS regions are determined by the changing geometry of the linkage and can be revealed through simulations of the initial design.

The loci of characteristic multipliers were spirals on the complex plane. The magnitudes of the characteristic multipliers increased as the operating speed increased. In Parts I and II, the magnitudes of one pair of complex characteristic multipliers were much larger than the other two pairs. This lead to the conclusion that the following undesirable phenomena would occur if the dominant characteristic multipliers were locally close to point (1,0) on the complex plane: (1), the formation of the RMS peak; (2), the rise in RMS value if the design damping ratio is higher than

the true damping ratio; and (3), the generation of narrower low RMS operating zone surrounding the design speed at lower damping and higher design speed. The relative positions of the characteristic multipliers remain the same for different design speeds and damping ratios. Thus, a locus plot of the dominant characteristic multipliers from the first trial as shown in Fig. 2 in Part II may reveal speed ratios that will result in a better design. Speeds whose dominant characteristic multipliers are locally close to the critical point (1,0) should not be considered as design speeds.

In Part III, for the linkage modeled with finite elements, magnitudes of six pairs of complex characteristic multipliers were much larger than the other ten pairs. The interactions among these six dominant characteristic multipliers and the point (1,0) were much more complicated than in Part I. The difference in damping did not cause significant differences in the response, especially at higher speeds. The width of the low RMS operating zone surrounding the design speed was smaller for higher speeds than for lower speeds.

Due to fast convergence the first four terms of the infinite series of the matrix exponential (equation (5) in Part I) provided an accurate approximation of the transition matrix in a short time interval for the cam system considered in Parts I and II. In Part III, however, the first few terms of the corresponding infinite matrix exponential series did not show the same trend of convergence. A central finite difference scheme was then used in Part III to solve both synthesis and analysis equations formulated by the finite element method. To find the approximate transition matrix in a short time interval for the system of analysis equations in Part III, an approach (D'Azzo and D'Azzo, 1988) different from the infinite matrix exponential was used (see Appendix C).

The synthesis and analysis methods introduced in this work satisfactorily produced the desired output motions and provided the simulations for the models used. In a real cam design, the forces and linkage elements may be much more complicated, but the validity of the methods and basic steps would be the same.

The reasons why only one pair of dominant characteristic multipliers was found for the linkages considered in Parts I and II, and six pairs were present in Part III is worth further study. There are other areas that should also be pursued in the future. The possible effects due to different cam motions, in particular, the duration and position of dwells, on the steady state response should be studied. Whether the lowest RMS values obtained through iteration at different design conditions are limited by the round off errors or other numerical problems needs investigation. A more complete nonlinear model including Coriolis, normal and tangential components of the accelerations as well as shear deformation and rotary inertia of the moving curved beam (Gau and Shabana, 1990) should be investigated, or another model such as that proposed by Nagarajan and Turcic (1990a, 1990b) might be used to do the synthesis. The results could then be compared with the linear results. Experiments should be carried out to confirm the numerical results obtained in this research.

**APPENDIX A: INTRODUCTION TO THE NUMERICAL SCHEME
USED TO CARRY OUT HSU'S METHOD INVOLVING THE
TRANSITION MATRICES IN PART I**

Following is an introduction to the numerical scheme used to carry out Hsu's method involving the transition matrices in Part I. An alternate form of equations (52) in Part I suitable for Hsu's method is also presented.

Equation (1) gives the form of the system of inhomogeneous, periodic, linear, ordinary differential equations considered in Part I:

$$\dot{\mathbf{X}} = \mathbf{A}(t)\mathbf{X} + \mathbf{B}(t) \quad (1)$$

where $\mathbf{A}(t) = \mathbf{A}(t + T)$, \mathbf{A} is an $n \times n$ coefficient matrix, $\mathbf{B}(t) = \mathbf{B}(t + T)$, \mathbf{B} is an $n \times 1$ forcing vector, and T is the period for both \mathbf{A} and \mathbf{B} . The steady state solution for equation (1) as derived in Part I is

$$\mathbf{X}(t) = \Phi(t, t_0)\mathbf{X}(t_0) + \int_{t_0}^t \Phi(t, \tau)\mathbf{B}(\tau)d\tau \quad (2)$$

where $\Phi(t, \tau)$ is the transition matrix and $\mathbf{X}(t_0)$ is the periodic initial condition which is given by equation (4) of Part I,

$$\mathbf{X}(t_0) = [\mathbf{I} - \Phi(t_0 + T, t_0)]^{-1} \int_{t_0}^{t_0+T} \Phi(t_0 + T, \tau)\mathbf{B}(\tau)d\tau$$

The integration in equation (2) can be approximated numerically by summing the response to each impulse $\mathbf{B}(\tau)d\tau$. Suppose the period between the time instants

t_0 and $t_0 + T$ is divided into n equally spaced intervals ($t_0 + T > t_{n-1} > t_{n-2} \cdots > t_m > \cdots > t_1 > t_0$) so that the transition matrix for each interval can be numerically approximated, for example, by equation (5) of Part I. Furthermore, based on the transition property of the transition matrix (equation (6) in Part I), the periodic steady state response at the time instant t_m can be expressed through equation (2) as:

$$\begin{aligned}
\mathbf{X}(t_m) = & \Phi(t_m, t_{m-1})\Phi(t_{m-1}, t_{m-2}) \cdots \Phi(t_3, t_2)\Phi(t_2, t_1)\Phi(t_1, t_0)\mathbf{X}(t_0) \\
& + \Phi(t_m, t_{m-1})\Phi(t_{m-1}, t_{m-2}) \cdots \Phi(t_3, t_2)\Phi(t_2, t_1)\Phi(t_1, t_0)\mathbf{B}(t_0)\Delta t \\
& + \Phi(t_m, t_{m-1})\Phi(t_{m-1}, t_{m-2}) \cdots \Phi(t_3, t_2)\Phi(t_2, t_1)\mathbf{B}(t_1)\Delta t \\
& + \Phi(t_m, t_{m-1})\Phi(t_{m-1}, t_{m-2}) \cdots \Phi(t_3, t_2)\mathbf{B}(t_2)\Delta t \\
& \vdots \quad \vdots \\
& + \Phi(t_m, t_{m-1})\Phi(t_{m-1}, t_{m-2})\mathbf{B}(t_{m-2})\Delta t \\
& + \Phi(t_m, t_{m-1})\mathbf{B}(t_{m-1})\Delta t
\end{aligned} \tag{3}$$

It can easily be deduced from equation (3) that

$$\mathbf{X}(t_{m+1}) = \Phi(t_{m+1}, t_m) [\mathbf{X}(t_m) + \mathbf{B}(t_m)\Delta t] \tag{4}$$

Equation (4) is useful for writing a computer program. For a more accurate approximation, the values of the parameters at the center of each interval may be used to evaluate Φ and \mathbf{B} .

In order to apply Hsu's method to equations (52) in Part I, the system of three second order equations need to be rewritten as a system of six first order equations

in the form of equation (1):

$$\begin{aligned} \begin{Bmatrix} \theta'_{6t} \\ \theta''_{6t} \\ \delta\theta'_5 \\ \delta\theta''_5 \\ \delta r'_3 \\ \delta r''_3 \end{Bmatrix} &= \begin{bmatrix} 0 & 1 & 0 & 0 & 0 & 0 \\ -1/\Omega^2 & -2\zeta/\Omega & 1/\Omega^2 & 2\zeta/\Omega & 0 & 0 \\ 0 & 0 & 0 & 1 & 0 & 0 \\ 1/(m_d\Omega^2) & 2\zeta/(m_d\Omega) & a_{4,3} & a_{4,4} & a_{4,5} & a_{4,6} \\ 0 & 0 & 0 & 0 & 0 & 1 \\ 0 & 0 & a_{6,3} & a_{6,4} & a_{6,5} & a_{6,6} \end{bmatrix} \begin{Bmatrix} \theta_{6t} \\ \theta'_{6t} \\ \delta\theta_5 \\ \delta\theta'_5 \\ \delta r_3 \\ \delta r'_3 \end{Bmatrix} \\ &+ \begin{Bmatrix} 0 \\ 2\zeta\theta'_5/\Omega + \theta_5/\Omega^2 \\ 0 \\ -\theta''_5 - 2\zeta\theta'_5/(m_d\Omega) - \theta_5/(m_d\Omega^2) \\ 0 \\ x'' \end{Bmatrix} \quad (5) \end{aligned}$$

where

$$\begin{aligned} a_{4,3} &= -\left\{1 + S_4 \sin^2(\theta_4 - \theta_5) - \zeta\Omega D_4(\theta'_5 - \theta'_4) \sin[2(\theta_4 - \theta_5)]\right\} / (m_d\Omega^2) \\ a_{4,4} &= -2\zeta [1 + D_4 \sin^2(\theta_4 - \theta_5)] / (m_d\Omega) \\ a_{4,5} &= -S_4 \cos\theta_4 \sin(\theta_4 - \theta_5) / (m_d\Omega^2) \\ a_{4,6} &= -2\zeta D_4 \cos\theta_4 \sin(\theta_4 - \theta_5) / (m_d\Omega) \\ a_{6,3} &= -\left\{S_4 \cos\theta_4 \sin(\theta_4 - \theta_5) - 2\zeta\Omega D_4(\theta'_5 - \theta'_4) \cos\theta_4 \cos(\theta_4 - \theta_5)\right\} / (m_c\Omega^2) \\ a_{6,4} &= -2\zeta D_4 \cos\theta_4 \sin(\theta_4 - \theta_5) / (m_c\Omega) \\ a_{6,5} &= -[S_3 + S_4 \cos^2\theta_4] / (m_c\Omega^2) \\ a_{6,6} &= -2\zeta [D_3 + D_4 \cos^2\theta_4] / (m_c\Omega) \end{aligned}$$

By comparing equations (5) and (1), it is apparent that $\mathbf{A}(t)$ is the 6×6 coefficient matrix above and $\mathbf{B}(t)$ is the 6×1 forcing vector on the right hand side.

**APPENDIX B: A SYSTEM OF EQUATIONS DERIVED FROM THE
GOVERNING EQUATIONS BY CENTRAL FINITE DIFFERENCE
SCHEME IN PART III**

The following is a system of n equations obtained by combining the equation (equation (9) in part III) for each of n equally spaced time steps in a whole period of T . The superscripts stand for time step numbers.

$$\left[\begin{array}{ccccccccc} P^1 & S^1 & 0 & 0 & 0 & \dots & \dots & \dots & 0 & 0 & R^1 \\ R^2 & P^2 & S^2 & 0 & 0 & \dots & \dots & \dots & 0 & 0 & 0 \\ 0 & R^3 & P^3 & S^3 & 0 & \dots & \dots & \dots & 0 & 0 & 0 \\ 0 & 0 & R^4 & P^4 & S^4 & 0 & \dots & \dots & 0 & 0 & 0 \\ \vdots & \vdots \\ 0 & 0 & 0 & 0 & \dots & \dots & 0 & R^{n-2} & P^{n-2} & S^{n-2} & 0 \\ 0 & 0 & 0 & 0 & 0 & \dots & \dots & 0 & R^{n-1} & P^{n-1} & S^{n-1} \\ S^n & 0 & 0 & 0 & 0 & 0 & \dots & \dots & 0 & R^n & P^n \end{array} \right] \left\{ \begin{array}{c} U^1 \\ U^2 \\ U^3 \\ U^4 \\ \vdots \\ U^{n-2} \\ U^{n-1} \\ U^n \end{array} \right\}$$

$$= 2(\Delta t)^2 \left\{ \begin{array}{c} \mathbf{Q}^1 \\ \mathbf{Q}^2 \\ \mathbf{Q}^3 \\ \mathbf{Q}^4 \\ \vdots \\ \mathbf{Q}^{n-2} \\ \mathbf{Q}^{n-1} \\ \mathbf{Q}^n \end{array} \right\}$$

where

$$\mathbf{R}^k = [2\mathbf{M} - \mathbf{C}\Delta t]^k$$

$$\mathbf{P}^k = [-4\mathbf{M} + 2(\Delta t)^2 \mathbf{K}]^k$$

$$\mathbf{S}^k = [2\mathbf{M} + \mathbf{C}\Delta t]^k$$

$$\Delta t = T/n$$

APPENDIX C: METHOD TO FIND THE CHARACTERISTIC MULTIPLIERS FOR THE ANALYSIS EQUATIONS IN PART III

In Part III, a numerical approach different from equation (5) in Part I is used to find the transition matrix in a short time interval for the system of analysis equations. This is because in each short time interval the first few terms of the corresponding infinite matrix exponential series (equation (5) in Part I) did not show the trend of convergence. This different approach (D'Azzo and D'Azzo, 1988) finds the transition matrix for a system with constant coefficient matrix \mathbf{A} (equation (1) in Part I) for the time duration, Δt . For a 6×6 constant coefficient matrix, \mathbf{A} , the transition matrix is

$$\Phi(t_0 + \Delta t, t_0) = \mathbf{P}^{-1} \begin{bmatrix} e^{\lambda_1 \Delta t} & 0 & 0 & 0 & 0 & 0 \\ 0 & e^{\lambda_2 \Delta t} & 0 & 0 & 0 & 0 \\ 0 & 0 & e^{\lambda_3 \Delta t} & 0 & 0 & 0 \\ 0 & 0 & 0 & e^{\lambda_4 \Delta t} & 0 & 0 \\ 0 & 0 & 0 & 0 & e^{\lambda_5 \Delta t} & 0 \\ 0 & 0 & 0 & 0 & 0 & e^{\lambda_6 \Delta t} \end{bmatrix} \mathbf{P}$$

where the λ_i are the eigenvalues of \mathbf{A} , and the \mathbf{P} is composed of the corresponding eigenvectors of \mathbf{A} .

This approach cannot be applied to the synthesis equations in Part III because

in each short time interval some of the corresponding λ_i are positive real numbers or complex conjugates with positive real parts with large magnitudes. These positive real numbers or positive real parts make $e^{\lambda_i \Delta t}$ big enough to cause floating overflow in the computer. The generation of these λ_i with positive real numbers or positive real parts is due to the unsymmetric elimination of the *last row* and the *first column* of the symmetric matrices in equations (4) in Part III. If the elimination were symmetric, (for example, the elimination of the *last row* and the *last column*) then the λ_i would all be negative real numbers or complex conjugates with negative real parts. The floating overflow problem would then never occur. For analysis problems in Part III, the elimination is symmetric since the linkage is treated as a structure in each short time interval. The *last row* and the *last column* of the matrices in equations (4) in part III are eliminated when the boundary conditions are applied and all the λ_i are negative real numbers or complex conjugates with negative real parts.

After the transition matrix for a short time interval is found, the discrete transition matrix for the whole period is then calculated through equation (6) in Part I. The characteristic multipliers are the eigenvalues of this discrete transition matrix and can easily be obtained numerically.

APPENDIX D: FORTRAN PROGRAMS FOR PARTS I AND II

```

C...Main program for Part I
c      RMC=mc, RMD=md, DSR=OMEGA, T4=THETA 4, T5=THETA 5,
C      T6=THETA 6, EX=DELTA X
c      KLISYN: no. of intervals used for synthesis
c      KLIMIT: no. of intervals used for analysis
PARAMETER NKEEP=360,NKY=216000
IMPLICIT REAL*8(A-H,O-Z)
DIMENSION COEFF(5),DSRT(20),XDATA(0:NKY),ZETAA(5),NAAN(10)
COMMON /CT6/T6(0:NKEEP)
COMMON /NPI/PI
COMMON /NAME1/NCAM,D,R3,R4,S3,S4,D4,D3
COMMON /NAME2/DSR
COMMON /XDA/XDATA,COEFF
COMMON /NRM/RMC,RMD
COMMON /NGK/KLISYN,KLIMIT,KSKIP,MSTEP,MCASTEP,NXFCA
COMMON /CTT/PERIOD,DELS,DELA,NSY,NDATA,NSEA
COMMON /NAA/ZETA,MXT,MEXCA,MXTCA,NCOEFF
& ,MOEVA,NMEOUT,MSTEADY,MEVAME,MEVARMS,MDISALL,MRMS
DATA R3/1.0/ R4/2.0/ S3/1.0/ S4/1.0/ D/0./ D4/1./ D3/1./
OPEN(91,FILE='LUMIMPI.DAT',STATUS='OLD')
READ(91,*)RMC,RMD,ZETA
READ(91,*)MOUT,NCAM,KLISYN,KLIMIT,MXT
READ(91,*)MEXCA,MXTCA,MCASTEP,MSTEP,NXFCA
READ(91,*)NCOEFF,NDATA,MOEVA,NMEOUT
READ(91,*)MSTEADY,MEVAME,MEVARMS,MDISALL,MRMS
READ(91,*)(NAAN(I),I=1,7)
READ(91,*)NUM,NITE,NSEA,NOA
READ(91,*)DSTA,DINC
DO 725 I=1,NOA

```

```

25      READ(91,*)ZETAA(I)
CLOSE (91)
DO 901 I=1,NUM
901    DSRT(I)=DSTA+(I-1)*DINC
IF (MEVARMS .EQ. 1) OPEN(19,FILE='EVRME',STATUS='NEW')
IF (MEVAME .EQ. 1) THEN
OPEN(16,FILE='EVAME',STATUS='NEW')
ENDIF
IF (MRMS .EQ. 1) THEN
OPEN(14,FILE='RMSME',STATUS='NEW')
OPEN(81,FILE='T6P61',STATUS='OLD') !desired output
DO 29 I=0,NKEEP
29      READ(81,*)T6(I)
CLOSE (81)
ENDIF
ZETAS=ZETA
PI=ACOS(-1.)
PERIOD=2.*PI
DELA=PERIOD/KLIMIT
DELS=PERIOD/KLISYN
COEFF(1)=1.
COEFF(2)=DELA
COEFF(3)=COEFF(2)**2/2.
COEFF(4)=COEFF(2)**3/6.
HD=PERIOD/NKY
DO 864 I=0,NKY
864    XDATA(I)=HD*I
DO 98 I=1,NUM
DSR=DSRT(I)
DO 98 II=1,NITE
NSY=II
ZETA=ZETAS
CALL SYNL6IMP !initial and iterated synthesis subroutine
IF (NAAN(II) .EQ. 1) CALL XFA6CVALL !analysis subroutine
CLOSE (NSY)
IF (NSEA .EQ. II) THEN
NSY=30                      !for RMS file
DO 265 JJ=1,NOA
NSY=NSY+1
ZETA=ZETAA(JJ)

```

```

        CALL XFA6CVALL
265      CLOSE (NSY)
        ENDIF
98      CONTINUE
        END

c...initial and iterated synthesis
c...using Hsu's step functions
        SUBROUTINE SYNL6IMP
        PARAMETER KDIM=216000,CHECK='FALSE'
        IMPLICIT REAL*8 (A-H,O-Z)
        DIMENSION XEXME(0:KDIM),FME(0:KDIM),ER4KEEP(0:KDIM)
&      ,XME(0:KDIM),XER4ME(KDIM),XKT5ME(KDIM),XT(0:KDIM)
&      ,XDATA(0:KDIM),ET5(0:KDIM),T5(0:KDIM)
        COMMON /XDA/XDATA
        COMMON /NPI/PI
        COMMON /NAME1/NCAM,D,R3,R4,S3,S4,D4,D3
        COMMON /NAME2/DSR
        COMMON /NR1/AA,BB,CCEX,EE,GG,ZZ,ZZI,YY,UU,RR
        COMMON /XG/XT
        COMMON /NRM/RMC,RMD
        COMMON /NGK/KLISYN,KLIMIT,KSKIP,MSTEP,MCASTEP,NXFCA
        COMMON /CTT/PERIOD,DELS,DELA,NSY,NDATA,NSEA
        COMMON /NAA/ZETA,MXT,MEXCA,MXTCA,NCUEFF
&      ,MOEVA,NMEOUT,MSTEADY,MEVAME,MEVARMS,MDISALL,MRMS
        IF (NSY .GE. 2) GOTO 919
        CCT5=1./(2.*ZETA*DSR) ! T5 begins 000000000000000000000000
        AA=DSR/(2.*ZETA)
        CALL SYNL6M2(0.,T6,DT6,DDT6)
        XKT5=0.5*DELS*(AA*DDT6+DT6+CCT5*T6) !1st F, i.e., F0
        DO 896 I=1,KLISYN
          XKT5=EXP(-CCT5*DELS)*XKT5
          CALL SYNL6M2(DELS*I,T6,DT6,DDT6)
          FT5=DELS*(AA*DDT6+DT6+CCT5*T6)
          XKT5=XKT5+0.5*FT5
          XKT5ME(I)=XKT5 !save XKT5
          XKT5=XKT5+0.5*FT5
896      CONTINUE
        HT5=EXP(-CCT5*PERIOD)
        T50=XKT5ME(KLISYN)/(1.-HT5) ! I.C. *** T5 ends 000000

```

```

CCER4=S4/(2.*ZETA*DSR*D4)
BB=1.-1./(4.*ZETA**2)
EE=1./(2.*ZETA*DSR)**2
GG=DSR/(2.*ZETA*D4)
CCEX=S3/(2.*ZETA*DSR*D3)
RR=S4/(2.*ZETA*DSR*D4)
ZZ=1./(2.*ZETA*DSR)
ZZI=2.*ZETA*DSR*D4
UU=2.*ZETA*DSR*D3
YY=RMC*DSR**2
DO 243 I=0,KLISYN
243   T5(I)=EXP(-CCT5*DELS*I)*T50+XKT5ME(I)
919   IF (NSY .GE. 2) THEN
      DO 809 I=0,KLISYN
         XTR3=XT(I)-R3
         T5RP=ACOS( (1.+XTR3**2-R4**2)/(2.*XTR3)) T5_RIGID_PRE. ITE.
809   ET5(I)=T5(I)-T5RP
      ENDIF
      IF (NSY .EQ. 1) THEN
         T5R=T5(0)
         T4=PI-ASIN(SIN(T5R)/R4)
      ELSE IF (NSY .GE. 2) THEN
         XTR3=XT(0)-R3
         T5R=ACOS( (1.+XTR3**2-R4**2) / (2.*XTR3) )
         T4=ATAN2(SIN(T5R),(COS(T5R)-XTR3))
      ENDIF
      CALL SYNL6M3(0.,T6,DT6,DDT6,DDDT6)
      DDT5=AA*DDDT6+BB*DDT6-EE*(T6-T5(0)) !DD(T5_total)
      XKER4=0.5*DELS*GG*(-DDT6-RMD*DDT5)/SIN(T4-T5R)
      DO 956 I=1,KLISYN
         XKER4=EXP(-CCER4*DELS)*XKER4
         TIME=DELS*I
         CALL SYNL6M3(TIME,T6,DT6,DDT6,DDDT6)
         DDT5=AA*DDDT6+BB*DDT6-EE*(T6-T5(I)) !T5_TOTAL DD(T5_total)
         IF (NSY .EQ. 1) THEN
            T5R=T5(I)
            T4=PI-ASIN(SIN(T5R)/R4)
         ELSE IF (NSY .GE. 2) THEN
            XTR3=XT(I)-R3
            T5R=ACOS( (1.+XTR3**2-R4**2) / (2.*XTR3) )

```

```

T4=ATAN2(SIN(T5R),(COS(T5R)-XTR3))
ENDIF
FER4=DELS*GG*(-DDT6-RMD*DDT5)/SIN(T4-T5R)
XKER4=XKER4+0.5*FER4
XKER4ME(I)=XKER4 ! save XKER4
XKER4=XKER4+0.5*FER4
956 CONTINUE
HER4=EXP(-CCER4*PERIOD)
ER40=XKER4ME(KLISYN)/(1.-HER4) ! I.C.! ER4 ends
ER4KEEP(0)=ER40
DO 21 LL=1,KLISYN ! EX =delta x begins *****
21   ER4KEEP(LL)=EXP(-CCER4*DELS*LL)*ER40+XKER4ME(LL)
IF (NSY .EQ. 1) THEN
  DER4=DQDDER(1,XDATA(0),NDATA,XDATA,ER4KEEP,CHECK)
  DDER4=DQDDER(2,XDATA(0),NDATA,XDATA,ER4KEEP,CHECK)
  CALL FORCING(0.,ER4KEEP(0),DER4,DDER4,T50,FEX,X,DX)
ELSE IF (NSY .GE. 2) THEN
  DXT=DQDDER(1,XDATA(0),NDATA,XDATA,XT,CHECK)
  DDXT=DQDDER(2,XDATA(0),NDATA,XDATA,XT,CHECK)
  DER4=DQDDER(1,XDATA(0),NDATA,XDATA,ER4KEEP,CHECK)
  DDER4=DQDDER(2,XDATA(0),NDATA,XDATA,ER4KEEP,CHECK)
  DET5=DQDDER(1,XDATA(0),NDATA,XDATA,ET5,CHECK)
  DDET5=DQDDER(2,XDATA(0),NDATA,XDATA,ET5,CHECK)
  CALL ITEFORCING(0.,ER4KEEP(0),DER4,DDER4,FEX,XT(0),DXT
& ,DDXT,ET5(0),DET5,DDET5)
ENDIF
FME(0)=FEX
IF (NSY .EQ. 1) XME(0)=X
XKEX=0.5*DELS*FEX ! 1st term of XKEX, i.e., F0 related term
DO 266 I=1,KLISYN
  XKEX=EXP(-CCEX*DELS)*XKEX
  TIME=DELS*I
  IF (NSY .EQ. 1) THEN
    DER4=DQDDER(1,XDATA(I),NDATA,XDATA,ER4KEEP,CHECK)
    DDER4=DQDDER(2,XDATA(I),NDATA,XDATA,ER4KEEP,CHECK)
    CALL FORCING(TIME,ER4KEEP(I),DER4,DDER4,T5(I),FEX,X,DX)
  ELSE IF (NSY .GE. 2) THEN
    DXT=DQDDER(1,XDATA(I),NDATA,XDATA,XT,CHECK)
    DDXT=DQDDER(2,XDATA(I),NDATA,XDATA,XT,CHECK)
    DER4=DQDDER(1,XDATA(I),NDATA,XDATA,ER4KEEP,CHECK)

```

```

DDER4=DQDDER(2,XDATA(I),NDATA,XDATA,ER4KEEP,CHECK)
DET5=DQDDER(1,XDATA(I),NDATA,XDATA,ET5,CHECK)
DDET5=DQDDER(2,XDATA(I),NDATA,XDATA,ET5,CHECK)
CALL ITEFORCING(TIME,ER4KEEP(I),DER4,DDER4,FEX,XT(I),DXT
&           ,DDXT,ET5(I),DET5,DDET5)

ENDIF
FME(I)=FEX
IF (NSY .EQ. 1) XME(I)=X
XKEX=XKEX+0.5*DELS*FEX !do not forget DELS
XKEXME(I)=XKEX !save XKEX
XKEX=XKEX+0.5*DELS*FEX
266 CONTINUE !*****end of XKEX *****
HEX=EXP(-CCEX*PERIOD)
EXO=XKEXME(KLISYN)/(1.-HEX) ! I.C. ***
DEX0=(-S3*EXO+FME(0))/UU
XKEXME(0)=0.
IF(MEXCA .EQ. 1) OPEN(9,FILE='CAEX',STATUS='NEW')
IF(MXTCA .EQ. 1) OPEN(10,FILE='CAXT',STATUS='NEW')
DO 265 I=0,KLISYN
  IF(I/MSTEP*MSTEP .EQ. I) THEN !to save disk quota
    TIME=DELS*I
    EX=EXP(-CCEX*TIME)*EXO+XKEXME(I)
    IF(MEXCA .EQ. 1 .AND. I/MCASTEP*MCASTEP.EQ.I) THEN
      WRITE(9,1896)EX,DEX,TIME
    ENDIF
    IF (MXT .EQ. 1) THEN
      IF (NSY .EQ. 1) XT(I/MSTEP)=XME(I)+EX
      IF (NSY .GE. 2) XT(I/MSTEP)=XT(I)+EX
      IF(MXTCA .EQ. 1 .AND. I/MCASTEP*MCASTEP .EQ. I)
        &      WRITE(10,1896)XT(I/MSTEP),EX,TIME
    ENDIF
  ENDIF
265 CONTINUE ! EX ends
1896 FORMAT(1X,4E17.9)
CLOSE (9)
CLOSE (10)
END
C
c...forcing terms for initial synthesis
SUBROUTINE FORCING(TIME,ER4,DER4,DDER4,T5,F,X,DX)

```

```

IMPLICIT REAL*8 (A-H,O-Z)
COMMON /NPI/PI
COMMON /NRM/RMC,RMD
COMMON /NAME1/NCAM,D,R3,R4,S3,S4,D4,D3
COMMON /NR1/AA,BB,CCEX,EE,GG,ZZ,ZZI,YY,UU,RR
T4=PI-ASIN(SIN(T5)/R4)
CT4=COS(T4)
CT4U=CT4**3
ST4=SIN(T4)
ST4Q=ST4**2
CT5=COS(T5)
ST5=SIN(T5)
ST4T5=SIN(T4-T5)
SCQT4=ST4/CT4**2
CALL SYNL6M3(TIME,T6,DT6,DDT6,DDDT6)
DT5=AA*DDT6+DT6+ZZ*(T6-T5)
DT5Q=DT5**2
DDT5=AA*DDDT6+BB*DDT6-EE*(T6-T5)
DT4=CT5*DT5/(R4*CT4)
DT4Q=DT4**2
DT45=DT4-DT5
X=CT5-R4*CT4+R3
DX=ST4T5*DT5/CT4
DDT4=(DDT5*CT5-DT5Q*ST5+R4*DT4Q*ST4)/(R4*CT4)
DDX=-DDT5*ST5-DT5Q*CT5+R4*DDT4*ST4+R4*DT4Q*CT4
F=(YY*DDX-YY*DDER4/CT4+(-ZZI*CT4
& -YY*2.*DT4*SCQT4-UU/CT4)
& *DER4+(-S4*CT4-YY*(2.*DT4Q*ST4Q/CT4U + DT4Q/CT4
& + DDT4*SCQT4)-UU*DT4*SCQT4 - S3/CT4) *ER4) /UU
RETURN
END
C
c...forcing terms for iterated synthesis
SUBROUTINE ITEFORCING(TIME,ER4,DER4,DDER4,F,XT,DXT,DDXT
& ,ET5,DET5,DDET5)
IMPLICIT REAL*8 (A-H,O-Z)
COMMON /NPI/PI
COMMON /NRM/RMC,RMD
COMMON /NAME1/NCAM,D,R3,R4,S3,S4,D4,D3
COMMON /NR1/AA,BB,CCEX,EE,GG,ZZ,ZZI,YY,UU,RR

```

```

XTR3=XT-R3
T5=ACOS( (1.+XTR3**2-R4**2) / (2.*XTR3) ) !T5_RIGID
ST5=SIN(T5)
ST5Q=ST5**2
CT5=COS(T5)
CT5Q=CT5**2
T4=ATAN2(ST5,(CT5-XTR3))
ST4=SIN(T4)
CT4=COS(T4)
CT4Q=CT4**2
ST4T5=SIN(T4-T5)
CT4T5=COS(T4-T5)
DT5=CT4*DXT/ST4T5
DT5Q=DT5**2
DT4=CT5*DXT/(R4*ST4T5)
DT4Q=DT4**2
DT54=DT5-DT4
DDT5=(CT4*DDXT-R4*DT4Q+DT5Q*CT4T5)/ST4T5
DDT4=(DDXT*CT5-R4*DT4Q*CT4T5+DT5Q)/(R4*ST4T5)
CT4U=CT4**3
ST4Q=ST4**2
SCQT4=ST4/CT4**2
DDT54=DDT5-DDT4
F=(YY*DDXT-YY*DDER4/CT4+(-ZZI*CT4
& -YY*2.*DT4*SCQT4-UU/CT4)*DER4
& +(-S4*CT4-YY*(2.*DT4Q*st4q/CT4U + DT4Q/CT4 + DDT4*SCQT4)-
& UU*DT4*SCQT4 - S3/CT4) *ER4) /UU
& +ST4T5/CT4*DET5 - CT4T5/CT4*DT54*ET5
& +ST4T5/st4q*ET5*ST4*DT4
& +S3/UU*ST4T5/CT4*ET5
& +YY/UU* (-CT4T5/CT4*DT54*DET5 + ST4T5*ST4/CT4Q*DT4*DET5
& +ST4T5/CT4*DDET5 - ST4T5/CT4*DT54**2*ET5
& -CT4T5*DT54/CT4Q*ST4*DT4*ET5 - CT4T5/CT4*DDT54*ET5
& -CT4T5/CT4*DT54*DET5 - CT4T5/CT4Q*DT54*ET5*ST4*DT4
& +ST4T5/CT4U*ET5*2.*ST4Q*DT4Q + ST4T5/CT4Q*DET5*ST4*DT4
& +ST4T5/CT4*ET5*DT4Q + ST4T5/CT4Q*ET5*ST4*DDT4 )
RETURN
END

```

```

c...desired output
SUBROUTINE SYNL6M3(X,T6,DT6,DDT6,DDDT6)
IMPLICIT REAL*8 (A-H,O-Z)
COMMON /NPI/PI
COMMON /NAME1/NCAM,D,R3,R4,S3,S4
COMMON /NBETA/IBE,BE6,BE7,BE8,BE9,BE10,BE11
PH=X
IF (IBE .EQ. 0) THEN
  BE=2./3.*PI
  BE6=BE**6
  BE7=BE6*BE
  BE8=BE7*BE
  BE9=BE8*BE
  BE10=BE9*BE
  BE11=BE10*BE
  IBE=1
ENDIF
2 IF (PH.LE.(2.0*PI)) GO TO 4
PH=PH-2.0*PI
GO TO 2
4 GO TO (6,7,5),NCAM
5 CPH=COS(PH)
T6=(PI/4.0)-((PI*CPH)/12.0)
D2T6DP=(PI*CPH)/12.0
GOTO 60
6 T6I=PI/6.00
T6F=PI/3.00
DEL=T6F-T6I
GO TO 10
7 T6I=PI/6.0
T6F=2.00*PI/3.0
DEL=T6F-T6I
10 IF ((PI/6.0)-PH) 15,20,20
15 IF (((5.0*PI)/6.0)-PH) 25,40,30
25 IF (((7.0*PI)/6.0)-PH) 35,40,40
35 IF (((11.0*PI)/6.0)-PH) 20,20,50
20 T6=T6I
DT6=0.
DDT6=0.
DDDT6=0.

```

```

GO TO 60
30  ANG=PH-(PI/6.0)
    AN2=ANG*ANG
    AN3=AN2*ANG
    AN4=AN3*ANG
    AN5=AN4*ANG
    AN6=AN5*ANG
    AN7=AN6*ANG
    AN8=AN7*ANG
    AN9=AN8*ANG
    AN10=AN9*ANG
    AN11=AN10*ANG
    T6=T6I+DEL*(462.*AN6/BE6-1980.*AN7/BE7+3465.*AN8/BE8-3080.
& *AN9/BE9+1386.*AN10/BE10-252.*AN11/BE11)
    DT6=DEL*(2772.*AN5/BE6-13860.*AN6/BE7+27720.*AN7/BE8-27720.*
& AN8/BE9+13860.*AN9/BE10-2772.*AN10/BE11)
    DDT6=DEL*(13860.*AN4/BE6-83160.*AN5/BE7+194040.*AN6/BE8
& -221760.*AN7/BE9+124740.*AN8/BE10-27720.*AN9/BE11)
    DDDT6=DEL*(55440.*AN3/BE6-415800.*AN4/BE7+1164240.*AN5/BE8
& -1552320.*AN6/BE9+997920.*AN7/BE10-249480.*AN8/BE11)
    GOTO 60
40  T6=T6F
    DT6=0.
    DDT6=0.
    DDDT6=0.
    GO TO 60
50  ANG=PH-(7.D0*PI/6.0D0)
    AN2=ANG*ANG
    AN3=AN2*ANG
    AN4=AN3*ANG
    AN5=AN4*ANG
    AN6=AN5*ANG
    AN7=AN6*ANG
    AN8=AN7*ANG
    AN9=AN8*ANG
    AN10=AN9*ANG
    AN11=AN10*ANG
    T6=T6F-DEL*(462.*AN6/BE6-1980.*AN7/BE7+3465.*AN8/BE8-3080.
& *AN9/BE9+1386.*AN10/BE10-252.*AN11/BE11)
    DT6=-DEL*(2772.*AN5/BE6-13860.*AN6/BE7+27720.*AN7/BE8-27720.*
```

```

&     AN8/BE9+13860.*AN9/BE10-2772.*AN10/BE11)
DDT6=-DEL*(13860.*AN4/BE6-83160.*AN5/BE7+194040.*AN6/BE8
&   -221760.*AN7/BE9+124740.*AN8/BE10-27720.*AN9/BE11)
DDDT6=-DEL*(55440.*AN3/BE6-415800.*AN4/BE7+1164240.*AN5/BE8
&   -1552320.*AN6/BE9+997920.*AN7/BE10-249480.*AN8/BE11)
60    RETURN
      END

c...analysis for Part I
c...using Hsu's step functions (impulses), the parameter values are
c...evaluated at the center of the small time interval
      SUBROUTINE XFA6CVALL
      IMPLICIT REAL*8(A-H,O-Z)
      PARAMETER CHECK=.FALSE.,N=6,LDA=N,LDB=N,IPATH=1,NKEEP=360
& ,NUMJA=4,KSYNDIM=216000
& ,LDC=N,NCA=N,NCB=N,NCC=N,NRA=N,NRB=N,NRC=N,LDEVEC=N
      COMPLEX*16 EVAL(N),DIS
      DIMENSION A(LDA,NCA),B(LDB,NCB),C(LDC,NCC),XF(N),
& PHISUB(N,N),PHI(N,N),COEFF(5),PHIINV(N,N),F(N),
& HCoeff(2),XK(N),XFIC(N),XMED(N),RI_H(N,N),
& XKME(NKEEP,N),PHIME(NKEEP,N,N),PHIALL(N,N),
& ASU(4:6,3:6),FSU(N),AL(4:6,3:6),AR(4:6,3:6),
& FL(N),FR(N),T5RIG(0:360)
& ,XK1P(N),CA(6),XT(0:KSYNDIM),XDATA(0:KSYNDIM)
      COMMON /NAME1/NCAM,D,R3,R4,S3,S4,D4,D3
      COMMON /NAME2/DSR
      COMMON /NAMEX1/AA,BB,CC,EE,GG,ZZ,WW,UU,YY,RR
      COMMON /NAMEY/ZD,DQ,Z5D,R5DQ,Z3D,R3DQ,ZDD
      COMMON /NAMEZ/ZI,ZD4,S45Q,Z5D4,ZDN
      COMMON /CT6/T6(0:360)
      COMMON /NPI/PI
      COMMON /XDA/XDATA,COEFF
      COMMON /XG/XT
      COMMON /NRM/RMC,RMD
      COMMON /NGK/KLISYN,KLIMIT,KSKIP,MSTEP,MCASTEP,NXFCA
      COMMON /CTT/PERIOD,DELS,DELA,NSY,NDATA,NSEA
      COMMON /NAA/ZETA,MXT,MEXCA,MXTCA,NCOEFF
& ,MOEVA,NMEOUT,MSTEADY,MEVAME,MEVARMS,MDISALL,MRMS
      DATA A(1,1)/0./ A(1,2)/1./ A(1,3)/0./ A(1,4)/0./ A(1,5)/0./
& A(1,6)/0./ A(2,5)/0./ A(2,6)/0./ A(3,1)/0./ A(3,2)/0./

```

```

& A(3,3)/0./ A(3,4)/1./ A(3,5)/0./ A(3,6)/0./ A(5,1)/0./
& A(5,2)/0./ A(5,3)/0./ A(5,4)/0./ A(5,5)/0./ A(5,6)/1./
& A(6,1)/0./ A(6,2)/0./
MUL=KLISYN/KLIMIT
YY=2.*ZETA*D3/(RMC*DSR)
WW=2.*ZETA*D4/(RMC*DSR)
UU=S4/(RMC*DSR**2)
RR=S3/(RMC*DSR**2)
ZD=ZETA*DSR
DQ=DSR**2
Z5D=2.*ZETA/(RMD*DSR)
R5DQ=RMD*DSR**2
Z3D=2.*ZETA/(RMC*DSR)
R3DQ=RMC*DSR**2
ZDD=2.*ZETA/DSR
S45Q=S4/(RMD*DSR**2)
Z5D4=Z5D*D4
ZD4=2.*ZETA*DSR*D4
ZDN=ZETA*DSR*D4
A(2,1)=-1./DQ
A(2,2)=-ZDD
A(2,3)=1./DQ
A(2,4)=ZDD
A(4,1)=1./R5DQ
A(4,2)=Z5D
DO 806 JJ=1,N !....INITIALIZE PHI(I,I)
DO 806 II=1,N
  IF (II .NE. JJ) THEN
    PHI(II,JJ)=0.
  ELSE
    PHI(II,JJ)=1.
  ENDIF
806  CONTINUE
DO 249 II=1,5,2 !***** constants assignment
  FL(II)=0.
  FR(II)=0.
249  F(II)=0.
DO 3076 II=1,N !***** assign the value at time=0.
3076  XK(II)=0.
DXT=DQDDER(1,XDATA(0),NDATA,XDATA,XT,CHECK)

```

```

DDXT=DQDDER(2,XDATA(0),NDATA,XDATA,XT,CHECK)
CALL COEFOR(XT(0),DXT,DDXT,ASU,FSU,T5RIG(0))
DO 406 JJ=3,6
    DO 406 II=4,6,2
406     AL(II,JJ)=ASU(II,JJ) !***** end of time=0 assignment
    DO 2673 II=2,N,2
2673     FL(II)=FSU(II)
    DO 7832 K=1,KLIMIT
        KDD=K*MUL
        DXT=DQDDER(1,XDATA(KDD),NDATA,XDATA,XT,CHECK)
        DDXT=DQDDER(2,XDATA(KDD),NDATA,XDATA,XT,CHECK)
        CALL COEFOR(XT(KDD),DXT,DDXT,ASU,FSU,T5ME)
        IF (K/NMEOUT*NMEOUT .EQ. K) T5RIG(K/NMEOUT)=T5ME
        DO 731 JJ=3,6
            DO 731 II=4,6,2
731         AR(II,JJ)=ASU(II,JJ)
            DO 501 II=2,N,2
501         FR(II)=FSU(II)
            DO 865 JJ=3,6           !averageing
                DO 865 II=4,6,2
865         A(II,JJ)=0.5*(AL(II,JJ)+AR(II,JJ))
            DO 591 II=2,N,2
591         F(II)=0.5*(FL(II)+FR(II)) !averaging ends
            DO 208 JJ=3,6           !reassignment
                DO 208 II=4,6,2
208         AL(II,JJ)=AR(II,JJ)
            DO 606 JJ=2,N,2
606         FL(JJ)=FR(JJ)           !reassignment end
            CALL DPOLRG(N,A,LDA,NCoeff,COEFF,PHISUB,LDB) !CAL. PHISUB
                !PHISUB: transition matrix for the samll time interval
747         DO 4198 II=1,N
4198         XK(II)=XK(II)+F(II)*COEFF(2)
            CALL DMURRV(N,N,PHISUB,N,N,XK,IPATH,N,XMED)
            DO 502 JJ=1,N
502         XK(JJ)=XMED(JJ) ! [XK] = [XMED]
C...CALCULATE PHI(TK)
847         CALL DMRRRR(NRA,NCA,PHISUB,LDA,NRB,NCB,PHI,LDB,NRC
            & ,NCC,C,LDC)
            CALL DCRGRG(N,C,LDA,PHI,LDB)      !COPY C TO PHI
            IF (K/NMEOUT*NMEOUT .EQ. K) THEN !!!!store PHI and XK

```

```

KMESTO=K/NMEOUT
DO 524 JJ=1,N
  XKME(KMESTO,JJ)=XK(JJ)
  DO 524 II=1,N
    PHIME(KMESTO,II,JJ)=PHI(II,JJ)
524      CONTINUE
      ENDIF
7832    CONTINUE
      DO 8241 II=1,N
        DO 8241 JJ=1,N
8241      PHIALL(JJ,II)=PHI(JJ,II)
      IF (Msteady .EQ. 0) STOP !the above find E. VALUES only
C...FIND THE INVERSE OF (I-H) AND NAME IT PHIINV
      NHCOEF=2
      HCOEFF(1)=1.
      HCOEFF(2)=-1.
      CALL DPOLRG(N,PHI,N,NHCOEF,HCOEFF,RI_H,N)
      CALL DLINRG(N,RI_H,N,PHIINV,N)
      DO 904 II=1,N
904      XK1P(II)=XKME(NKEEP,II)
      CALL DMURRV(N,N,PHIINV,N,N,XK1P,IPATH,N,XFIC)
C...[XFIC]: the calculated steady state i.c. [XFIC]=inv[I-H]*[Xk1P]
      RMS=0. !RMS values
      RSQU=0.
      DO 632 K=1,NKEEP
        DO 182 JJ=1,N
          DO 182 II=1,N
            PHI(II,JJ)=PHIME(K,II,JJ)
182      CONTINUE
      CALL DMURRV(N,N,PHI,N,N,XFIC,IPATH,N,XF)
      DO 403 II=1,N
        XK(II)=XKME(K,II)
403      CONTINUE
      CALL DAXPY(N,1.,XK,1,XF,1)
      IF (NXFCA .EQ. 1) THEN
        WRITE(89,6420)5*K*DELA,T5RIG(K),XF(1)
      ENDIF
      IF (MRMS .EQ. 1) THEN
        DIFF=ABS(T6(K)-XF(1))
        RSQU=RSQU+DIFF**2

```

```

ENDIF !end of RMS
632  CONTINUE
RMS=SQRT(RSQU/NKEEP)
WRITE(NSY+70,930)DSR,RMS
IF (MEVARMS .EQ. 1 .AND. NSEA .EQ. NSY) THEN !begin EVARMS
IF (MOEVA .EQ. 1) THEN      ! beginning of E.Values
  CALL DEVLRG(N,PHIALL,N,EVAL)
ENDIF
IF (MEVAME .EQ. 1) WRITE(16,802)DSR,EVAL !!!end of E.Values
DO 23 I=1,6
23    CA(I)=ABS(EVAL(I))
CM=CA(1)
IMAX=1
DO 78 I=2,6
  IF (CA(I) .GT. CM) THEN
    IMAX=I
    CM=CA(I)
  ENDIF
78    CONTINUE
CA(IMAX)=0.
DM=CA(1)
JMAX=1
DO 18 I=2,6
  IF (CA(I) .GT. DM) THEN
    JMAX=I
    DM=CA(I)
  ENDIF
18    CONTINUE
DIS=(1.,0)
IF (MDISALL .EQ. 1) THEN !#####beginning of dis. all E.V.
  DO 892 J=1,6
892   DIS=DIS*((1.,0)-EVAL(J))
  RDIS=REAL(DIS)
  ENDIF          ##### distance square from all e.v.
  QDIST=REAL((1.-EVAL(IMAX))*(1.-EVAL(JMAX)))!the largest two
  IF (CONJG(EVAL(IMAX)) .EQ. EVAL(JMAX)) THEN
    WRITE(19,77)DSR,EVAL(IMAX),RMS,QDIST,RDIS
  ELSE IF(DIMAG(EVAL(IMAX)) .EQ. 0. .AND.
&           DIMAG(EVAL(JMAX)) .EQ. 0.) THEN
    WRITE(19,77)DSR,REAL(EVAL(IMAX)),DIMAG(EVAL(IMAX)),RMS

```

```

& ,QDIST,RDIS
    WRITE(19,77)DSR,REAL(EVAL(JMAX)),DIMAG(EVAL(JMAX)),RMS
& ,QDIST,RDIS
ELSE
    WRITE(19,77)DSR,EVAL(IMAX),EVAL(JMAX),RMS,QDIST,RDIS
ENDIF
ENDIF           !end of EVARMS
CLOSE (89)
6420 FORMAT(1X,4E15.7)
930  FORMAT(1X,F8.5,3(4G14.6,/))
802  FORMAT(1X,F8.5,2(2(1X,'(,G14.6,',',G14.6,''))'),/
&           2(1X,'(,G14.6,',',G14.6,'')))
77   FORMAT(1X,F8.5,6G14.6)
END
c
SUBROUTINE COEFOR(XT,DXT,DDXT,ASU,FSU,T5)
IMPLICIT REAL*8(A-H,O-Z)
DIMENSION ASU(4:6,3:6),FSU(6)
COMMON /NPI/PI
COMMON /NAME1/NCAM,D,R3,R4,S3,S4,D4,D3
COMMON /NAMEX1/AA,BB,CC,EE,GG,ZZ,WW,UU,YY,RR
COMMON /NAMEY/ZD,DQ,Z5D,R5DQ,Z3D,R3DQ,ZDD
COMMON /NAMEZ/ZI,ZD4,S45Q,Z5D4,ZDN
XTR3=XT-R3
T5=ACOS( (1.+XTR3**2-R4**2) / (2.*XTR3) )
ST5=SIN(T5)
ST5Q=ST5**2
CT5=COS(T5)
CT5Q=CT5**2
T4=ATAN2(ST5,(CT5-XTR3))
CT4=COS(T4)
CT4Q=CT4**2
ST4T5=SIN(T4-T5)
ST4T5Q=ST4T5**2
S2T45=SIN(2.*(T4-T5))
CT4T5=COS(T4-T5)
DT5=CT4*DXT/ST4T5
DT5Q=DT5**2
DT4=CT5*DXT/(R4*ST4T5)
DT4Q=DT4**2

```

```
DT54=DT5-DT4
DDT5=(CT4*DDXT-R4*DT4Q+DT5Q*CT4T5)/ST4T5
ASU(4,3)=-(1.+S4*ST4T5Q-ZDN*DT54*S2T45)/R5DQ
ASU(4,4)=-Z5D*(1.+D4*ST4T5Q)
ASU(4,5)=-S45Q*CT4*ST4T5
ASU(4,6)=-Z5D4*CT4*ST4T5
ASU(6,3)=-(S4*CT4*ST4T5-ZD4*DT54*CT4*CT4T5)/R3DQ
ASU(6,4)=-WW*CT4*ST4T5
ASU(6,5)=-(S3+S4*CT4Q)/R3DQ
ASU(6,6)=-Z3D*(D3+D4*CT4Q)
FSU(2)=ZDD*DT5+T5/DQ
FSU(4)=-DDT5-Z5D*DT5-T5/R5DQ
FSU(6)=DDXT
RETURN
END
```

APPENDIX E: FORTRAN PROGRAMS FOR PART III

```

C...main program, finite element synthesis and steady state by
c..... central finite difference scheme
PARAMETER NG=16,KDIM=360,NEL=6,NDF=6
IMPLICIT REAL*8(A-H,O-Z)
DIMENSION RL(NEL),B(2:NEL),TH(2:NEL),RD(1),IJK(NDF,NEL)
& ,NANSYS(5),NANALYSIS(5)
& ,XDATA(KDIM),XX(KDIM),T5DES(KDIM),DSRT(20),RATIOAA(5)
COMMON /NFEM/NCAM,KSTART,KRUN,KLIMIT,NMARGIN,NRI,IJK
COMMON /NKK/NGALL,NCABAL,NCOUNT,NSYNPLOT
COMMON /RFEM/DSR,RD,E,RMU,R4,R,RHO,B,TH,RL,PI,IS
COMMON /RFX/XX
COMMON /RAD/XDATA
COMMON /RC/KLIMIT_1,KLIMIT_2,PERIOD,H,RH,THQ,P1,P2,P3,P4,P5,P6
COMMON /T5C/T5DES
COMMON /NJJ/ICOMA,ICOMS
COMMON /NHK/NSY,WN,NCT,NANSYS,NSEA
OPEN(71,FILE='FDIMPI',STATUS='OLD')
READ(71,*)NCOUNT,NGALL,NCABAL,NSYNPLOT
READ(71,*)NCAM,KSN,(NANSYS(I),I=1,5)
READ(71,*)(NANALYSIS(I),I=1,5)
READ(71,*)KSTART,KLIMIT,KRUN,NMARGIN
READ(71,*)NRI,NOA,NITE,NAN1ST,NSEA
READ(71,*)(RATIOAA(JJ),JJ=1,NOA)
READ(71,*)RATIOS,RATIOA,RD(1),E,RMU
READ(71,*)R4,R,RHO !R:radius of curvature
READ(71,*)((IJK(J,IE),J=1,NDF),IE=1,NEL)
DO 801 I=2,NEL
     READ(71,*)B(I),TH(I)
     READ(71,*)(RL(I),I=1,2)

```

```

      READ(71,*)NREA,NMORE
      DO 77 I=1,NREA
77      READ(71,*)DSRT(I)
      READ(71,*)DSTA,DINC
      CLOSE (71)
      DO 901 I=1,NMORE
901      DSRT(NREA+I)=DSTA+(I-1)*DINC
      OPEN(61,FILE='FERMSALL',STATUS='NEW')
      KLIMIT_1=KLIMIT-1
      KLIMIT_2=KLIMIT-2
      PI=ACOS(-1.0)
      PERIOD=2.*PI
      H=PERIOD/KLIMIT
      THQ=2.*H**2
      PMARGIN=H*NMargin
      P1=PMARGIN
      P2=PI/6.-PMARGIN
      P3=PI*5./6.+PMARGIN
      P4=PI*7./6.-PMARGIN
      P5=PI*11./6.+PMARGIN
      P6=PERIOD-PMARGIN
      OPEN(82,FILE='T6P3',STATUS='OLD')
      DO 864 I=1,KLIMIT
      READ(82,*)T5DES(I)
      XDATA(I)=H*(I-1)
      T4=PI-ASIN(RL(2)*SIN(T5DES(I))/R4)
      XX(I)=RL(2)*COS(T5DES(I))-R4*COS(T4)
864      CONTINUE
      CLOSE (82)
      G=E/(2.*(1.+RMU))
      RKN=G*PI*RD(1)**4/32./RL(1)
      RI=NRI*RHO*PI*RL(1)*(RD(1)/2.)**4/2.
      WN=SQRT(RKN/RI)
      DO 99 KK=1,NREA+NMORE
      DSR=DSRT(KK)
      DO 99 II=1,NITE
      ICOMS=0
      NSY=II
      NAN=0
      RH=RATIOS*H

```

```

CALL FDIMPSA !synthesis and analysis program
IF (NANALYSIS(II) .EQ. 0) GOTO 87
NCT=II
NSY=0
NAN=1
ICOMA=0
RH=RATIOA*H
CALL FDIMPSA
CLOSE (61)
87 IF (NSEA .EQ. II) THEN
    DO 265 JJ=1,NOA
        NCT=JJ+30
        NSY=0
        NAN=1
        ICOMA=0
        RH=RATIOAA(JJ)*H
        CALL FDIMPSA
        CLOSE (61)
    ENDIF
99 CONTINUE
END

C...FDIMPSA.FOR finite element synthesis and analysis by
c..... central finite difference algorithm
SUBROUTINE FDIMPSA
PARAMETER NG=16,KDIM=360,NEL=6,NDF=6
IMPLICIT REAL*8(A-H,O-Z)
DIMENSION RL(NEL),B(2:NEL),TH(2:NEL),RD(1)
& ,RK(NG,NG),F(NG),RM(NG,NG),IJK(NDF,NEL),NANSYS(5)
& ,A(KDIM,-1:1,NG,NG),Z(KDIM,NG,NG),Q(KDIM,NG),D(KDIM,NG)
& ,Y(KDIM,NG,NG),XX(KDIM),XT(KDIM),XDATA(KDIM),T5DES(KDIM)
& ,T5RIG(KDIM)
COMMON /NFEM/NCAM,KSTART,KRUN,KLIMIT,NMARGIN,NRI,IJK
COMMON /NKK /NGALL,NCABAL,NCOUNT,NSYNPLOT
COMMON /RFEM/DSR,RD,E,RMU,R4,R,RHO,B,TH,RL,PI,IS
COMMON /RFX/XX
COMMON /RAD/XDATA
COMMON /RC/KLIMIT_1,KLIMIT_2,PERIOD,H,RH,THQ,P1,P2,P3,P4,P5,P6
COMMON /T5C/T5DES
COMMON /NHK/NSY,WN,NCT,NANSYS,NSEA

```

```

COMMON /CXJ/XT

C
      DO 330 L=1,KLIMIT
      DO 330 IC=1,NG
      Q(L,IC)=0.
      DO 330 IR=1,NG
      A(L,-1,IR,IC)=0.
      A(L,0,IR,IC)=0.
      A(L,1,IR,IC)=0.
      Z(L,IR,IC)=0.
330   Y(L,IR,IC)=0.
      DO 209 IS=1,KLIMIT
      IF (NSY .EQ. 1) THEN
      P=XDATA(IS)
      IF(P .GE. P1 .AND. P .LE. P2 .OR. P .GE. P3 .AND. P .LE. P4
& .OR. P .GE. P5 .AND. P .LE. P6) GOTO 747
      CALL FEM_MKF(P,RM,RK,F) !beginning of the period is no.1
                           !end of the period is KLIMIT+1
      ELSE IF (NSY .GE. 2)THEN
      DXT=DQDDER(1,XDATA(IS),KLIMIT,XDATA,XT,LCHECK)
      DDXT=DQDDER(2,XDATA(IS),KLIMIT,XDATA,XT,LCHECK)
      CALL FEM_SY2(XDATA(IS),T5RIG(IS),XT(IS),DXT,DDXT,RM,RK,F)
      ELSE IF (NSY .EQ. 0)THEN
      DXT=DQDDER(1,XDATA(IS),KLIMIT,XDATA,XT,LCHECK)
      DDXT=DQDDER(2,XDATA(IS),KLIMIT,XDATA,XT,LCHECK)
      CALL FEM_ANA(XDATA(IS),T5RIG(IS),XT(IS),DXT,DDXT,RM,RK,F)
      ENDIF
747   DO 208 IC=1,NG
      DO 279 IR=1,NG
      IF (IS .EQ. 1) THEN
      Z(1,IR,IC)=2.*RM(IR,IC)-RH*RK(IR,IC)
      ELSE IF (IS .EQ. KLIMIT) THEN
      Y(KLIMIT_1,IR,IC)=2.*RM(IR,IC)-RH*RK(IR,IC)
      ELSE
      A(IS,-1,IR,IC)=2.*RM(IR,IC)-RH*RK(IR,IC)
      ENDIF
C.....
      IF (IS .EQ. KLIMIT_1) THEN
      Z(KLIMIT_1,IR,IC)=2.*RM(IR,IC)+RH*RK(IR,IC)
      ELSE IF (IS .EQ. KLIMIT) THEN

```

```

Y(1,IR,IC)=2.*RM(IR,IC)+RH*RK(IR,IC)
ELSE
  A(IS,1,IR,IC)=2.*RM(IR,IC)+RH*RK(IR,IC)
ENDIF
C...
IF (IS .EQ. KLIMIT) THEN
  Z(KLIMIT,IR,IC)=-4.*RM(IR,IC)+THQ*RK(IR,IC)
ELSE
  A(IS,0,IR,IC)=-4.*RM(IR,IC)+THQ*RK(IR,IC)
ENDIF
C.....
279   CONTINUE
208   Q(IS,IC)=THQ*F(IC)
      ATEM=Q(IS,4) !switching 4 & 5 rows due to zero element
      Q(IS,4)=Q(IS,5)
      Q(IS,5)=ATEM
      DO 901 IC=1,NG
        IF (IS .EQ. KLIMIT) THEN
          ATEM=Z(IS,4,IC)
          Z(IS,4,IC)=Z(IS,5,IC)
          Z(IS,5,IC)=ATEM
        ELSE
          ATEM=A(IS,0,4,IC)
          A(IS,0,4,IC)=A(IS,0,5,IC)
          A(IS,0,5,IC)=ATEM
        ENDIF
C
      IF (IS .EQ. KLIMIT_1) THEN
        ATEM=Z(KLIMIT_1,4,IC)
        Z(KLIMIT_1,4,IC)=Z(KLIMIT_1,5,IC)
        Z(KLIMIT_1,5,IC)=ATEM
      ELSE IF (IS .EQ. KLIMIT) THEN
        ATEM=Y(KLIMIT_1,4,IC)
        Y(KLIMIT_1,4,IC)=Y(KLIMIT_1,5,IC)
        Y(KLIMIT_1,5,IC)=ATEM
      ELSE
        ATEM=A(IS,1,4,IC)
        A(IS,1,4,IC)=A(IS,1,5,IC)
        A(IS,1,5,IC)=ATEM
      ENDIF

```

```

C.....
      IF (IS .EQ. 1) THEN
        ATEM=Z(1,4,IC)
        Z(1,4,IC)=Z(1,5,IC)
        Z(1,5,IC)=ATEM
      ELSE IF (IS .EQ. KLIMIT) THEN
        ATEM=Y(1,4,IC)
        Y(1,4,IC)=Y(1,5,IC)
        Y(1,5,IC)=ATEM
      ELSE
        ATEM=A(IS,-1,4,IC)
        A(IS,-1,4,IC)=A(IS,-1,5,IC)
        A(IS,-1,5,IC)=ATEM
      ENDIF
901    CONTINUE
209    CONTINUE
      DO 8099 JJ=1,KLIMIT_1           ! K=1 TO KLIMIT-1
      DO 812 II=1,NG
      DO 809 NN=0,1
      DO 809 MM=1,NG
        IF ( NN .EQ. 0 .AND. MM .LE. II) GOTO 809
        RAT=A(JJ+NN,0-NN,MM,II)/A(JJ,0,II,II)
        IF (RAT .EQ. 0) GOTO 809
        Q(JJ+NN,MM)=Q(JJ+NN,MM)-RAT*Q(JJ,II)
        DO 765 LL=II,NG
765      A(JJ+NN,0-NN,MM,LL)=A(JJ+NN,0-NN,MM,LL)
      &      -RAT*A(JJ,0,II,LL)
      DO 809 ZC=1,NG
        Z(JJ+NN,MM,ZC)=Z(JJ+NN,MM,ZC)-RAT*Z(JJ,II,ZC)
        IF (JJ .LE. KLIMIT_2) THEN
          A(JJ+NN,1-NN,MM,ZC)=A(JJ+NN,1-NN,MM,ZC)-RAT*
      &      A(JJ,1,II,ZC)
        ENDIF
809    CONTINUE
        IF (JJ .LE. KLIMIT_2) THEN !%%%%%% last row
        DO 4809 MM=1,NG
          RAT=Y(JJ,MM,II)/A(JJ,0,II,II)
          IF (RAT .EQ. 0) GOTO 4809
          DO 195 LL=II,NG
195      Y(JJ,MM,LL)=Y(JJ,MM,LL)-RAT*A(JJ,0,II,LL)

```

```

DO 903 LL=1,NG
903      Y(JJ+1,MM,LL)=Y(JJ+1,MM,LL)-RAT*A(JJ,1,II,LL)
          Q(KLIMIT,MM)=Q(KLIMIT,MM)-RAT*Q(JJ,II)
          DO 4809 ZC=1,NG
          Z(KLIMIT,MM,ZC)=Z(KLIMIT,MM,ZC)-RAT*Z(JJ,II,ZC)
4809      CONTINUE
          ENDIF                                !%%%%%% last row ends
812      CONTINUE
          IF (JJ .EQ. KLIMIT_2) THEN
              DO 36 IC=1,NG
                  DO 36 IR=1,NG
                      A(KLIMIT,-1,IR,IC)=Y(KLIMIT_1,IR,IC)
                  ENDIF
8099      CONTINUE
          DO 1309 II=1,NG           ! K=KLIMIT *****
          DO 1309 MM=1,NG
              IF ( MM .LE. II) GOTO 1309
              RAT=Z(KLIMIT,MM,II)/Z(KLIMIT,II,II)
              IF (RAT .EQ. 0) GOTO 1309
              Q(KLIMIT,MM)=Q(KLIMIT,MM)-RAT*Q(KLIMIT,II)
              DO 1378 LL=II,NG
                  Z(KLIMIT,MM,LL)=Z(KLIMIT,MM,LL)-RAT*Z(KLIMIT,II,LL)
1378      1309      CONTINUE           ! k=klimit ends *****
C...back substituting
          DO 94 I=NG,1,-1 !$$$$$$$$$$$$$$$$$ D(KLIMIT,I) $$$$$$$$$$$
          DSUM=0
          DO 32 J=I+1,NG
              DSUM=DSUM+Z(KLIMIT,I,J)*D(KLIMIT,J)
              D(KLIMIT,I)=(Q(KLIMIT,I)-DSUM)/Z(KLIMIT,I,I)
32      94      CONTINUE !$$$$$$$$$$$$$$$$$$$$$$$$$$$$$ D(KLIMIT,I) ends $$$$
          DO 2194 I=NG,1,-1       !$$$$$ D(KLIMIT-1,I)
          DSUM=0
          DO 681 K=1,NG
              DSUM=DSUM+Z(KLIMIT_1,I,K)*D(KLIMIT,K)
              DO 3132 J=I+1,NG
                  DSUM=DSUM+A(KLIMIT_1,0,I,J)*D(KLIMIT_1,J)
                  D(KLIMIT_1,I)=(Q(KLIMIT_1,I)-DSUM)/A(KLIMIT_1,0,I,I)
3132      2194     CONTINUE           !$$$$$$$$$$$$$$$$$ D(1,I)
          DO 2147 M=KLIMIT-2,1,-1 !$$$$$ D(KLIMIT-2,I) to D(1,I)
          M1=M+1

```

```

DO 9194 I=NG,1,-1
DSUM=0
DO 2812 K=1,NG
  DSUM=DSUM+Z(M,I,K)*D(KLIMIT,K)+A(M,1,I,K)*D(M1,K)
DO 324 J=I+1,NG
  DSUM=DSUM+A(M,O,I,J)*D(M,J)
  D(M,I)=(Q(M,I)-DSUM)/A(M,O,I,I)
9194  CONTINUE
2147  CONTINUE !$$$$$$$$$$$$$D(KLIMIT-2,I) to D(1,I) ends
IF (NSY .NE. 0) THEN
  IF (NSYNPLOT .EQ. 1) THEN
    OPEN(20,FILE='FDOA1',STATUS='NEW')
    OPEN(21,FILE='FDOA2',STATUS='NEW')
    OPEN(22,FILE='FDOX',STATUS='NEW')
    OPEN(23,FILE='FDOY',STATUS='NEW')
    DO 3207 JJ=1,KLIMIT,NCOUNT
      WRITE(20,9062)H*(JJ-1),D(JJ,1),D(JJ,4),D(JJ,5),D(JJ,8)
      WRITE(21,9062)H*(JJ-1),D(JJ,11),D(JJ,14),D(JJ,15)
      WRITE(22,9062)H*(JJ-1),D(JJ,2),D(JJ,6),D(JJ,9),D(JJ,12)
      & ,D(JJ,16)
3207  WRITE(23,9062)H*(JJ-1),D(JJ,3),D(JJ,7),D(JJ,10),D(JJ,13)
CLOSE (20)
CLOSE (21)
CLOSE (22)
CLOSE (23)
ENDIF
DO 864 I=1,KLIMIT
  IF (NSY .EQ. 1 ) XT(I)=XX(I)+D(I,16)
  IF (NSY .NE. 1 ) XT(I)=XT(I)+D(I,16)
  IF (NANSYS(1) .EQ. NSY .OR. NANSYS(2) .EQ. NSY
& .OR. NANSYS(3) .EQ. NSY .OR. NANSYS(4) .EQ. NSY
& .OR. NANSYS(5) .EQ. NSY ) THEN !select iteration no.
    WRITE(50+NSY,9382)XT(I),D(I,16),XDATA(I)
  ENDIF
864  CONTINUE
CLOSE (50+NSY)
ELSE IF (NSY .EQ. 0) THEN
  IF (NGALL .EQ. 1) THEN
    OPEN(10,FILE='FANAA1',STATUS='NEW')
    OPEN(11,FILE='FANAA2',STATUS='NEW')

```

```

OPEN(12,FILE='FANAX',STATUS='NEW')
OPEN(13,FILE='FANAY',STATUS='NEW')
ENDIF
IF (NCABAL .EQ. 1) OPEN(14,FILE='FANAT5',STATUS='NEW')
DIFQ=0.
DO 207 JJ=1,KLIMIT,NCOUNT
  IF (NGALL .EQ. 1) THEN
    WRITE(10,9062) XDATA(JJ),D(JJ,1),D(JJ,2),D(JJ,5),D(JJ,6)
    WRITE(11,9062) XDATA(JJ),D(JJ,9),D(JJ,12),D(JJ,15),D(JJ,16)
    WRITE(12,9062) XDATA(JJ),D(JJ,3),D(JJ,7),D(JJ,10),D(JJ,13)
    WRITE(13,9062) XDATA(JJ),D(JJ,4),D(JJ,8),D(JJ,11),D(JJ,14)
  ENDIF
  T5ALL=D(JJ,1)+T5RIG(JJ)
  T5DIF=T5DES(JJ)-T5ALL
  IF (NCABAL .EQ. 1) THEN
    WRITE(35+NCT,9982) XDATA(JJ),T5DIF,T5ALL,T5RIG(JJ)
  ENDIF
  DIFQ=DIFQ+T5DIF**2
207  CONTINUE
WRITE(NCT,9982) DSR,DSR/WN,SQRT(DIFQ/KLIMIT)
CLOSE (NCT)
IF (NGALL .EQ. 1) THEN
  CLOSE (10)
  CLOSE (11)
  CLOSE (12)
  CLOSE (13)
ENDIF
IF (NCABAL .EQ. 1) THEN
  CLOSE (35+NCT)
ENDIF
ENDIF
9982 FORMAT(1X,5E16.8)
9382 FORMAT(1X,E24.16,E16.8,E13.5)
9062 FORMAT(1X,6E13.5)
END

SUBROUTINE FEM_MKF(TIME,SMCUT,SKCUT,SMRIGCUT)
PARAMETER NEL=6,NDF=6,N=NDF,NTF=17,NG=NTF-1,NTH=32,IPATH=1
IMPLICIT REAL*8(A-H,O-Z)
DIMENSION RL(NEL),B(2:NEL),TH(2:NEL),RD(1)

```

```

& ,EA(2:NEL),EI(2:NEL),RLS(2:NEL),RLC(2:NEL),RALW(2:NEL)
& ,ET(2:NEL),SKE(NEL,NDF,NDF),SKET(NDF,NDF)
& ,SKEA(N,N),SKEB(N,N),SMEA(N,N),SMEB(N,N)
& ,SME(NEL,NDF,NDF),SMET(NDF,NDF),TR(N,N)
& ,TRT(N,N),SM(NTF,NTF),SK(NTF,NTF),DDRIG(NTF),SMCUT(NG,NG)
& ,SMRIG(NTF),SMRIGCUT(NG),SKCUT(NG,NG),IJK(NDF,NEL)
COMMON /NFEM/NCAM,KSTART,KRUN,KLIMIT,NMARGIN,NRI,IJK
COMMON /RFEM/DSR,RD,E,RMU,R4,R,RHO,B,TH,RL,PI,IS
COMMON /NAME1/NCAMM
COMMON /NJJ/ICOMA,ICOMS
COMMON /NIS/PERIOD,SME,SKE,ZET,GAR
IF (ICOMS .NE. 7) THEN
  NCAMM=NCAM
  DQ=DSR**2
  PI=4.*ATAN(1.)
  PERIOD=2.*PI
  DEL=PERIOD/KLIMIT
  PMARGIN=DEL*Nmargin
  P1=PMARGIN
  P2=PI/6.-PMARGIN
  P3=PI*5./6.+PMARGIN
  P4=PI*7./6.-PMARGIN
  P5=PI*11./6.+PMARGIN
  P6=PERIOD-PMARGIN
  G=E/(2.*(1.+RMU))
  ALP=0.5*ASIN(R4/2./R)
  BET=0.5*(PI-ALP)
  GAR=ASIN((1.-COS(ALP))/(2.*SIN(ALP/2.)))
  ZET=ASIN((COS(ALP)-COS(2.*ALP)) / (2.*SIN(ALP/2.)) )
  RI=NRI*RHO*PI*RL(1)*(RD(1)/2.)**4/2.
  RMD=1./DQ
  DO 29 I=3,NEL
29   RL(I)=2.*R*SIN(ALP/2.)
  DO 105 I=1,1
    SMEME=RHO*PI*RL(I)*(RD(I)/2.)**4/2./3.
    SME(I,1,1)=(RI+SMEME)/RMD
    SME(I,1,2)=SMEME/2./RMD
    SME(I,2,1)=SME(I,1,2)
    SME(I,2,2)=SMEME/RMD
    SKE(I,1,1)=G*PI*RD(I)**4/32./RL(I)

```

```

SKE(I,1,2)=-SKE(I,1,1)
SKE(I,2,1)=SKE(I,1,2)
SKE(I,2,2)=SKE(I,1,1)
105    CONTINUE
DO 201 I=2,NEL
RALW(I)=RHO*B(I)*TH(I)*RL(I)
SME(I,1,1)=RALW(I)/3./RMD
SME(I,1,2)=0.
SME(I,1,3)=0.
SME(I,1,4)=RALW(I)/6./RMD
SME(I,1,5)=0.
SME(I,1,6)=0.
SME(I,2,2)=RALW(I)*13./35./RMD
SME(I,2,3)=RALW(I)*11.*RL(I)/210./RMD
SME(I,2,4)=0.
SME(I,2,5)=RALW(I)*9./70./RMD
SME(I,2,6)=-RALW(I)*13.*RL(I)/420./RMD
SME(I,3,3)=RALW(I)*RL(I)**2/105./RMD
SME(I,3,4)=0.
SME(I,3,5)=-SME(I,2,6)
SME(I,3,6)=-RALW(I)*RL(I)**2/140./RMD
SME(I,4,4)=RALW(I)/3./RMD
SME(I,4,5)=0.
SME(I,4,6)=0.
SME(I,5,5)=SME(I,2,2)
SME(I,5,6)=-SME(I,2,3)
SME(I,6,6)=SME(I,3,3)

```

C

```

EA(I)=E*B(I)*TH(I)
EI(I)=E*B(I)*TH(I)**3/12.
RLS(I)=RL(I)**2
RLC(I)=RLS(I)*RL(I)
SKE(I,1,1)=EA(I)/RL(I)
SKE(I,1,2)=0.
SKE(I,1,3)=0.
SKE(I,1,4)=-SKE(I,1,1)
SKE(I,1,5)=0.
SKE(I,1,6)=0.
SKE(I,2,2)=12.*EI(I)/RLC(I)
SKE(I,2,3)=6.*EI(I)/RLS(I)

```

```

SKE(I,2,4)=0.
SKE(I,2,5)=-SKE(I,2,2)
SKE(I,2,6)=SKE(I,2,3)
SKE(I,3,3)=4.*EI(I)/RL(I)
SKE(I,3,4)=0.
SKE(I,3,5)=-SKE(I,2,3)
SKE(I,3,6)=2.*EI(I)/RL(I)
SKE(I,4,4)=EA(I)/RL(I)
SKE(I,4,5)=0.
SKE(I,4,6)=0.
SKE(I,5,5)=SKE(I,2,2)
SKE(I,5,6)=SKE(I,3,5)
SKE(I,6,6)=SKE(I,3,3)
DO 201 JJ=1,N
  DO 201 II=JJ+1,N
    SME(I,II,JJ)=SME(I,JJ,II)
  201   SKE(I,II,JJ)=SKE(I,JJ,II)
  ICOMS=7
ENDIF
DO 18 JJ=1,NTF !.....assemble
  DO 18 II=1,NTF
    SM(II,JJ)=0.
  18   SK(II,JJ)=0.
  DO 2500 I=1,1
    DO 2500 IA=1,NDF
      IJKIA=IJK(IA,I)
      IF(IJKIA .EQ. 0) GOTO 2500
      DO 2500 JB=1,NDF
        IJKJB=IJK(JB,I)
        IF(IJKJB .EQ. 0) GOTO 2500
        SM(IJKIA,IJKJB)=SME(I,IA,JB)+SM(IJKIA,IJKJB)
        SK(IJKIA,IJKJB)=SKE(I,IA,JB)+SK(IJKIA,IJKJB)
2500 CONTINUE
CALL DSYNL3D2(TIME,T6,DT6,DDT6)
T4=PI-ASIN(RL(2)*SIN(T6)/R4)
DT4=RL(2)*COS(T6)*DT6/R4/COS(T4)
DDT4=(RL(2)*DDT6*COS(T6)-RL(2)*DT6**2*SIN(T6)
& +R4*DT4**2*SIN(T4))/(R4*COS(T4))
ET(2)=T6
ET(3)=T4+PI+ZET

```

```

ET(4)=T4+PI+GAR
ET(5)=T4+PI-GAR
ET(6)=T4+PI-ZET
DO 200 I=2,NEL
  TR(1,1)=COS(ET(I))
  TR(1,2)=SIN(ET(I))
  TR(2,1)=-TR(1,2)
  TR(2,2)=TR(1,1)
  TR(3,3)=1.
  TR(4,4)=TR(1,1)
  TR(4,5)=TR(1,2)
  TR(5,4)=-TR(4,5)
  TR(5,5)=TR(4,4)
  TR(6,6)=1.
  TRT(1,1)=COS(ET(I))
  TRT(1,2)=-SIN(ET(I))
  TRT(2,1)=-TRT(1,2)
  TRT(2,2)=TRT(1,1)
  TRT(3,3)=1.
  TRT(4,4)=TRT(1,1)
  TRT(4,5)=TRT(1,2)
  TRT(5,4)=-TRT(4,5)
  TRT(5,5)=TRT(4,4)
  TRT(6,6)=1.
  DO 723 JJ=1,NDF      !...transformation
    DO 723 KK=1,NDF
      SMEA(JJ,KK)=SME(I,JJ,KK)
      SKEA(JJ,KK)=SKE(I,JJ,KK)
    CALL DMRRRR(N,N,SMEA,N,N,N,TR,N,N,N,SMEB,N)
    CALL DMRRRR(N,N,TRT,N,N,N,SMEB,N,N,N,SMET,N)
    CALL DMRRRR(N,N,SKEA,N,N,N,TR,N,N,N,SKEB,N)
    CALL DMRRRR(N,N,TRT,N,N,N,SKEB,N,N,N,SKET,N)
    DO 200 IA=1,NDF
      IJKIA=IJK(IA,I)
      IF(IJKIA .EQ. 0) GOTO 200
    DO 200 JB=1,NDF
      IJKJB=IJK(JB,I)
      IF(IJKJB .EQ. 0) GOTO 200
      SM(IJKIA,IJKJB)=SMET(IA,JB)+SM(IJKIA,IJKJB)
      SK(IJKIA,IJKJB)=SKET(IA,JB)+SK(IJKIA,IJKJB)
 723

```

```

200  CONTINUE
      DDRIG(1)=DDT6
      DDRIG(2)=DDT6
      DDRIG(3)=(-RL(2)*DDT6*SIN(T6)+RL(2)*DT6**2*COS(T6))
      DDRIG(4)=(RL(2)*DDT6*COS(T6)+RL(2)*DT6**2*SIN(T6))
      DDRIG(5)=DDT6
      DDRIG(6)=DDT4
      DDRIG(9)=DDT4
      DDRIG(12)=DDT4
      DDRIG(15)=DDT4
      DDRIG(16)=DDT4
      DDRIG(7)=DDRIG(3)-RL(3)*DDT4*SIN(ET(3))+RL(3)*DT4**2*COS(ET(3))
      DDRIG(8)=DDRIG(4)+RL(3)*DDT4*COS(ET(3))
      &           +RL(3)*DT4**2*SIN(ET(3))
      DDRIG(10)=DDRIG(7)-RL(4)*DDT4*SIN(ET(4))
      &           +RL(4)*DT4**2*COS(ET(4))
      DDRIG(11)=DDRIG(8)+RL(4)*DDT4*COS(ET(4))
      &           +RL(4)*DT4**2*SIN(ET(4))
      DDRIG(13)=DDRIG(10)-RL(5)*DDT4*SIN(ET(5))
      &           +RL(5)*DT4**2*COS(ET(5))
      DDRIG(14)=DDRIG(11)+RL(5)*DDT4*COS(ET(5))
      &           +RL(5)*DT4**2*SIN(ET(5))
      DDRIG(17)=-RL(2)*DDT6*SIN(T6)-RL(2)*DT6**2*COS(T6)
      &           +R4*DDT4*SIN(T4)+R4*DT4**2*COS(T4)
      CALL DMURRV(NTF,NTF,SM,NTF,NTF,DDRIG,IPATH,NTF,SMRIG)
      DO 17 II=1,NTF-1
         SMRIGCUT(II)=-SMRIG(II) !take negative (move to RHS)
      DO 17 JJ=1,NTF-1
         SKCUT(JJ,II)=SK(JJ,II+1)
17      SMCUT(JJ,II)=SM(JJ,II+1)
      END

C...desired output
      SUBROUTINE DSYNL3D2(X,T6,DT6,DDT6)
      IMPLICIT REAL*8 (A-H,O-Z)
      PARAMETER PI=3.141592653589793
      COMMON /NAME1/NCAM
      PH=X
2 IF (PH.LE.(2.0*PI)) GO TO 4
      PH=PH-2.0*PI

```

```

GO TO 2
4 GO TO (6,7,5),NCAM
5 CPH=COS(PH)
T6=(PI/4.0)-((PI*CPH)/12.0)
D2T6DP=(PI*CPH)/12.0
GOTO 60
6 T6I=PI/6.00
T6F=PI/3.00
DEL=T6F-T6I
GO TO 10
7 T6I=PI/6.0
T6F=2.00*PI/3.0
DEL=T6F-T6I
10 IF ((PI/6.0)-PH) 15,20,20
15 IF (((5.0*PI)/6.0)-PH) 25,40,30
25 IF (((7.0*PI)/6.0)-PH) 35,40,40
35 IF (((11.0*PI)/6.0)-PH) 20,20,50
20 T6=T6I
DT6=0.
DDT6=0.
GO TO 60
30 ANG=PH-(PI/6.0)
AN2=ANG*ANG
AN3=AN2*ANG
AN4=AN3*ANG
AN5=AN4*ANG
AN6=AN5*ANG
AN7=AN6*ANG
BETA=2.0*PI/3.0
BE4=BETA**4
BE5=BE4*BETA
BE6=BE5*BETA
BE7=BE6*BETA
T6=T6I+DEL*(35.0*AN4/BE4-84.0*AN5/BE5+70.0*AN6/BE6
& -20.0*AN7/BE7)
DT6=DEL*(140.0*AN3/BE4-420.0*AN4/BE5
& +420.0*AN5/BE6-140.0*AN6/BE7)
DDT6=DEL*(420.0*AN2/BE4-1680.0*AN3/BE5
& +2100.0*AN4/BE6-840.0*AN5/BE7)
GOTO 60

```

```

40 T6=T6F
DT6=0.
DDT6=0.
GO TO 60
50 ANG=PH-(7.D0*PI/6.0D0)
AN2=ANG*ANG
AN3=AN2*ANG
AN4=AN3*ANG
AN5=AN4*ANG
AN6=AN5*ANG
AN7=AN6*ANG
BETA=2.O*PI/3.0
BE4=BETA**4
BE5=BE4*BETA
BE6=BE5*BETA
BE7=BE6*BETA
T6=T6F-DEL*(35.0*AN4/BE4-84.0*AN5/BE5
& +70.0*AN6/BE6-20.0*AN7/BE7)
DT6=-DEL*(140.0*AN3/BE4-420.0*AN4/BE5
& +420.0*AN5/BE6-140.0*AN6/BE7)
DDT6=-DEL*(420.0*AN2/BE4-1680.0*AN3/BE5
& +2100.0*AN4/BE6-840.0*AN5/BE7)
60 RETURN
END

SUBROUTINE FEM_SY2(TIME,T5,XT,DXT,DDXT,SMCUT,SKCUT,SMRIGCUT)
PARAMETER NEL=6,NDF=6,N=NDF,NTF=17,NG=NTF-1,NTH=32,IPATH=1
IMPLICIT REAL*8(A-H,O-Z)
DIMENSION RL(NEL),B(2:NEL),TH(2:NEL),RD(1)
& ,EA(2:NEL),EI(2:NEL),RLS(2:NEL),RLC(2:NEL),RALW(2:NEL)
& ,ET(2:NEL),SKE(NEL,NDF,NDF),SKET(NDF,NDF)
& ,SKEA(N,N),SKEB(N,N),SMEA(N,N),SMEB(N,N)
& ,SME(NEL,NDF,NDF),SMET(NDF,NDF),TR(N,N)
& ,TRT(N,N),SM(NTF,NTF),SK(NTF,NTF),DDRIG(NTF),FRIG(NTF)
& ,SMCUT(NG,NG),SMRIG(NTF),SMRIGCUT(NG),SKCUT(NG,NG)
& ,IJK(NDF,NEL)
COMMON /NFEM/NCAM,KSTART,KRUN,KLIMIT,NMARGIN,NRI,IJK
COMMON /RFEM/DSR,RD,E,RMU,R4,R,RHO,B,TH,RL,PI,IS
COMMON /NAME1/NCAMM
COMMON /NJJ/ICOMA,ICOMS

```

```

COMMON /NIA/SME,SKE,ZET,GAR
IF (ICOMS .NE. 7) THEN
  NCAMM=NCAM
  DQ=DSR**2
  G=E/(2.*(1.+RMU))
  ALP=0.5*ASIN(R4/2./R)
  BET=0.5*(PI-ALP)
  GAR=ASIN((1.-COS(ALP))/(2.*SIN(ALP/2.)))
  ZET=ASIN((COS(ALP)-COS(2.*ALP)) / (2.*SIN(ALP/2.)) )
  RI=NRI*RHO*PI*RL(1)*(RD(1)/2.)**4/2.
  RMD=1./DQ
  DO 29 I=3,NEL
    RL(I)=2.*R*SIN(ALP/2.)
  DO 105 I=1,1
    SMEME=RHO*PI*RL(I)*(RD(I)/2.)**4/2./3.
    SME(I,1,1)=(RI+SMEME)/RMD
    SME(I,1,2)=SMEME/2./RMD
    SME(I,2,1)=SME(I,1,2)
    SME(I,2,2)=SMEME/RMD
    SKE(I,1,1)=G*PI*RD(I)**4/32./RL(I)
    SKE(I,1,2)=-SKE(I,1,1)
    SKE(I,2,1)=SKE(I,1,2)
    SKE(I,2,2)=SKE(I,1,1)
105  CONTINUE
  DO 201 I=2,NEL
    RALW(I)=RHO*B(I)*TH(I)*RL(I)
    SME(I,1,1)=RALW(I)/3./RMD
    SME(I,1,2)=0.
    SME(I,1,3)=0.
    SME(I,1,4)=RALW(I)/6./RMD
    SME(I,1,5)=0.
    SME(I,1,6)=0.
    SME(I,2,2)=RALW(I)*13./35./RMD
    SME(I,2,3)=RALW(I)*11.*RL(I)/210./RMD
    SME(I,2,4)=0.
    SME(I,2,5)=RALW(I)*9./70./RMD
    SME(I,2,6)=-RALW(I)*13.*RL(I)/420./RMD
    SME(I,3,3)=RALW(I)*RL(I)**2/105./RMD
    SME(I,3,4)=0.
    SME(I,3,5)=-SME(I,2,6)

```

```

SME(I,3,6)=-RALW(I)*RL(I)**2/140./RMD
SME(I,4,4)=RALW(I)/3./RMD
SME(I,4,5)=0.
SME(I,4,6)=0.
SME(I,5,5)=SME(I,2,2)
SME(I,5,6)=-SME(I,2,3)
SME(I,6,6)=SME(I,3,3)

C
EA(I)=E*B(I)*TH(I)
EI(I)=E*B(I)*TH(I)**3/12.
RLS(I)=RL(I)**2
RLC(I)=RLS(I)*RL(I)
SKE(I,1,1)=EA(I)/RL(I)
SKE(I,1,2)=0.
SKE(I,1,3)=0.
SKE(I,1,4)=-SKE(I,1,1)
SKE(I,1,5)=0.
SKE(I,1,6)=0.
SKE(I,2,2)=12.*EI(I)/RLC(I)
SKE(I,2,3)=6.*EI(I)/RLS(I)
SKE(I,2,4)=0.
SKE(I,2,5)=-SKE(I,2,2)
SKE(I,2,6)=SKE(I,2,3)
SKE(I,3,3)=4.*EI(I)/RL(I)
SKE(I,3,4)=0.
SKE(I,3,5)=-SKE(I,2,3)
SKE(I,3,6)=2.*EI(I)/RL(I)
SKE(I,4,4)=EA(I)/RL(I)
SKE(I,4,5)=0.
SKE(I,4,6)=0.
SKE(I,5,5)=SKE(I,2,2)
SKE(I,5,6)=SKE(I,3,5)
SKE(I,6,6)=SKE(I,3,3)
DO 201 JJ=1,N
    DO 201 II=JJ+1,N
        SME(I,II,JJ)=SME(I,JJ,II)
        SKE(I,II,JJ)=SKE(I,JJ,II)
201     ICOMS=7
ENDIF
DO 18 JJ=1,NTF !.....assemble

```

```

DO 18 II=1,NTF
SM(II,JJ)=0.
SK(II,JJ)=0.
18   DO 2500 I=1,1
      DO 2500 IA=1,NDF
         IJKIA=IJK(IA,I)
         IF(IJKIA .EQ. 0) GOTO 2500
         DO 2500 JB=1,NDF
            IJKJB=IJK(JB,I)
            IF(IJKJB .EQ. 0) GOTO 2500
            SM(IJKIA,IJKJB)=SME(I,IA,JB)+SM(IJKIA,IJKJB)
            SK(IJKIA,IJKJB)=SKE(I,IA,JB)+SK(IJKIA,IJKJB)
2500   CONTINUE
      T5=ACOS( (RL(2)**2+XT**2-R4**2) / (2.*RL(2)*XT) )
      ST5=SIN(T5)
      RST5=RL(2)*ST5
      ST5Q=ST5**2
      CT5=COS(T5)
      RCT5=RL(2)*CT5
      CT5Q=CT5**2
      T4=ATAN2(RST5,RCT5-XT)
      CT4=COS(T4)
      R4CT4=R4*CT4
      CT4Q=CT4**2
      ST4T5=SIN(T4-T5)
      CT4T5=COS(T4-T5)
      DT5=CT4*DXT/(RL(2)*ST4T5)
      DT5Q=DT5**2
      DT4Q=DT4**2
      DDT5=(CT4*DDXT-R4*DT4Q+RL(2)*DT5Q*CT4T5)/(RL(2)*ST4T5)
      DT4=CT5*DXT/(R4*ST4T5)
      DDT4=(RCT5*DDT5-RST5*DT5Q+R4*ST4*DT4Q)/R4CT4
      ET(2)=T5
      ET(3)=T4+PI+ZET
      ET(4)=T4+PI+GAR
      ET(5)=T4+PI-GAR
      ET(6)=T4+PI-ZET
      DO 200 I=2,NEL !*****
      TR(1,1)=COS(ET(I))
      TR(1,2)=SIN(ET(I))

```

```

TR(2,1)=-TR(1,2)
TR(2,2)=TR(1,1)
TR(3,3)=1.
TR(4,4)=TR(1,1)
TR(4,5)=TR(1,2)
TR(5,4)=-TR(4,5)
TR(5,5)=TR(4,4)
TR(6,6)=1.
TRT(1,1)=COS(ET(I))
TRT(1,2)=-SIN(ET(I))
TRT(2,1)=-TRT(1,2)
TRT(2,2)=TRT(1,1)
TRT(3,3)=1.
TRT(4,4)=TRT(1,1)
TRT(4,5)=TRT(1,2)
TRT(5,4)=-TRT(4,5)
TRT(5,5)=TRT(4,4)
TRT(6,6)=1.
DO 723 JJ=1,NDF !.....assemble
    DO 723 KK=1,NDF
        SMEA(JJ,KK)=SME(I,JJ,KK)
        SKEA(JJ,KK)=SKE(I,JJ,KK)
723     CALL DMRRRR(N,N,SMEA,N,N,N,TR,N,N,N,SMEB,N)
        CALL DMRRRR(N,N,TRT,N,N,N,SMEB,N,N,N,SMET,N)
        CALL DMRRRR(N,N,SKEA,N,N,N,TR,N,N,N,SKEB,N)
        CALL DMRRRR(N,N,TRT,N,N,N,SKEB,N,N,N,SKET,N)
        DO 200 IA=1,NDF
            IJKIA=IJK(IA,I)
            IF(IJKIA .EQ. 0) GOTO 200
            DO 200 JB=1,NDF
                IJKJB=IJK(JB,I)
                IF(IJKJB .EQ. 0) GOTO 200
                SM(IJKIA,IJKJB)=SMET(IA,JB)+SM(IJKIA,IJKJB)
                SK(IJKIA,IJKJB)=SKET(IA,JB)+SK(IJKIA,IJKJB)
200     CONTINUE
        CALL DSYNL3T6DDT6(TIME,T6SYN,DDT6SYN)
c... subroutine DSYNL3T6DDT6 is a reduction of subroutine DSYNL3D2
        DDRIG(1)=DDT6SYN
        DDRIG(2)=DDT5
        DDRIG(3)=(-RL(2)*DDT5*SIN(T5)+RL(2)*DT5**2*COS(T5))

```

```

DDRIG(4)=(RL(2)*DDT5*COS(T5)+RL(2)*DT5**2*SIN(T5))
DDRIG(5)=DDT5
DDRIG(6)=DDT4
DDRIG(9)=DDT4
DDRIG(12)=DDT4
DDRIG(15)=DDT4
DDRIG(16)=DDT4
DDRIG(7)=DDRIG(3)-RL(3)*DDT4*SIN(ET(3))
&           +RL(3)*DT4**2*COS(ET(3))
DDRIG(8)=DDRIG(4)+RL(3)*DDT4*COS(ET(3))
&           +RL(3)*DT4**2*SIN(ET(3))
DDRIG(10)=DDRIG(7)-RL(4)*DDT4*SIN(ET(4))
&           +RL(4)*DT4**2*COS(ET(4))
DDRIG(11)=DDRIG(8)+RL(4)*DDT4*COS(ET(4))
&           +RL(4)*DT4**2*SIN(ET(4))
DDRIG(13)=DDRIG(10)-RL(5)*DDT4*SIN(ET(5))
&           +RL(5)*DT4**2*COS(ET(5))
DDRIG(14)=DDRIG(11)+RL(5)*DDT4*COS(ET(5))
&           +RL(5)*DT4**2*SIN(ET(5))
DDRIG(17)=DDXT
CALL DMURRV(NTF,NTF,SM,NTF,NTF,DDRIG,IPATH,NTF,SMRIG)
DO 17 II=1,NTF-1
  SMRIGCUT(II)=-SMRIG(II)-SK(II,1)*(T6SYN-T5)
  !take negative (move to RHS)
  DO 17 JJ=1,NTF-1
    SKCUT(JJ,II)=SK(JJ,II+1)
    SMCUT(JJ,II)=SM(JJ,II+1)
17 END

SUBROUTINE FEM_ANA(TIME,T5,XT,DXT,DDXT,SMCUT,SKCUT,SMRIGCUT)
PARAMETER NEL=6,NDF=6,N=NDF,NTF=17,NG=NTF-1,NTH=32,IPATH=1
IMPLICIT REAL*8(A-H,O-Z)
DIMENSION RL(NEL),B(2:NEL),TH(2:NEL),RD(1)
& ,EA(2:NEL),EI(2:NEL),RLS(2:NEL),RLC(2:NEL),RALW(2:NEL)
& ,ET(2:NEL),SKE(NEL,NDF,NDF),SKET(NDF,NDF)
& ,SKEA(N,N),SKEB(N,N),SMEA(N,N),SMEB(N,N)
& ,SME(NEL,NDF,NDF),SMET(NDF,NDF),TR(N,N),IJK(NDF,NEL)
& ,TRT(N,N),SM(NTF,NTF),SK(NTF,NTF),DDRIG(NTF),FRIG(NTF)
& ,SMCUT(NG,NG),SMRIG(NTF),SMRIGCUT(NG),SKCUT(NG,NG)
COMMON /NFEM/NCAM,KSTART,KRUN,KLIMIT,NMARGIN,NRI,IJK

```

```

COMMON /RFEM/DSR,RD,E,RMU,R4,R,RHO,B,TH,RL,PI,IS
COMMON /NJJ/ICOMA,ICOMS
COMMON /NIA/SME,SKE,ZET,GAR
IF (ICOMA .NE. 7) THEN
  DQ=DSR**2
  G=E/(2.*(1.+RMU))
  ALP=0.5*ASIN(R4/2./R)
  BET=0.5*(PI-ALP)
  GAR=ASIN((1.-COS(ALP))/(2.*SIN(ALP/2.)))
  ZET=ASIN((COS(ALP)-COS(2.*ALP)) / (2.*SIN(ALP/2.)) )
  RI=NRI*RHO*PI*RL(1)*(RD(1)/2.)**4/2.
  RMD=1./DQ
  DO 29 I=3,NEL
    RL(I)=2.*R*SIN(ALP/2.)
  DO 105 I=1,1
    SMEME=RHO*PI*RL(I)*(RD(I)/2.)**4/2./3.
    SME(I,1,1)=(RI+SMEME)/RMD
    SME(I,1,2)=SMEME/2./RMD
    SME(I,2,1)=SME(I,1,2)
    SME(I,2,2)=SMEME/RMD
    SKE(I,1,1)=G*PI*RD(I)**4/32./RL(I)
    SKE(I,1,2)=-SKE(I,1,1)
    SKE(I,2,1)=SKE(I,1,2)
    SKE(I,2,2)=SKE(I,1,1)
105  CONTINUE
  DO 201 I=2,NEL
    RALW(I)=RHO*B(I)*TH(I)*RL(I)
    SME(I,1,1)=RALW(I)/3./RMD
    SME(I,1,2)=0.
    SME(I,1,3)=0.
    SME(I,1,4)=RALW(I)/6./RMD
    SME(I,1,5)=0.
    SME(I,1,6)=0.
    SME(I,2,2)=RALW(I)*13./35./RMD
    SME(I,2,3)=RALW(I)*11.*RL(I)/210./RMD
    SME(I,2,4)=0.
    SME(I,2,5)=RALW(I)*9./70./RMD
    SME(I,2,6)=-RALW(I)*13.*RL(I)/420./RMD
    SME(I,3,3)=RALW(I)*RL(I)**2/105./RMD
    SME(I,3,4)=0.

```

```

SME(I,3,5)=-SME(I,2,6)
SME(I,3,6)=-RALW(I)*RL(I)**2/140./RMD
SME(I,4,4)=RALW(I)/3./RMD
SME(I,4,5)=0.
SME(I,4,6)=0.
SME(I,5,5)=SME(I,2,2)
SME(I,5,6)=-SME(I,2,3)
SME(I,6,6)=SME(I,3,3)

C
EA(I)=E*B(I)*TH(I)
EI(I)=E*B(I)*TH(I)**3/12.
RLS(I)=RL(I)**2
RLC(I)=RLS(I)*RL(I)
SKE(I,1,1)=EA(I)/RL(I)
SKE(I,1,2)=0.
SKE(I,1,3)=0.
SKE(I,1,4)=-SKE(I,1,1)
SKE(I,1,5)=0.
SKE(I,1,6)=0.
SKE(I,2,2)=12.*EI(I)/RLC(I)
SKE(I,2,3)=6.*EI(I)/RLS(I)
SKE(I,2,4)=0.
SKE(I,2,5)=-SKE(I,2,2)
SKE(I,2,6)=SKE(I,2,3)
SKE(I,3,3)=4.*EI(I)/RL(I)
SKE(I,3,4)=0.
SKE(I,3,5)=-SKE(I,2,3)
SKE(I,3,6)=2.*EI(I)/RL(I)
SKE(I,4,4)=EA(I)/RL(I)
SKE(I,4,5)=0.
SKE(I,4,6)=0.
SKE(I,5,5)=SKE(I,2,2)
SKE(I,5,6)=SKE(I,3,5)
SKE(I,6,6)=SKE(I,3,3)
DO 201 JJ=1,N
    DO 201 II=JJ+1,N
        SME(I,II,JJ)=SME(I,JJ,II)
201        SKE(I,II,JJ)=SKE(I,JJ,II)
        ICOMA=7
    ENDIF

```

```

DO 18 JJ=1,NTF
DO 18 II=1,NTF
  SM(II,JJ)=0.
18   SK(II,JJ)=0.
    DO 2500 I=1,1      !.....assemble
      DO 2500 IA=1,NDF
        IJKIA=IJK(IA,I)
        IF(IJKIA .EQ. 0) GOTO 2500
        DO 2500 JB=1,NDF
          IJKJB=IJK(JB,I)
          IF(IJKJB .EQ. 0) GOTO 2500
          SM(IJKIA,IJKJB)=SME(I,IA,JB)+SM(IJKIA,IJKJB)
          SK(IJKIA,IJKJB)=SKE(I,IA,JB)+SK(IJKIA,IJKJB)
2500   CONTINUE           !.....assemble ends
      T5=ACOS( (RL(2)**2+XT**2-R4**2) / (2.*RL(2)*XT) )
      ST5=SIN(T5)
      RST5=RL(2)*ST5
      ST5Q=ST5**2
      CT5=COS(T5)
      RCT5=RL(2)*CT5
      CT5Q=CT5**2
      T4=ATAN2(RST5,RCT5-XT)
      CT4=COS(T4)
      R4CT4=R4*CT4
      CT4Q=CT4**2
      ST4T5=SIN(T4-T5)
      CT4T5=COS(T4-T5)
      DT5=CT4*DXT/(RL(2)*ST4T5)
      DT5Q=DT5**2
      DT4Q=DT4**2
      DDT5=(CT4*DDXT-R4*DT4Q+RL(2)*DT5Q*CT4T5)/(RL(2)*ST4T5)
      DT4=CT5*DXT/(R4*ST4T5)
      DDT4=(RCT5*DDT5-RST5*DT5Q+R4*ST4*DT4Q)/R4CT4
      ET(2)=T5
      ET(3)=T4+PI+ZET
      ET(4)=T4+PI+GAR
      ET(5)=T4+PI-GAR
      ET(6)=T4+PI-ZET
      DO 200 I=2,NEL
        TR(1,I)=COS(ET(I))

```

```

TR(1,2)=SIN(ET(I))
TR(2,1)=-TR(1,2)
TR(2,2)=TR(1,1)
TR(3,3)=1.
TR(4,4)=TR(1,1)
TR(4,5)=TR(1,2)
TR(5,4)=-TR(4,5)
TR(5,5)=TR(4,4)
TR(6,6)=1.
TRT(1,1)=COS(ET(I))
TRT(1,2)=-SIN(ET(I))
TRT(2,1)=-TRT(1,2)
TRT(2,2)=TRT(1,1)
TRT(3,3)=1.
TRT(4,4)=TRT(1,1)
TRT(4,5)=TRT(1,2)
TRT(5,4)=-TRT(4,5)
TRT(5,5)=TRT(4,4)
TRT(6,6)=1.
DO 723 JJ=1,NDF !transformation
  DO 723 KK=1,NDF
    SMEA(JJ,KK)=SME(I,JJ,KK)
    SKEA(JJ,KK)=SKE(I,JJ,KK)
723 CALL DMRRRR(N,N,SMEA,N,N,N,TR,N,N,N,SMEB,N)
      CALL DMRRRR(N,N,TRT,N,N,N,SMEB,N,N,N,SMET,N)
      CALL DMRRRR(N,N,SKEA,N,N,N,TR,N,N,N,SKEB,N)
      CALL DMRRRR(N,N,TRT,N,N,N,SKEB,N,N,N,SKET,N)
DO 200 IA=1,NDF !assemble
  IJKIA=IJK(IA,I)
  IF(IJKIA .EQ. 0) GOTO 200
  DO 200 JB=1,NDF
    IJKJB=IJK(JB,I)
    IF(IJKJB .EQ. 0) GOTO 200
    SM(IJKIA,IJKJB)=SMET(IA,JB)+SM(IJKIA,IJKJB)
    SK(IJKIA,IJKJB)=SKET(IA,JB)+SK(IJKIA,IJKJB)
200 CONTINUE           !assemble ends
  DDRIG(1)=DDT5
  DDRIG(2)=DDT5
  DDRIG(3)=(-RL(2)*DDT5*SIN(T5)+RL(2)*DT5**2*COS(T5))
  DDRIG(4)=(RL(2)*DDT5*COS(T5)+RL(2)*DT5**2*SIN(T5))

```

```

DDRIG(5)=DDT5
DDRIG(6)=DDT4
DDRIG(9)=DDT4
DDRIG(12)=DDT4
DDRIG(15)=DDT4
DDRIG(16)=DDT4
DDRIG(7)=DDRIG(3)-RL(3)*DDT4*SIN(ET(3))
&           +RL(3)*DT4**2*COS(ET(3))
DDRIG(8)=DDRIG(4)+RL(3)*DDT4*COS(ET(3))
&           +RL(3)*DT4**2*SIN(ET(3))
DDRIG(10)=DDRIG(7)-RL(4)*DDT4*SIN(ET(4))
&           +RL(4)*DT4**2*COS(ET(4))
DDRIG(11)=DDRIG(8)+RL(4)*DDT4*COS(ET(4))
&           +RL(4)*DT4**2*SIN(ET(4))
DDRIG(13)=DDRIG(10)-RL(5)*DDT4*SIN(ET(5))
&           +RL(5)*DT4**2*COS(ET(5))
DDRIG(14)=DDRIG(11)+RL(5)*DDT4*COS(ET(5))
&           +RL(5)*DT4**2*SIN(ET(5))
DDRIG(17)=DDXT
CALL DMURRV(NTF,NTF,SM,NTF,NTF,DDRIG,IPATH,NTF,SMRIG)
DO 17 II=1,NTF-1
  SMRIGCUT(II)=-SMRIG(II) !take negative (move to RHS)
  DO 17 JJ=1,NTF-1
    SKCUT(JJ,II)=SK(JJ,II)
    SMCUT(JJ,II)=SM(JJ,II)
17 END

```

```

c...main program to calculate characteristic multipliers
c  RATIO=Rayleigh damping coefficient
c  DSR=OMEGA (speed ratio)
c  R=radius of curvature, RHO= density, RD=diameter, RL=length
c  RMU=Poisson ratio
      PARAMETER NEL=6,NDF=6,N=NDF,NTF=17,NG=NTF-1,NTH=32
      & ,IPATH=1,NKEEP=4,NTHD=64,KDIM=360,LCHECK='FALSE'
      IMPLICIT REAL*8(A-H,O-Z)
      DIMENSION RL(NEL),B(2:NEL),TH(2:NEL),RD(1)
      & ,EA(2:NEL),EI(2:NEL),RLS(2:NEL),RLC(2:NEL),RALW(2:NEL)
      & ,ET(2:NEL),SM(NTF,NTF),SMINV(NTF,NTF),SK(NTF,NTF)
      & ,SKNOR(NG,NG),HA(NTH,NTH),PHISUB(NTH,NTH)
      & ,RM(NG,NG),SMRIG(NTF),RMINV(NG,NG),RK(NG,NG)
      & ,PHI(NTH,NTH),COLB(NTH),XDATA(KDIM),XT(KDIM)
      & ,IJK(NDF,NEL)
      COMPLEX*16 EVAL(NTH),EVEC(NTH,NTH)
      & ,EVECT(NTH,NTH),TA(NTH,NTH),T(NTH,NTH),PHISUBC(NTH,NTH)
      COMMON /NFEM/KLIMIT,NRI,IJK
      COMMON /RFEM/DSR,RD,E,RMU,R4,R,RHO,B,TH,RL,PI,K
      OPEN(5,FILE='FEMHSUI.DAT',STATUS='OLD')
      READ(71,*)MSTDWRI,MOEVA,MEVAWRI
      READ(71,*)MEVAME,MONPIV
      READ(71,*)KSN
      READ(71,*)KLIMIT,NRI
      READ(71,*)DSR,RATIO
      READ(71,*)RD(1),E,RMU,R4,R,RHO
      READ(71,*)((IJK(J,IE),J=1,NDF),IE=1,NEL)
      DO 801 I=2,NEL
801      READ(71,*)B(I),TH(I)
      READ(71,*)(RL(I),I=1,2)
      CLOSE (71)
      DQ=DSR**2
      PI=4.*ATAN(1.)
      PERIOD=2.*PI
      DEL=PERIOD/KLIMIT*KSN
      G=E/(2.*(1.+RMU))
      RKN=G*PI*RD(1)**4/32./RL(1)
      RI=NRI*RHO*PI*RL(1)*(RD(1)/2.)**4/2.
      WN=SQRT(RKN/RI)
      DO 864 I=1,KLIMIT

```

```

864      XDATA(I)=DEL*(I-1)
      DO 109 II=1,NTH-1,2
109      HA(II,II+1)=1.
      OPEN(81,FILE='FEMXT',STATUS='OLD') !contain xt obtained
                                         !in synthesis
      DO 709 JJ=1,KLIMIT
709      READ(81,*)XT(JJ)
      CLOSE (81)
      DO 78321 K=1,KLIMIT
      P=(K-1)*DEL
      DXT=DQDDER(1,XDATA(IS),KLIMIT,XDATA,XT,LCHECK)
      DDXT=DQDDER(2,XDATA(IS),KLIMIT,XDATA,XT,LCHECK)
      CALL HSU_ANA(P,XT,DXT,DDXT,RM,RK)
      CALL DLINRG(NG,RM,NG,RMINV,NG)
      CALL DMRRRR(NG,NG,RMINV,NG,NG,NG,RK,NG,NG,NG,SKNOR,NG)
      DO 643 II=1,NTH-1,2
      DO 643 JJ=1,NTH-1,2
          HA(II+1,JJ)=-SKNOR((II+1)/2,(JJ+1)/2)
          HA(II+1,JJ+1)=RATIO*HA(II+1,JJ)
643      CONTINUE
      IF (K .EQ. 1) THEN !***** assign the value at time=0.****
      DO 806 JJ=1,NTH !....INITIALIZE PHI(I,I)
      DO 806 II=1,NTH
          IF (II .NE. JJ) THEN
              PHI(II,JJ)=0.
          ELSE
              PHI(II,JJ)=1.
          ENDIF
806      CONTINUE
      ENDIF !***** end of time=0 assignment **
      CALL DEVCRG(NTH,HA,NTH,EVAL,EVEC,NTH)
      CALL DLINCG(NTH,EVEC,NTH,EVECT,NTH)
      DO 67 I=1,NTH
67      T(I,I)=EXP(EVAL(I)*DEL)
      CALL DMCRCR(NTH,NTH,T,NTH,NTH,NTH,NTH,EVECT,NTH,NTH,NTH,TA,NTH)
      CALL DMCRCR(NTH,NTH,EVEC,NTH,NTH,NTH,NTH,TA,NTH,NTH,NTH
      & ,PHISUBC,NTH)
      DO 908 IC=1,NTH
      DO 908 IR=1,NTH
908      PHISUB(IR,IC)=DREAL(PHISUBC(IR,IC))

```

```

CALL BCRMUL(PHISUB,PHI,COLB,NTH,NTH) !...CALCULATE PHI(TK)
78321 CONTINUE
IF (MOEVA .EQ. 1) THEN      ! beginning of E.Values
  CALL DEVLRG(NTH,PHI,NTH,EVAL)
  IF (MEVAWRI .EQ. 1) THEN
    WRITE(13,9242)DSR,DSR/WM
    WRITE(13,9062)EVAL
  ENDIF
ENDIF
IF (MEVAME .EQ. 1) WRITE(16,9062)DSR,EVAL !end of E.Values
9062 FORMAT(1X,6E13.5)
9242 FORMAT(1X,5E14.6)
END

SUBROUTINE HSU_ANA(TIME,XT,DXT,DDXT,SMCUT,SKCUT)
PARAMETER NEL=6,NDF=6,N=NDF,NTF=17,NG=NTF-1,NTH=32
& ,IPATH=1,NKEEP=4
IMPLICIT REAL*8(A-H,O-Z)
DIMENSION RL(NEL),B(2:NEL),TH(2:NEL),RD(1)
& ,EA(2:NEL),EI(2:NEL),RLS(2:NEL),RLC(2:NEL),RALW(2:NEL)
& ,ET(2:NEL),SKE(NEL,NDF,NDF),SKET(NDF,NDF)
& ,SKEA(N,N),SKEB(N,N),SMEA(N,N),SMEB(N,N)
& ,SME(NEL,NDF,NDF),SMET(NDF,NDF),TR(N,N)
& ,TRT(N,N),SM(NTF,NTF),SK(NTF,NTF)
& ,SMCUT(NG,NG),SKCUT(NG,NG),IJK(NDF,NEL)
COMMON /NFEM/KLIMIT,NRI,IJK
COMMON /RFEM/DSR,RD,E,RMU,R4,R,RHO,B,TH,RL,PI,K
COMMON /NCOM/PERIOD,SME,SKE,ICOM,ZET,GAR
IF (ICOM .NE. 7) THEN
  DQ=DSR**2
  PI=4.*ATAN(1.)
  PERIOD=2.*PI
  DEL=PERIOD/KLIMIT
  G=E/(2.*(1.+RMU))
  ALP=0.5*ASIN(R4/2./R)
  BET=0.5*(PI-ALP)
  GAR=ASIN((1.-COS(ALP))/(2.*SIN(ALP/2.)))
  ZET=ASIN((COS(ALP)-COS(2.*ALP)) / (2.*SIN(ALP/2.)) )
  RI=NRI*RHO*PI*RL(1)*(RD(1)/2.)**4/2.
  RMD=1./DQ

```

```

DO 29 I=3,NEL
29    RL(I)=2.*R*SIN(ALP/2.)
DO 105 I=1,1
      SMEME=RHO*PI*RL(I)*(RD(I)/2.)**4/2./3.
      SME(I,1,1)=(RI+SMEME)/RMD
      SME(I,1,2)=SMEME/2./RMD
      SME(I,2,1)=SME(I,1,2)
      SME(I,2,2)=SMEME/RMD
      SKE(I,1,1)=G*PI*RD(I)**4/32./RL(I)
      SKE(I,1,2)=-SKE(I,1,1)
      SKE(I,2,1)=SKE(I,1,2)
      SKE(I,2,2)=SKE(I,1,1)

105   CONTINUE
DO 201 I=2,NEL
      RALW(I)=RHO*B(I)*TH(I)*RL(I)
      SME(I,1,1)=RALW(I)/3./RMD
      SME(I,1,2)=0.
      SME(I,1,3)=0.
      SME(I,1,4)=RALW(I)/6./RMD
      SME(I,1,5)=0.
      SME(I,1,6)=0.
      SME(I,2,2)=RALW(I)*13./35./RMD
      SME(I,2,3)=RALW(I)*11.*RL(I)/210./RMD
      SME(I,2,4)=0.
      SME(I,2,5)=RALW(I)*9./70./RMD
      SME(I,2,6)=-RALW(I)*13.*RL(I)/420./RMD
      SME(I,3,3)=RALW(I)*RL(I)**2/105./RMD
      SME(I,3,4)=0.
      SME(I,3,5)=-SME(I,2,6)
      SME(I,3,6)=-RALW(I)*RL(I)**2/140./RMD
      SME(I,4,4)=RALW(I)/3./RMD
      SME(I,4,5)=0.
      SME(I,4,6)=0.
      SME(I,5,5)=SME(I,2,2)
      SME(I,5,6)=-SME(I,2,3)
      SME(I,6,6)=SME(I,3,3)

C
      EA(I)=E*B(I)*TH(I)
      EI(I)=E*B(I)*TH(I)**3/12.
      RLS(I)=RL(I)**2

```

```

RLC(I)=RLS(I)*RL(I)
SKE(I,1,1)=EA(I)/RL(I)
SKE(I,1,2)=0.
SKE(I,1,3)=0.
SKE(I,1,4)=-SKE(I,1,1)
SKE(I,1,5)=0.
SKE(I,1,6)=0.
SKE(I,2,2)=12.*EI(I)/RLC(I)
SKE(I,2,3)=6.*EI(I)/RLS(I)
SKE(I,2,4)=0.
SKE(I,2,5)=-SKE(I,2,2)
SKE(I,2,6)=SKE(I,2,3)
SKE(I,3,3)=4.*EI(I)/RL(I)
SKE(I,3,4)=0.
SKE(I,3,5)=-SKE(I,2,3)
SKE(I,3,6)=2.*EI(I)/RL(I)
SKE(I,4,4)=EA(I)/RL(I)
SKE(I,4,5)=0.
SKE(I,4,6)=0.
SKE(I,5,5)=SKE(I,2,2)
SKE(I,5,6)=SKE(I,3,5)
SKE(I,6,6)=SKE(I,3,3)
DO 201 JJ=1,N
  DO 201 II=JJ+1,N
    SME(I,II,JJ)=SME(I,JJ,II)
201    SKE(I,II,JJ)=SKE(I,JJ,II)
    ICOM=7
    ENDIF
    DO 18 JJ=1,NTF
      DO 18 II=1,NTF
        SM(II,JJ)=0.
18      SK(II,JJ)=0.
      DO 2500 I=1,1
        DO 2500 IA=1,NDF
          IJKIA=IJK(IA,I)
          IF(IJKIA .EQ. 0) GOTO 2500
          DO 2500 JB=1,NDF
            IJKJB=IJK(JB,I)
            IF(IJKJB .EQ. 0) GOTO 2500
            SM(IJKIA,IJKJB)=SME(I,IA,JB)+SM(IJKIA,IJKJB)

```

```

SK(IJKIA,IJKJB)=SKE(I,IA,JB)+SK(IJKIA,IJKJB)
2500  CONTINUE
      T5=ACOS( (RL(2)**2+XT**2-R4**2) / (2.*RL(2)*XT) )
      ST5=SIN(T5)
      RST5=RL(2)*ST5
      ST5Q=ST5**2
      CT5=COS(T5)
      RCT5=RL(2)*CT5
      CT5Q=CT5**2
      T4=ATAN2(RST5,RCT5-XT)
      CT4=COS(T4)
      R4CT4=R4*CT4
      CT4Q=CT4**2
      ST4T5=SIN(T4-T5)
      CT4T5=COS(T4-T5)
      DT5=CT4*DXT/(RL(2)*ST4T5)
      DT5Q=DT5**2
      DT4Q=DT4**2
      DDT5=(CT4*DDXT-R4*DT4Q+RL(2)*DT5Q*CT4T5)/(RL(2)*ST4T5)
      DT4=CT5*DXT/(R4*ST4T5)
      DDT4=(RCT5*DDT5-RST5*DT5Q+R4*ST4*DT4Q)/R4CT4
      ET(2)=T5
      ET(3)=T4+PI+ZET
      ET(4)=T4+PI+GAR
      ET(5)=T4+PI-GAR
      ET(6)=T4+PI-ZET
      DO 200 I=2,NEL !...transformation
      TR(1,1)=COS(ET(I))
      TR(1,2)=SIN(ET(I))
      TR(2,1)=-TR(1,2)
      TR(2,2)=TR(1,1)
      TR(3,3)=1.
      TR(4,4)=TR(1,1)
      TR(4,5)=TR(1,2)
      TR(5,4)=-TR(4,5)
      TR(5,5)=TR(4,4)
      TR(6,6)=1.
      TRT(1,1)=COS(ET(I))
      TRT(1,2)=-SIN(ET(I))
      TRT(2,1)=-TRT(1,2)

```

```

      TRT(2,2)=TRT(1,1)
      TRT(3,3)=1.
      TRT(4,4)=TRT(1,1)
      TRT(4,5)=TRT(1,2)
      TRT(5,4)=-TRT(4,5)
      TRT(5,5)=TRT(4,4)
      TRT(6,6)=1.
      DO 723 JJ=1,NDF
         DO 723 KK=1,NDF
            SMEA(JJ,KK)=SME(I,JJ,KK)
            SKEA(JJ,KK)=SKE(I,JJ,KK)
723   CALL DMRRRR(N,N,SMEA,N,N,N,TR,N,N,N,SMEB,N)
      CALL DMRRRR(N,N,TR,N,N,N,SMEB,N,N,N,SMET,N)
      CALL DMRRRR(N,N,SKEA,N,N,N,TR,N,N,N,SKEB,N)
      CALL DMRRRR(N,N,TR,N,N,N,SKEB,N,N,N,SKET,N)
      DO 200 IA=1,NDF !...assemble****
      IJKIA=IJK(IA,I)
      IF(IJKIA .EQ. 0) GOTO 200
      DO 200 JB=1,NDF
         IJKJB=IJK(JB,I)
         IF(IJKJB .EQ. 0) GOTO 200
         SM(IJKIA,IJKJB)=SMET(IA,JB)+SM(IJKIA,IJKJB)
         SK(IJKIA,IJKJB)=SKET(IA,JB)+SK(IJKIA,IJKJB)
200    CONTINUE           !assemble ends *****
      DO 17 II=1,NTF-1
         DO 17 JJ=1,NTF-1
            SKCUT(JJ,II)=SK(JJ,II)
17       SMCUT(JJ,II)=SM(JJ,II)
9055    FORMAT(1X,6E11.3)
9062    FORMAT(1X,6G11.3)
      END

C....matrix multiplication: B=A*B
      SUBROUTINE BCRMUL(A,B,COLB,M,N)
      IMPLICIT REAL*8(A-H,O-Z)
      DIMENSION A(M,M),B(M,N),COLB(M)
      DO 10 J=1,N
         DO 9 I=1,M
            COLB(I)=B(I,J)
9          DO 10 I=1,M

```

```
B(I,J)=0.  
DO 10 K=1,M  
10      B(I,J)=B(I,J)+A(I,K)*COLB(K)  
END
```

REFERENCES

- Chen, F. Y. 1973. "Analysis and Design of Cam-Driven Mechanisms with Nonlinearities". *Journal of Engineering for Industry*, 95:685–694.
- Cronin, D. L., and LaBouff, G. A. 1981. "Resonances and Instabilities in Dynamic Systems Incorporating a Cam". *Journal of Mechanical Design*, 103:914–921.
- D'Azzo, J. J., and D'Azzo, C. H. 1988. *Linear control system analysis and design: Conventional and modern* 3rd ed. McGraw-Hill, New York.
- Flugrad, D. R., Jr. 1986. "Cam Synthesis and Analysis for an Elastic Follower Linkage". *Journal of Mechanisms, Transmissions, and Automation in Design*, 108:367–372.
- Gau, W., and Shabana, A. A. 1990. "Effects of Shear Deformation and Rotary Inertia on the Nonlinear Dynamics of Rotating Curved Beams". *Journal of Vibration and Acoustics*, 112:183–193.
- Gupta, K. C., and Wiederrick, J. L. 1983. "Development of Cam Profiles Using the Convolution Operator". *Journal of Mechanisms, Transmissions, and Automation in Design*, 105:654–657.
- Hsu, C. S. 1974. "On Approximating a General Linear Periodic System". *Journal of Mathematical Analysis and Applications*, 45, No.1:234–251.
- Hsu, C. S., and Cheng, W. H. 1973. "Applications of the Theory of Impulsive Parametric Excitation and New Treatments of General Parametric Excitation Problems". *Journal of Applied Mechanics*, 97:78–86.
- Hsu, C. S., and Cheng, W. H. 1974. "Steady State Response of a Dynamical System under Combined Parametric and Forcing Excitations". *Journal of Applied Mechanics*, 98:371–378.

- Johnson, R. C. 1959. "Dynamic Analysis and Design of Relatively Flexible Cam Mechanisms Having More Than One Degree of Freedom". *Journal of Engineering for Industry*, 81:323-331.
- Midha, A., and Turcic, D. A. 1980. "On the Periodic Response of Cam Mechanism with Flexible Follower and Camshaft". *Journal of Dynamic Systems, Measurement, and Control*, 102:255-264.
- Midha, A., Erdman, A. G., and Frohrib, D. A. 1978. "Finite Element Approach to Mathematical Modelling of High-Speed Elastic Linkages". *Mechanism and Machine Theory*, 13:603-618.
- Nagarajan, S., and Turcic, D. A. 1990a. "Lagrangian Formulation of the Equations of Motion for Elastic Mechanisms with Mutual Dependence between Rigid Body and Elastic Motions. Part I: Element Level Equations". *Journal of Dynamic Systems, Measurement, and Control*, 112:203-214.
- Nagarajan, S., and Turcic, D. A. 1990b. "Lagrangian Formulation of the Equations of Motion for Elastic Mechanisms with Mutual Dependence between Rigid Body and Elastic Motions. Part II: System Equations". *Journal of Dynamic Systems, Measurement, and Control*, 112:215-224.
- Sandor, G., and Zhuang, X. 1985. "A Linearized Lumped Parameter Approach to Vibration and Stress Analysis of Elastic Linkages". *Mechanism and Machine Theory*, 20, No.5:427-437.
- Tsay, D. M., and Huey, C. O., Jr. 1989. "Synthesis and Analysis of Cam-Follower Systems with Two Degrees of Freedom". *Advances in Design Automation - 1989*. ASME, 3:281-288.
- Wiederrick, J. L., and Roth, B. 1975. "Dynamic Synthesis of Cams Using Finite Trigonometric Series". *Journal of Engineering for Industry*, 97:603-618.

ACKNOWLEDGEMENTS

My major professor, Dr. Donald R. Flugrad, Jr., helped me shaping the direction of this research; he gave me support, nice advice, and valuable suggestions. My co-major professor, Dr. James E. Bernard, made important comments and suggestions on both mathematical and engineering aspects of this work. My committee members, Dr. Jeffrey C. Huston, Dr. J. Adin Mann III, Dr. kenneth G. McConnell, and Dr. Martin J. Vanderploeg also made valuable comments.

My next door neighbor, Michelle E. Quick, who is a linguistics and Russian major senior at Iowa State University made a great effort to smooth and polish the English of the draft. My friends at Iowa State University constantly gave me assistance and unforgettable care.

Finally I must express my gratitude to my family in Hsinchu, Taiwan, who supported me anytime, anywhere.